

1-1-2014

Development And Human Performance Evaluation Of Control Modes Of An Exo-Skeletal Assistive Robotic Arm (esara)

Umer Khalid
Wayne State University,

Follow this and additional works at: http://digitalcommons.wayne.edu/oa_dissertations

 Part of the [Robotics Commons](#)

Recommended Citation

Khalid, Umer, "Development And Human Performance Evaluation Of Control Modes Of An Exo-Skeletal Assistive Robotic Arm (esara)" (2014). *Wayne State University Dissertations*. Paper 1145.

This Open Access Dissertation is brought to you for free and open access by DigitalCommons@WayneState. It has been accepted for inclusion in Wayne State University Dissertations by an authorized administrator of DigitalCommons@WayneState.

**DEVELOPMENT AND HUMAN PERFORMANCE EVALUATION OF CONTROL
MODES OF AN EXO-SKELETAL ASSISTIVE ROBOTIC ARM (eSARA)**

by

UMER KHALID

DISSERTATION

Submitted to the Graduate School

of Wayne State University,

Detroit, Michigan,

in partial fulfillment of the requirements

for the degree of

DOCTOR OF PHILOSOPHY

2015

MAJOR: ELECTRICAL AND COMPUTER
ENGINEERING

Approved by:

Advisor

Date

© COPYRIGHT BY

UMER KHALID

2015

All Rights Reserved

DEDICATION

I dedicated my dissertation to my father (my inspiration), Khalid Bashir and my late mother (my motivation), Shahida Khalid, my older brother (my role model) Dr. Waqas Khalid, my younger brother (my encouragement) Hamza Khalid and my wife (my perseverance) Dr. Dilshad Umer-Khalid

Your support and confidence in me helped me achieve my goal.

Thank you.

ACKNOWLEDGMENTS

I would like to thank Dr. Abhilash Pandya, Dr. Robert Erlandson, Dr. Yong Xu, Dr. Gerry Conti and Dr. Richard Ellis for their efforts and guidance in this research. I would like to specially thank Vince Brown for his participation and involvement in making this research a success.

In addition I would also like to thank Anthony M. Composto, Prem K. SivaKumar, Ajay V. Mudunuri, Tonya J. Whitehead, Melissa R. Wrobel, Fred W. Upton, and Computer Assisted Robotic Enhanced System (CARES) research group for their support.

TABLE OF CONTENTS

Dedication	ii
Acknowledgements	iii
List of Tables	viii
List of Figures.....	x
Chapter 1 : Introduction Background, Motivation, and Significance.....	1
1.1 Aims and Scopes of Research.....	2
1.2 Specific Research Objectives.....	3
1.3 Novelty and Significance of the Research	5
1.4 Background and Significance	7
1.4.1 Spinal Cord Anatomy	8
1.4.2 The Level of a Spinal Cord Injury (SCI)	9
1.4.3 Physical Limitations and Residual Functionality of Incomplete and Complete Spinal Cord Injuries	10
1.4.4 Physical Limitations and Mobility Challenges of the C6-C7 SCI Individuals (upper extremity challenges and residual functionalities)	11
1.4.5 SCI Statistics.....	12
1.5 International Classification of Functioning, Disability and Health (ICF) Framework to Establish with Research	13
1.5.1 ICF Structure.....	14
1.6 Overview of Current Assistive Devices and their Limitations	16
1.6.1 Types and Classifications of Assistive Devices.....	17
1.7 Chapter Summary	26
1.8 Organization of the Dissertation	27
1.8.1 Chapter 1: Introduction, Motivation, Background and Significance	27

1.8.2	Chapter 2: Development of a Prototype for Proof of Concept and Feasibility.....	27
1.8.3	Chapter 3: Development and Preliminary Testing of the Exo-Skeletal Assistive Robotic Arm (eSARA)	28
1.8.4	Chapter 4: Human Machine Interface (HMI) and Evaluation of the Exo-Skeletal Assistive Robotic Arm (eSARA).....	28
1.8.5	Chapter 5: Discussion, Conclusion, and Future Work.....	28
Chapter 2 : Voice-Activated Lightweight Reacher to Assist with.....		30
Upper Extremity Movement Limitations: A Case Study.....		30
2.1	Introduction.....	30
2.2	Development of Simple Assistive Reacher Arm (SARA) Platform.....	30
2.3	System Hardware	32
2.4	System Firmware and Electronics	33
2.5	Preparatory Assessment of the SCI Participant	35
2.6	EXPERIMENT 1: Case Study: Planar and 3D Movement by a Person with Spinal Cord Injury.....	37
2.6.1	Methods.....	37
2.6.2	Protocol.....	38
2.6.3	Results.....	41
2.7	EXPERIMENT 2	41
2.7.1	Methods.....	41
2.7.2	Protocol.....	43
2.7.3	Data Analysis	45
2.7.4	Results.....	45
2.8	Discussion and Conclusion.....	48
Conclusion:		50

Chapter 3 : Development of a Multi Modal, Exo-Skeletal Assistive Robotic Arm.....	51
3.1 Introduction and Motivation	51
3.1.1 Classification of Modes of Control.....	52
3.2 Methods for the Development of the Exo-Skeletal Assistive Robotic Arm (eSARA).....	53
3.2.1 System Hardware	56
3.2.2 System Architecture.....	68
3.2.3 System Software	78
3.2.4 Electrical Design.....	83
3.2.5 Preliminary Testing of the Exo-Skeletal Assistive Robotic Arm (eSARA) Platform.....	90
3.3 Discussion and Conclusion.....	100
Chapter 4 : Evaluation of Control Modes	103
4.1 Introduction and Motivation	103
4.2 Human Machine Interface (HMI) Structure and Process	104
4.3 Test-Bench for Human Machine Interface (HMI)	106
4.4 National Aeronautics and Space Administration (NASA) Task Load Index (TLX).....	107
4.4.1 Participants and Inclusion / Exclusion Criterion	108
4.5 EXPERIMENT 1: Fine Movement Experiment.....	109
4.5.1 Methods.....	109
4.5.2 Data Analysis	112
4.5.3 Results.....	114
4.5.4 Summary.....	136
4.6 EXPERIMENT 2: Gross Movement Experiment.....	137
4.6.1 Methods.....	137
4.6.2 Data Analysis	140

4.6.3	Results.....	142
4.6.4	Summary.....	163
4.7	NASA TLX Results.....	163
4.7.1	Healthy Participants.....	163
4.7.2	Healthy Restricted (Occupational Therapy Students) Participants.....	164
4.7.3	NASA TLX Result Summary.....	164
4.8	Modality Rating.....	165
4.9	Discussion and Conclusion.....	166
Chapter 5 : Discussion, Conclusion, and Future Work.....		169
	Summary:.....	169
5.1	Discussion and Conclusion.....	170
5.1.1	Modality Selection for the SCI Injury Level.....	172
5.1.2	Modality Match Methodology.....	173
5.2	Future Work.....	174
5.2.1	Device Upgrades.....	174
References.....		181
Abstract.....		197
Autobiographical Statement.....		200

LIST OF TABLES

Table 1: Summary of physical limitations and residual functionality of complete and	11
Table 2: ICF Structure.	15
Table 3: Power consumption of the device.	35
Table 4: MANOVA results for Experiment 2 based on estimated marginal means	47
Table 5: Available features for the L-16 actuators [96]	59
Table 6: Summary of the Arduino Duemilanove microcontroller board.	62
Table 7: Trigger and command words used in the voice control modality.	70
Table 8: Summary of the maximum force at the end effector resulting from the change in the	96
Table 9: Current consumption and battery life for all the three modalities and lift assist.	99
Table 10: Estimated marginal mean of time (minutes) values of the levels	115
Table 11: ANOVA analysis for the fine movement experiment of healthy	115
Table 12: Estimated marginal mean of time (minutes) values	116
Table 13: ANOVA results for the fine movement experiment with healthy	117
Table 14: Estimated marginal mean of time (minutes) values	118
Table 15: ANOVA results for the fine movement experiment of healthy	118
Table 16: Estimated marginal mean of time (minutes) values	124
Table 17: ANOVA results for fine movement experiment of occupational therapy	124
Table 18: Estimated marginal mean of time (minutes) values	125
Table 19: ANOVA results for fine movement experiment of occupational therapy	126
Table 20: Estimated marginal mean of time (minutes) values	127
Table 21: ANOVA results for fine movement experiment of occupational therapy	128
Table 22: Estimated marginal mean of time (minutes) values ts only	143
Table 23: ANOVA results for the gross movement experiment with healthy participants	144

Table 24: Estimated marginal mean of time (minutes) values	145
Table 25: ANOVA results for the gross movement experiment with healthy	146
Table 26: Estimated marginal mean of time (minutes) values	147
Table 27: ANOVA results for the gross movement experiment with healthy	147
Table 28: Estimated marginal mean of time (minutes) values	152
Table 29: ANOVA results for the gross movement experiment	152
Table 30: Estimated marginal mean of time (minutes) values	153
Table 31: ANOVA results for the gross movement experiment	154
Table 32: Estimated marginal mean of time (minutes) values	155
Table 33: ANOVA results for the gross movement	156
Table 34: Average of the NASA TLX results for the healthy participants	164
Table 35: Average of the NASA TLX results for the occupational therapy	164
Table 36: Most challenging level	165
Table 37: Control modalities ranked by the participants.	165

LIST OF FIGURES

Figure 1: Specific research objectives summarized	5
Figure 2: Shows the modality selection method fitting the user with upper extremity	7
Figure 3: Anatomy of the spinal cord showing the corresponding body parts [21].	9
Figure 4: ICF structure.	14
Figure 5: Framework of International Classification	16
Figure 6: Evolution of reachers from the basic model in 1918	17
Figure 7: Individual using assistive robotic arm mounted on a wheelchair [29-30].	18
Figure 8: Different iterations of the wheelchair robotic arm [31-32].	18
Figure 9: The extendable wheelchair robotic arm designed for opening door knobs [33].	19
Figure 10: The figure on the left shows the entire mobile manipulator	20
Figure 11: This figure shows the object placement experiment	20
Figure 12: Left: Four of the six doors that the robot successfully opened.	21
Figure 13: The Dusty robot on the left and the remote on the right	22
Figure 14: The Figure showing various body bots [7, 71-76, 82].	23
Figure 15: Variations of the modern exo-skeletal robotic arms [50-55].	24
Figure 16: Proposed model and the built robotic arm with 7 degrees of freedom [89, 90].	25
Figure 17: i-limb ultra-prosthetic hand by touch bionics [1].	25
Figure 18: The Luke Arm.	26
Figure 19: The Smart Assistive Reacher Arm	31
Figure 20: The L-12 linear actuator [96] (left), VR stamp module	32
Figure 21: The driver circuit for the reacher arm (left) and the block diagram	33
Figure 22: This Figure shows the Pilot Test being conducted	35
Figure 23: Polaris and the reflector unit	36

Figure 24: Participant's progress throughout the experiment	39
Figure 25: This figure shows the participant moving the object	40
Figure 26: (a) Cell phone falls	40
Figure 27: Left: Color coded test bench with three levels.....	42
Figure 28: Test bench levels and distance from the test bench.....	43
Figure 29: Start and end points of the experiment.	44
Figure 30: Errors within the test bench are shown (a-c).....	45
Figure 31: This figure shows participants performance at different points.....	46
Figure 32: Estimated mean values of the levels (in minutes)	46
Figure 33: Individual participant performance time in minutes.....	47
Figure 34: Box plot and average of the healthy participants'	48
Figure 35: Multi-modal control and end effector units.....	53
Figure 36: Final assembly of the Exo-Skeletal Assistive Robotic Arm (eSARA).....	54
Figure 37: Evolution of eSARA	55
Figure 38: (a) Zeiss S21 [98] stand used to support eSARA's weight	56
Figure 39: Firgelli L16-P actuators. The actuator on the top (50mm) was used.....	57
Figure 40: L16-P actuator load vs. force (left) and current vs. force plots (right) [96].....	58
Figure 41: The innovator X® elbow brace by Össur [99].....	59
Figure 42: Claw kit and 2-wire motor 393 from VEX Robotics [100].	60
Figure 43: Machined parts of eSARA a) Top of the arm used to hold the extension rail,	61
Figure 44: Arduino Duemilanove board with Atmel Atmega 328 chip [101, 102].....	64
Figure 45: Examples of the color coded push buttons used in the device.....	64
Figure 46: Slider used to control extension and grasping.....	65
Figure 47: VRbot by Veear [103].....	65
Figure 48: The FSR sensor by Interlink Electronics [104].....	66

Figure 49: Lithium polymer battery: 11.1V, 55.5Wh with 5000mAh.	66
Figure 50: Safety and power switches	67
Figure 51: Hierarchy of the system firmware.	68
Figure 52: Flow chart of the control mode and lift assist processes.	69
Figure 53: Voice control mode showing VRbot and the Graphic User Interface	71
Figure 54: Button Control mode.	72
Figure 55: Slider Control Mode.	72
Figure 56: The PID controller concept (left) and the PID algorithm (right).	74
Figure 57: PID Tuning	74
Figure 58: The calibrated BA (left) and the calibrated TA using BA as the primary actuator.	75
Figure 59: Distance travelled by biceps actuator vs. triceps actuator	76
Figure 60: Actual BA vs. TA potentiometer position feedback from the actuator counts	77
Figure 61: Atmega328 pin mapping to Arduino.	78
Figure 62: Handshake protocol between Arduino and VRbot.	80
Figure 63: Allocated command words for the VRbot.	81
Figure 64: (a) Equations used to define variables in the code	83
Figure 65: Full circuit diagram interfacing all the control modes for extension and grasping.	84
Figure 66: Atmega328 micro controller used for the button modality.	85
Figure 67: Atmega328 micro controller used for the slider modality.	85
Figure 68: Atmega328 micro controller used for the voice modality.	86
Figure 69: L298P motor-driver controlling the extension and grasping motors.	86
Figure 70: Modality control switch.	86
Figure 71: Full circuit diagram interfacing both of the pressure sensors for the lift assist feature.	87
Figure 72: Atmega328 micro controller used for the lift assist pressure sensors.	88
Figure 73: L298P motor-driver controlling the first set of biceps and triceps actuators.	89

Figure 74: L298P motor-driver controlling the second set of biceps and triceps actuators.....	89
Figure 75: Voltage regulation circuit.	89
Figure 76: This Figure shows stages of the Printed Circuit Board (PCB) for the	90
Figure 77: Figure showing eSARA with minimum and maximum extension.	91
Figure 78: Figure showing eSARA minimum and maximum lift assist angles	93
Figure 79: Side view of eSARA showing three flex angles for force calculations.	94
Figure 80: Calculations based on the measurements from Computer Aided Design	95
Figure 81: 17.85lb weight start and end point when moved with the eSARA platform.....	97
Figure 82: Current measuring experiment showing all the three modes, button, slider and voice... 98	98
Figure 83: The final assembly of the Exo-Skeletal Assistive Robotic Arm.....	104
Figure 84: HMI structure and process flow.	105
Figure 85: (a) Color coded Test bench with three levels to be used for the experiment.....	106
Figure 86: Structure of the NASA TLX for the fine movement and gross movement	108
Figure 87: (a) Test-bench (b) Color-coded pegs for the fine movement experiment.	109
Figure 88: Start and end points of the fine movement experiment.	110
Figure 89: (a-d) Errors counted within the testbench that must be rectified (e) error outside	111
Figure 90: One mode, all levels for fine movement.....	113
Figure 91: All modes, one level for fine movement.....	113
Figure 92: Time performance of healthy participants during the fine movement.....	114
Figure 93: Box and whisker plot of the time performance of healthy	116
Figure 94: Box and whisker plot of the time performance of healthy.....	117
Figure 95: Individual time performance of healthy participants	119
Figure 96: Individual time performance of healthy participants	120
Figure 97: Individual time performance of healthy participants	120
Figure 98: Individual time performance of healthy participant.....	121

Figure 99: Individual time performance of healthy participants (slider)	121
Figure 100: Individual time performance of healthy participants (voice)	122
Figure 101: Box and whisker plot of the time performance	123
Figure 102: Box and whisker plot of the time performance	125
Figure 103: Box and whisker plot of the time performance	127
Figure 104: Individual time performances of the occupational therapy participants	128
Figure 105: Individual time performances of the occupational therapy participants	129
Figure 106: Individual time performances of the occupational therapy participants	130
Figure 107: Individual time performance of the occupational therapy participants	130
Figure 108: Individual time performance of the occupational therapy participants	131
Figure 109: Individual time performance of the occupational therapy participants	131
Figure 110: Individual time performances of all participants	132
Figure 111: Individual time performances of all participants	133
Figure 112: Individual time performances of all participants	133
Figure 113: Individual time performances of all participants	134
Figure 114: Individual time performances of all participants	135
Figure 115: Individual time performances of all participants	135
Figure 116: (a) The test-bench (b) Color-coded bottles of various weights.	137
Figure 117: Start and end points for the gross movement experiment.	138
Figure 118: Bottles are marked with a red rectangle to show the additional support	139
Figure 119: (a) and (b) Examples of errors for the gross movement	140
Figure 120: One Mode all level for gross movement	141
Figure 121: All Modes One level for gross movement	142
Figure 122: Box and whisker plot of the time performance of healthy participants	143
Figure 123: Box and whisker plot of the time performance of healthy	145

Figure 124: Box and whisker plot of the time performance of healthy participants during the gross movement experiment using the voice modality on all three height levels.	146
Figure 125: Individual time performance of healthy participants	148
Figure 126: Individual time performance of healthy participants	148
Figure 127: Individual time performance of healthy participants	149
Figure 128: Individual time performance of healthy participants	149
Figure 129: Individual time performance of healthy participants	150
Figure 130: Individual time performance of healthy participants	150
Figure 131: Box and whisker plot of the time performance of occupational therapy	151
Figure 132: Box and whisker plot of the time performance of the occupational therapy	153
Figure 133: Box and whisker plot of the time performance of occupational therapy	155
Figure 134: Individual time performance of occupational therapy participants	156
Figure 135: Individual time performance of occupational therapy participants	157
Figure 136: Individual time performance of occupational therapy participants	157
Figure 137: Individual time performance of the occupational therapy participants	158
Figure 138: Individual time performance of the occupational therapy participants	158
Figure 139: Individual time performance of the occupational therapy participants	159
Figure 140: Individual time performance of all participants, and their average	160
Figure 141: Individual time performance of all participants and their average	160
Figure 142: Individual time performance of all participants and their average	161
Figure 143: Individual time performance of all participants and their average	161
Figure 144: Individual time performance of all participants and their average	162
Figure 145: Individual time performance of all participants and their average	162
Figure 146: Methodology for modality selection for SCI participants.	173

Chapter 1: Introduction Background, Motivation, and Significance

In everyday life, human beings often perform many simple tasks such as reaching over the edge of the table to grasp a piece of paper or bending down to pick up a fallen pen. Such simple tasks become a challenge for a person who has physical limitations. These physical deficiencies may be the result of a birth defect or a traumatic incident. In either case, the person becomes less self-sufficient. In the case of severe spinal injuries, some people are forced to accept and adapt a lifestyle they never thought existed. To overcome some of these obstacles, engineers have designed various assistive robotics over the years. These assistive devices come in a vast variety, ranging from simple reachers to smart prosthetic limbs with brain control capabilities [1] with the goal of giving some level of autonomy back to the physically challenged person.

This research was conducted to facilitate improved autonomy of a targeted group of individuals with spinal cord injury (SCI) at levels C5 to C7 relating to upper extremity injuries. The specific population was selected as the existing technology was either too expensive, too bulky or was unable to address their needs in regards to upper extremity mobility. The residual functionality in the limbs and the lack of motor ability of the wrist and fingers makes it difficult for the existing technology to be customized for specific injury level. The unavailability of existing devices to provide multimodal controls also limits support to the SCI individuals.

The motivation of this research was to provide multimodal control of an assistive device based on a range of basic human movements that were possible by the population under consideration (button pushing, lever sliding, and speech). The main idea was to create an evaluation methodology based on a user platform with multiple modes of control. The controls would be operational on the range of movement of the SCI participants. The multiple modality control would allow customization of the platform based on an individual's level of SCI.

Creating devices that allow multiple modes of operation would immensely improve the customizability of the device and influence the quality of life for the group under discussion. The techniques described herein may also prove useful for all individuals with temporary or permanent upper extremity movement restrictions.

1.1 Aims and Scopes of Research

Given that spinal cord injury results in a wide variety of deficits, even for the small range of levels (C5-C7) targeted here, a one-size-fits-all approach to assistive devices was not optimal. Furthermore, a custom solution for all individuals was impractical. The goal of this research was to understand the capabilities of C5-C7 injured individuals and develop and evaluate modes of control and methods of evaluation for a reacher/grasper prototype that would allow for a flexible interface. The focus of the research was to study the human interaction with the device when performing reaching and grasping tasks and to develop a testing methodology that would allow for practical levels of customization.

A series of experiments was conducted to test the Human Machine Interface (HMI) with generalized control modes to determine what mode best fits the level of injury for the participating SCI individual. The key testing method compared an SCI participant performance with the average of healthy individuals using the same device. If the modality could bring the SCI individual to the level of performance of the healthy individual using the same control scheme, it would be considered a successful implementation. It was hypothesized that given a range of spinal cord injuries a clear delineation of classes of modes of control and a method of evaluation of these modes will result in a usable interface.

To achieve this goal, the following hypotheses were proposed:

- (1) Reach and grasp tasks with designed platforms with multiple modes of control and useful features would be feasible to be used by an SCI participant.
 - a. Control modes can be matched to the functionality of SCI individuals.
 - b. Utilizing reach extension would be beneficial and feasible.
 - c. Lift assist would prove vital when lifting heavy objects.
 - d. Signs or reports of fatigue or distress (recorded during the experiments by verbally asking the participants) would be absent.
- (2) A methodology to evaluate multiple modes of operating the device can be created.
 - a. Multi-modal control would provide device customization.
 - b. Movement time and errors of the SCI participant, within the limits set by a healthy adult group using the same device for both ‘fine movement’ and ‘gross movement’ experiments, is a key metric of success.

1.2 Specific Research Objectives

To achieve the above hypotheses, the following specific research objectives were developed:

- (1) Develop a baseline platform of a light weight, voice activated, Simple Assistive Reacher Arm (SARA) and compare the performance of the SCI participant to normal individuals using the same device.

The first prototype was developed with a fixed reaching length and the most basic modality for use – voice activation. The reacher was then evaluated with a case study involving an SCI participant’s time performance to that of the healthy participant’s time performance. The aim was to simply test the most basic mode of operation and compare the result with healthy individuals to create a baseline approach for comparison.

(2) Create a methodology for testing and evaluation of multi-modes of control. This objective required expanding the existing platform and development of an Exo-Skeletal Assistive Robotic Arm (eSARA) with multiple modes of control that could be customized and optimized for use with a range of capabilities. This platform also consisted of an added feature called smart lift assist mechanism, to enable SCI participants to lift daily life objects with ease.

As more features were added, more dexterity and modes of control were needed. A second prototype was then designed with additional features such as extendable reaching length, lift assist, and most critically, different modes of controls for SCI individuals with upper extremity limitations. The control modes used were categorized as (1) ballistic modality with no extremity movement required (voice activated) (2) ballistic control mode (like pushing) that required minimal movement of the extremities and (3) continuous control mode (like sliding a joystick) that may require major (continuous) movement of the extremity.

(3) The third research objective was to conduct an extensive Human Machine Interface (HMI) study to evaluate all the control modes and the lift assist of the device. This HMI study was conducted to evaluate the level of control most feasible for the SCI participant based on the participant's level of injury.

The Figure 1 below summarizes these research objectives.

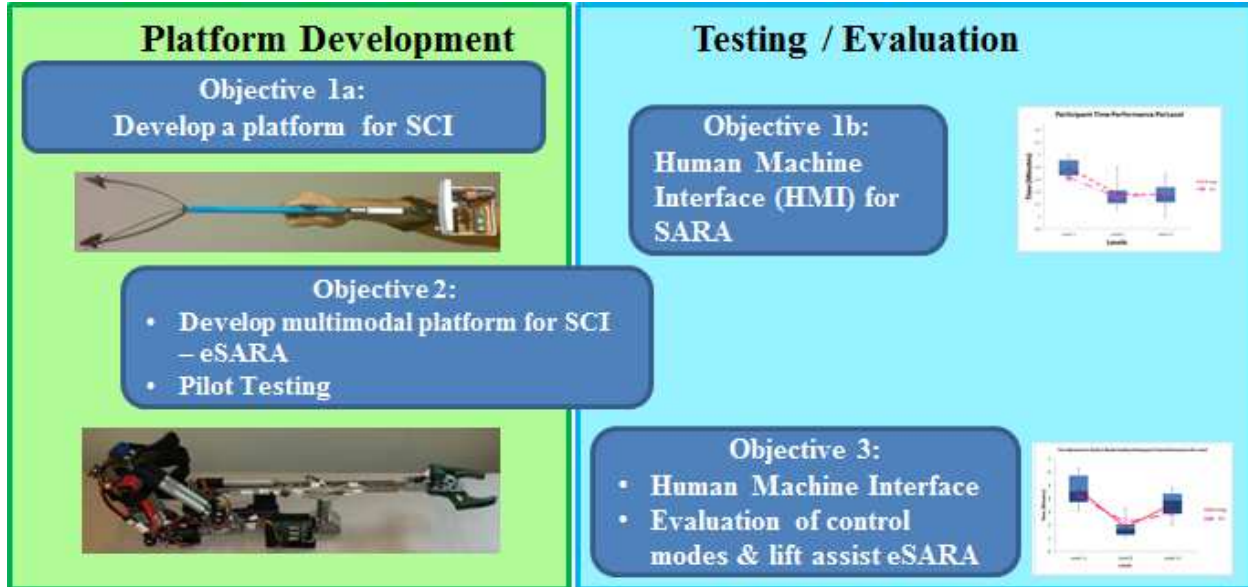


Figure 1: Specific research objectives summarized [Spinal Cord Injury individuals (SCI), Simple Assistive Reacher Arm (SARA), Exo-Skeletal Robotic Arm (eSARA)].

1.3 Novelty and Significance of the Research

This research was conducted to design and evaluate a reaching arm with different selectable modes of control and lift assist features. It has always been an issue to customize an assistive device for multiple users within a targeted population [2-6]. The issue of technology customization can be driven by the patients' physical differences (e.g. weight, height, or level of strength) or differences in the severity of the injury. One of the common issues when customizing assistive technology is the lack of flexibility to control the device. The majority of the assistive devices have one unique way, or mode, of controlling the device, limiting the usability of the device to a small population.

The modes considered for this research were categorized as ballistic control modes and continuous control modes for the user interface modalities. Both modes, ballistic and continuous, were studied with SCI individuals to determine suitability for a specific level of injury.

This research also focuses on devising a methodology to fit a modality to a specific SCI individual. The three modalities chosen for this research were based on simplistic and basic human movement characteristics. The modes of control for this research were:

1. Voice control mode, basic speech requiring very little or no physical involvement. This mode was categorized as ballistic modality with no extremity movement required.
2. Button control mode, basic pressing action repeatedly performed by SCI individuals with precision and very little effort. This mode was categorized as ballistic control mode that required minimal movement of the upper extremities.
3. Slider control mode, basic pushing or pulling repeatedly performed by SCI individuals with precision and very little effort. This mode was categorized as continuous control mode requiring the major (continuous) movement of the upper extremities.

To evaluate these modes two different test platforms were created. Both these platforms shared a test-bench that was also specifically designed to evaluate the control modes based on fine and gross movement. These platforms are discussed in detail in chapters 2 and 3, respectively. Evaluation of ballistic versus continuous mode of control and the Human Machine Interface (HMI) is discussed thoroughly in chapter 4.

Currently available reachers are mostly mechanical, requiring motor skills that preclude many users. Furthermore, use of voice control is generally lacking in the majority of these assistive reaching devices. Therefore, a voice interface is well-suited for users that have very limited extremity control.

Figure 2 summarizes the entire aim of the thesis. Briefly, to fit a user with upper extremity limitation to a device that can be customized for the given modes and can be used by all. The figure shows that each modality, ballistic (no/minor extremity movement) or continuous, were

given for the device. Then with the modality selection methodology developed in this research the outcome was targeted to the specific level of spinal cord injury (C5-C7).

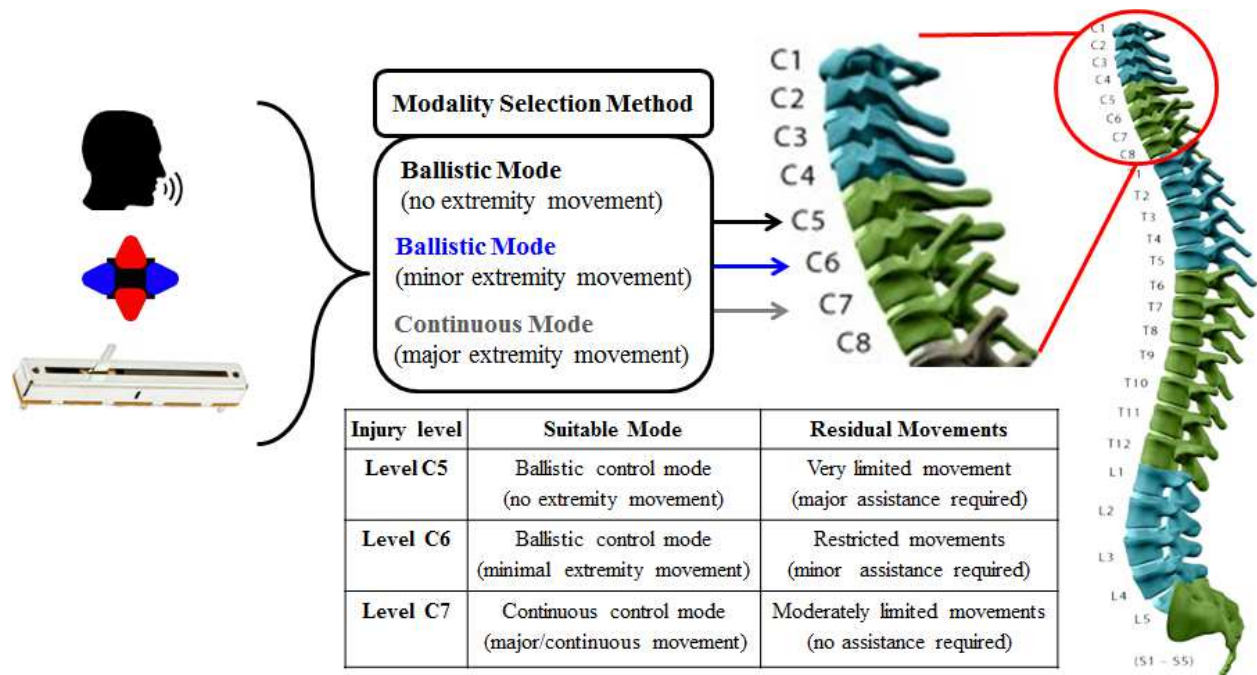


Figure 2: Shows the modality selection method fitting the user with upper extremity disability with a modality best suited for their injury.

The background and significance of this research is discussed in the next section (1.4). This section provides background on the spinal cord injury used as the framework for the research. This section also gives a brief overview of existing assistive devices and identifies gaps in the technology for users with upper extremity disability and residual functionality.

1.4 Background and Significance

Some exoskeletal arms and body suits that are available are not only extremely expensive and bulky but also require nerve endings to be connected to the electronics [2, 7-12]. Such devices generally rely on signals produced in the nerve endings called myo-electric signals. The majority of these devices require surgical procedures for connecting the nerve endings to the device. By measuring the myo-electric signals, it is possible to provide a replacement device for

lost limbs that uses the electro-myographic activity of a contracting muscle as a control signal. These devices are most commonly used for below-elbow amputees with retained elbow function. Some leading companies, such as Touch Bionics [1, 13-20], have developed limbs that mimic human hand movements and are controlled voluntarily by the patient. Again these devices are normally designed for treating amputation-related injuries. A vast majority of the assistive technology focuses more on technological advancements for amputations and less on residual functionality assistive devices. A simple, light weight, voice activated extender/reacher has yet to be developed that enables individuals with residual functionality to accomplish simple tasks.

1.4.1 Spinal Cord Anatomy

The classification of spinal cord injury is often linked to the specific location along the spinal cord/vertebrae with each of these injury locations resulting in drastically different deficits. To control various parts of the body there are numerous nerve endings that connect to the brain. These nerves run through the body and are connected to a major structure called the spinal cord. The spinal cord can be considered a superhighway for messages between the brain and the rest of the body. The spinal cord runs through numerous linked bones that surround most of its length called vertebrae [21]. These vertebrae are divided as follows:

- 7 cervical vertebrae (located in the neck)
- 12 thoracic vertebrae (located in the trunk)
- 5 lumbar vertebrae (located in the lower back)
- 5 sacral vertebrae (located in the pelvis)
- 4 fused vertebrae that form the coccyx

31 pairs of spinal nerves connect with the spinal cord through nerve roots and travel to specific parts of the body. For example, the pair of spinal nerves connecting with the spinal cord

in the region of the C2 vertebra travels to the head and neck. Injury to this portion of the spine results in severe deficits from the head and neck all through the body. The spinal nerves attaching to the cord in the region of the L4 vertebra run to specific muscles in the legs and specific areas of skin in the calves. Hence, injury at this level relates to deficits in the legs and calves. Figure 3 illustrates where in the body the spinal cord nerves extend.

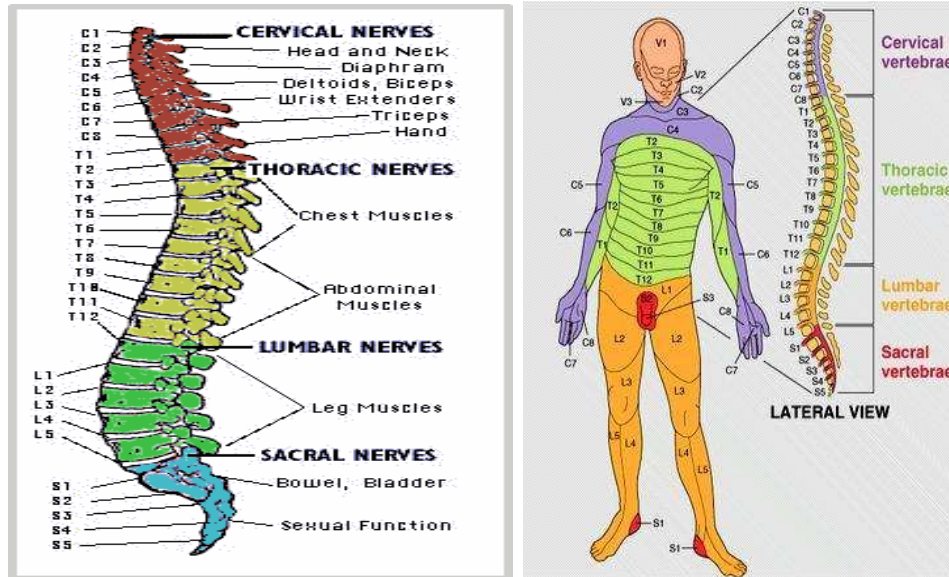


Figure 3: Anatomy of the spinal cord showing the corresponding body parts [21].

1.4.2 The Level of a Spinal Cord Injury (SCI)

The reference vertebra closest to the injury defines the level of the spinal cord injury. For example, an injury to the spinal cord at the level of the sixth cervical vertebra would be referred to as a C6 injury (“C” for cervical). An injury to the cord between the C6 and C7 vertebrae would be called a C6-7 injury. A T12 injury occurs at the level of the 12th thoracic (T) vertebra. An L3 injury occurs at the level of the third lumbar (L) vertebra [21, 22].

Spinal cord injuries alter communication between the brain and the parts of the body below the level of injury. This reduced communication or total loss of communication, to specific areas of the body can cause paralysis. The closer the injury is to the head, the greater the

area of the body affected. For example, an individual with a T10 injury (located in the lower middle back) may lose use of his legs (paraplegia) but his arms would not be affected. An individual with a C4 injury (located in the middle of the neck) may lose use of her legs and arms (referred to as quadriplegia)[23].

SCI is also classified according to the person's loss of motor and sensory function. The following are the main types of classifications:

- Quadriplegia consists of loss of movement and sensation in all four limbs. It usually occurs as a result of injury at T1 or above. Quadriplegia can affect the chest and may result in breathing aid requirements.
- Paraplegia consists of loss of movement and sensation in the lower half of the body. It usually occurs as a result of injuries at T1 or below.
- Triplegia consists of the loss of movement and sensation in one arm and both legs and usually results from incomplete SCI.

1.4.3 Physical Limitations and Residual Functionality of Incomplete and Complete Spinal Cord Injuries

Spinal injury results in either complete or incomplete loss of sensation and motor ability of the individual. Complete injuries result in total loss of sensation and function below the injury level where as incomplete injuries result in partial loss. Paraplegia and quadriplegia can be associated with either total or partial loss. An incomplete injury leaves the individual with some residual functionality below the level of the injury. For example, an individual may have weakness of the forearm but is still able to move his or her index finger. In some cases an individual may lose the ability to use muscles below the level of the injury only on one side of the body, while losing pain and temperature sensation on the other side of the body [24-28].

The International and American Spinal Injury Association (ASIA) [23, 29, 30] define an incomplete spinal cord injury as one in which the person has some spinal cord function preserved below the injury level. A complete injury results in total loss of sensation and muscle control below the level of the injury. According to ASIA, half of all spinal cord injuries result in complete spinal cord injury. These injuries do not require cutting of the cord but often result from bruising of the cord or loss of blood flow to the cord. Therefore, a complete injury does not mean that there is no hope of any improvement.

All spinal cord injury patients can improve slightly over a period of time, but only 0.9% fully recovers with the exception for the incomplete-preserved motor functions. A greater number of injuries result in quadriplegia. Chances of quadriplegia increase at age 45 and increase further after age 60 [21, 22].

1.4.4 Physical Limitations and Mobility Challenges of the C6-C7 SCI Individuals (upper extremity challenges and residual functionalities)

Table 1 compares the specific level of SCI and the resulting rehabilitation potential. Impairments and rehabilitation potential can vary depending on the type and severity of SCI. The table focuses only on upper extremity injuries (levels C5 to C7).

Injury Level	Result of Injury	Residual Functionality
Level C5	Quadriplegia that permits the right shoulder and elbow functionalities	Assistive devices were needed to help while eating. Self-assisting devices may be used. No ventilator needed
Level C6	Quadriplegia that permits shoulder, elbow and some wrist movements	Ability to propel wheelchair. No assistance required for feeding, groom, and dress self;
Level C7	Quadriplegia resulting in restricted shoulder, elbow, wrist, and hand functionalities	Ability to propel wheelchair, driving with assistance can be achieved

Table 1: Summary of physical limitations and residual functionality of complete and incomplete spinal cord injuries.

1.4.5 SCI Statistics

The majority of patients with injuries above the C3 level die before receiving medical treatment and those who survive are dependent on mechanical respirators to breathe. Similarly, fifty percent of all SCI cases are associated with other injuries as well [31, 32]. The following list provides spinal cord injury statistics showing the need for assistive technology.

- 270,000 Americans are currently living with an SCI.
- 52% of spinal cord injured individuals are considered paraplegic and 47% quadriplegic.
- Approximately 11,000 new injuries occur each year.
- 82% of SCI patients are male.
- 56% of injuries occur between the ages of 16 and 30.
- The average age at the time of injury is 31.
- The most rapidly increasing cause of injuries is violence; vehicular accident injuries are decreasing in number.
- 89% of all SCI individuals are discharged from hospitals to a private home; 4.3% are discharged to nursing homes.
- Only 52% of SCI individuals are covered by private health insurance at the time of injury.

The above statistics have increased the demand for assistive robotics to be developed to help improve the lives of the patients suffering from such injuries. Improvements have been made in order to resolve simple tasks such as moving objects from one position to another. Various machines, gadgets, and robotic devices have been developed to assist these individuals [33, 34]. Wheelchairs with motors have been developed so that SCI individuals are less dependent on

others and can manually maneuver themselves with ease. Certain equipment is also available that allows the physically challenged individuals to utilize computers without much trouble.

1.5 International Classification of Functioning, Disability and Health (ICF) Framework to Establish with Research

ICF provides a framework and classifications for rehabilitation purposes designed to serve various disciplines and different sectors. Its specific aims are summarized as follows:

- “To provide a scientific basis for understanding and studying health and health-related states, outcomes and determinants;
- To establish a common language for describing health and health-related states in order to improve communication between different users, such as health care workers, researchers, policy-makers and the public, including people with disabilities;
- To permit comparison of data across countries, health care disciplines, services and time;
- To provide a systematic coding scheme for health information systems” [35-39].

These aims are interrelated in order to construct a meaningful and practical system that can be used by various consumers for health policy, quality assurance, and outcome evaluation in different cultures.

ICF has been used for various purposes including:

- “As a statistical tool – in the collection and recording of data (e.g. in population studies and surveys or in management information systems);
- As a research tool – to measure outcomes, quality of life or environmental factors;
- As a clinical tool – in needs assessment, matching treatments with specific conditions, vocational assessment, rehabilitation and outcome evaluation;

- As a social policy tool – in social security planning, compensation systems and policy design and implementation;
- As an educational tool – in curriculum design and to raise awareness and undertake social action” [35-39].

1.5.1 ICF Structure

ICF has been accepted as one of the United Nations social classifications and was referred to in and incorporates The Standard Rules on the Equalization of Opportunities for Persons with Disabilities.

ICF can apply not only to people with disabilities but also people without disabilities. The health and health-related states associated with all health conditions can be described using ICF. In other words, ICF has universal application. Figure 4 and Table 2 outline the structure of the ICF.

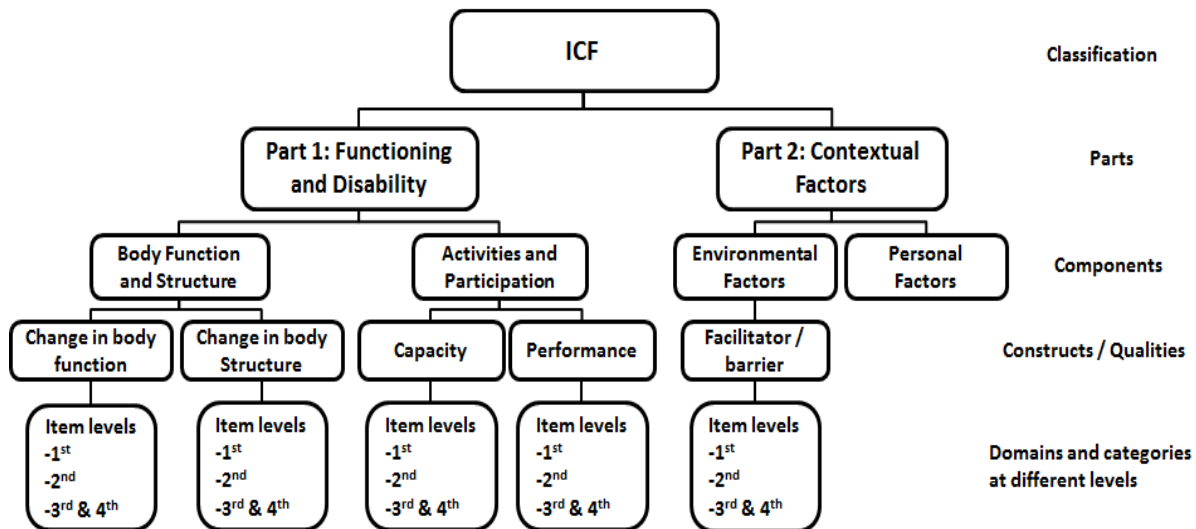


Figure 4: ICF structure.

The model in the figure above can be represented in the following table:

	Part 1: Functioning and Disability		Part 2: Contextual Factors	
Components	Body Functions and Structures	Activities and Participation	Environmental Factors	Personal Factors
Domains	Body Functions Body Structures	Life areas (tasks, actions)	External influences on functioning and disability	Internal influences on functioning and disability
Constructs	Changing in body functions (physiological) Change in body structures (anatomical)	Capacity Executing tasks in standard environment Performance executing tasks in the current environment	Facilitating or hindering impact of features of physical, social and attitudinal world	Impact of attributes of the person
Positive aspect	Functional and structural integrity	Activities Participation	Facilitators	Not applicable
	Functioning			
Negative aspect	Impairment	Activity limitation Participation restriction	Barriers / hindrances	Not applicable
	Disability			

Table 2: ICF Structure.

The ICF model can be used as a problem solving tool in occupational therapy and rehabilitation [37, 40]. The ICF can be used as a tool to evaluate the role of environment [36]. A further simplified model can be used for less complicated problem solving following the ICF framework [38, 39]. Figure 5 shows an individual's functioning in a specific domain as an interaction or complex relationship between the health condition and contextual factors (e.g. environmental and personal factors). There is a dynamic interaction among these entities where interventions in one entity have the potential to modify one or more of the others. These interactions are specific and not always in a predictable one-to-one relationship. The interaction works in two directions where the presence of disability may even modify the health condition

itself. To infer a limitation in capacity from one or more impairments, or a restriction of performance from one or more limitations, may often seem reasonable [41]. It is important, however, to collect data on these constructs independently and thereafter explore associations and causal links between them. If the full health experience is to be described, all components should be considered.

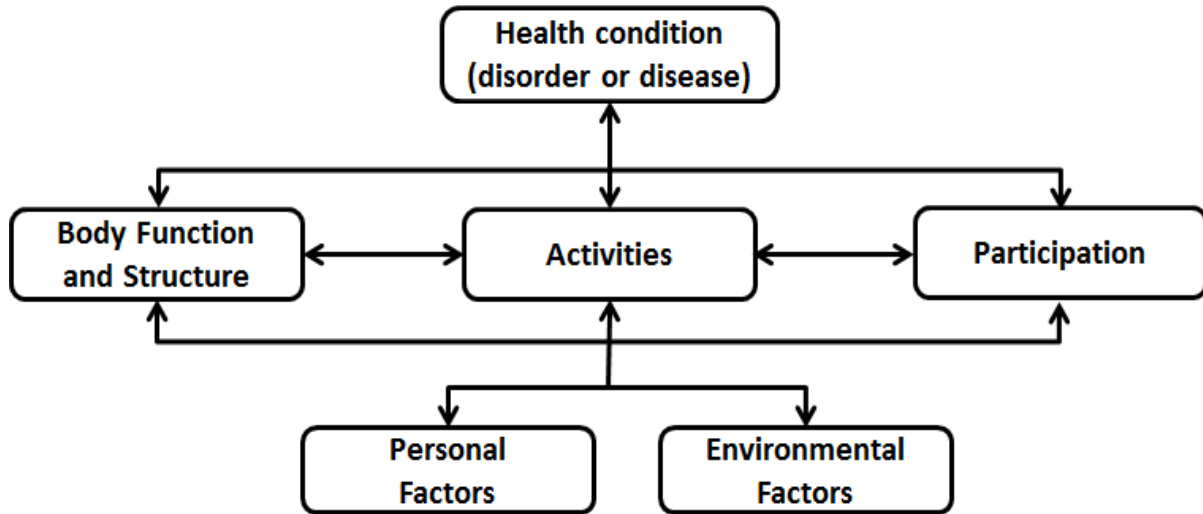


Figure 5: Framework of International Classification of Functioning, Disability and Health by the World Health Organization [35, 41].

1.6 Overview of Current Assistive Devices and their Limitations

Over the past several years there have been a lot of different assistive devices that have helped a number of spinal cord injured patients. These assistive devices range in complexity from a simple reacher to a fully functional robotic arm that works on the residual functionality present in an amputated arm. Other forms of assistive robots come as wheelchair extensions often designed as robotic arms that protrude out of the wheelchair and assist in different tasks [2, 3]. This section discusses the assistive devices focusing on their usability for SCI patients with

severe upper extremity disability. The devices were also assessed based on their appearance as user friendly and ability to draw less or no attention to the disability.

1.6.1 Types and Classifications of Assistive Devices

1.6.1.1 Assistive Reachers

Current reaching devices are not that different from the ones invented in the early 1900s (see Figure 6) [42-44]. These devices were designed to grasp an object and move it from one place to another, similar to the current reachers [4]. Some extendable reachers were developed based on the telescopic mechanism [45]. Besides assisting in self-gripping of an object, available reachers have also been designed for a variety of other purposes for assisting the physically challenged including functioning as a dressing aid [46] or walking assistance [47], whereas others provide assistance by self-gripping an object [48]. Some reachers are able to pick up tools with variable positions and take into account limitations of wrist or finger functionality [49-53].



Figure 6: Evolution of reachers from the basic model in 1918 to the modern day top to bottom [42-44, 47, 49].

1.6.1.2 Wheelchair Robotics

Wheelchair robotics have evolved to provide a friendly user interface to control the assistive robots [54, 55]. The robot was mounted on the left side of the wheelchair and the

controls on the right side for a right handed individual. The figure below illustrates the complexity of the robotics but also the ease of use.



Figure 7: Individual using assistive robotic arm mounted on a wheelchair [29-30].

The Weston wheelchair mounted with an assistive robot [56-62] was a typical example of wheelchair robotics. Using a normal wheelchair, a robotic arm is added behind the right shoulder and comes forward to cover a large radius towards the right. The following figures illustrate design similarities in the different iterations of the wheelchair robotic arm.



Figure 8: Different iterations of the wheelchair robotic arm [31-32].

Another example was an under actuated gripper to unlatch door knobs and handles [63]. The basic purpose of this assistive robotic design was to extend, grasp, and twist open door knobs.

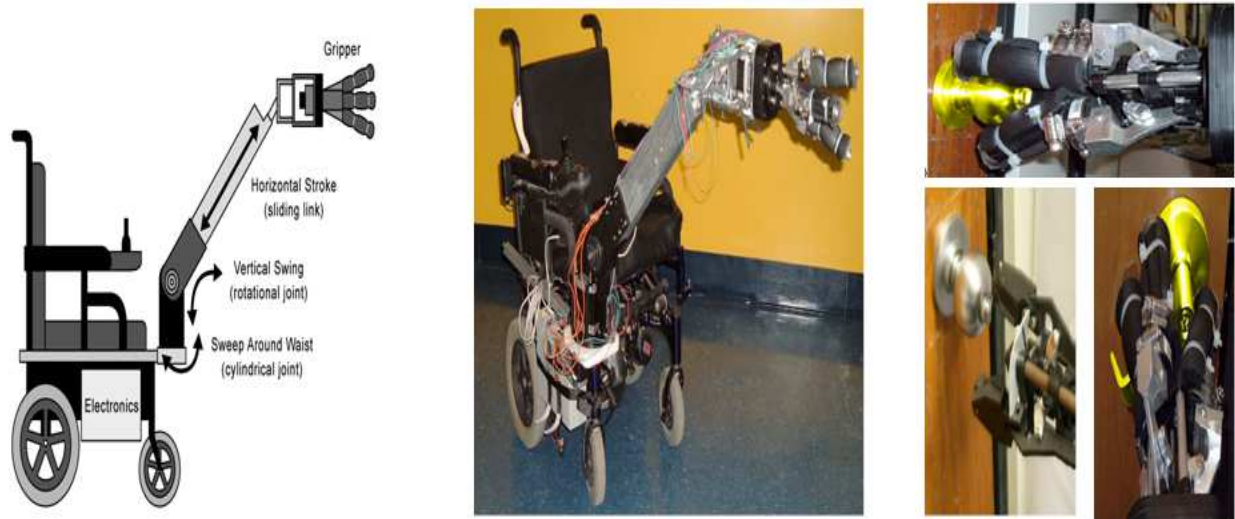


Figure 9: The extendable wheelchair robotic arm designed for opening door knobs [33].

Similarly, the wheelchair mounted robotic arm can be controlled with a virtual interface [64]. This robot provides methods for independent manipulation of objects in unstructured environments utilizing the wheelchair arm. The camera addresses the appropriateness of vision-based input and the complexity of the hierarchy, comparing the human visual to a menu based system. Rigorous calculations and tasks were taken into considerations for a simple human judgment call [65]. For example, to pick up an object from a table an individual with SCI would prefer his vision abilities to rely on rather than picking from a menu.

1.6.1.3 Mobile Robots (EL-E Robotic Arm)

Another assistive robot was developed to perform tasks based on a command from a laser pointer. The tasks included grasping a pen from one end of the room and bringing it to the user at the other end of the room. The robot was controlled by using a clickable device with a laser

mounted at one end. Pointing the laser on the object triggers the robot to move towards the object grasps the object and clicking on the control device brings the robot to the desired position. The EL-E assistive mobile manipulator was developed to perform such functions [5, 6]. In addition the robot can be controlled with a touch screen display.

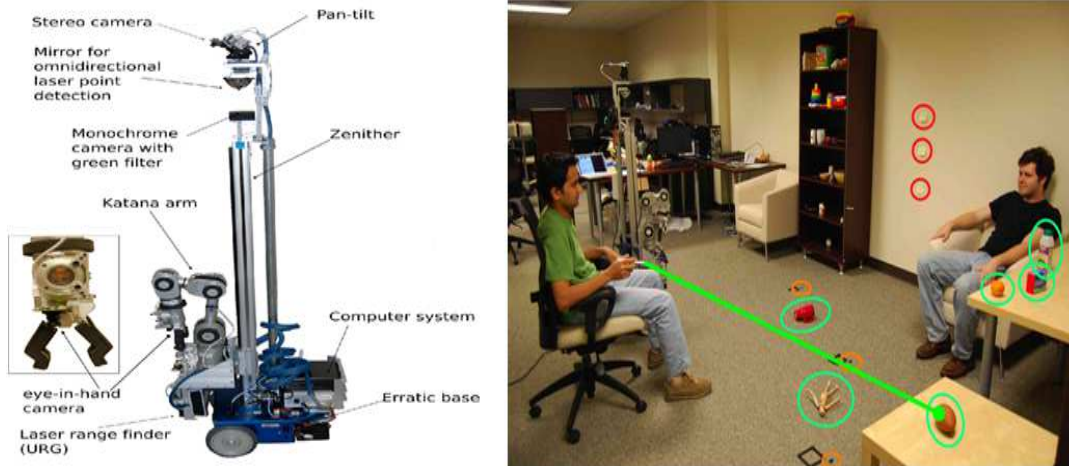


Figure 10: The figure on the left shows the entire mobile manipulator with integrated interface system. The figure on the right shows the starting configuration, users can select object buttons on the ground and table to be picked up by the robot [5, 6].

The EL-E was also used to fetch objects from a flat surface autonomously [66, 67]. The robot moves to a flat surface, calculates the depth differences, subtracts the background and then picks up the desired object and takes it to the user. The following figure illustrates the motions.



Figure 11: This figure shows the object placement experiment. The first image shows the three objects (TV remote, toothbrush and bowl) and the desired placement points (red circles). The second image shows the robot grasping the toothbrush, and the remaining three images show the robot placing the toothbrush, the TV remote, and the bowl [37-38].

The EL-E robot was also used to open doors [68, 69], a similar approach to that of the wheelchair robotic arm designed to open doors [63]. At first the EL-E robot was used to open doors with the laser pointer. Then a dog was used as a test participant in comparison to EL-E assistive robot to find the accuracy.



Figure 12: Left: Four of the six doors that the robot successfully opened and traversed. The first row shows the robot twisting the door handles and the second row shows the robot after it has reversed the doorway [68]. Right: A service dog opens a door using a bandanna tied to the door handle and the assistive robot opens a door in an analogous manner [69].

All the assistive robotics that have been discussed so far were either add on devices or an individual robot that was larger than the wheelchair in height. These robotic devices may be suitable for specified locations. However, wheelchair robotic arms have limited mobility and in some circumstances it is extremely difficult to maneuver around with assistive transportation systems. Due to the fixed dimensions of a standard wheelchair, addition of an overhanging third arm makes device usability extremely complex for SCI individuals.

Another problem with these systems was a lack of user friendliness and no attempt to fit the technology with the deficit observed. In other words, the limitation was a lack of the flexibility needed in the interface. Just to get in and out of a wheelchair can be a daily challenge for individuals with spinal cord injuries (SCI). To add an additional arm that comes out of the wheelchair and is always present adds an additional restriction to their already limited mobility.

1.6.1.4 Dusty, An Assistive Mobile

Dusty is an assistive mobile manipulator that retrieves dropped objects for people with motor impairments. It is a remote controlled assistive device developed to retrieve objects that were not within the reach of individuals with disabilities [70].

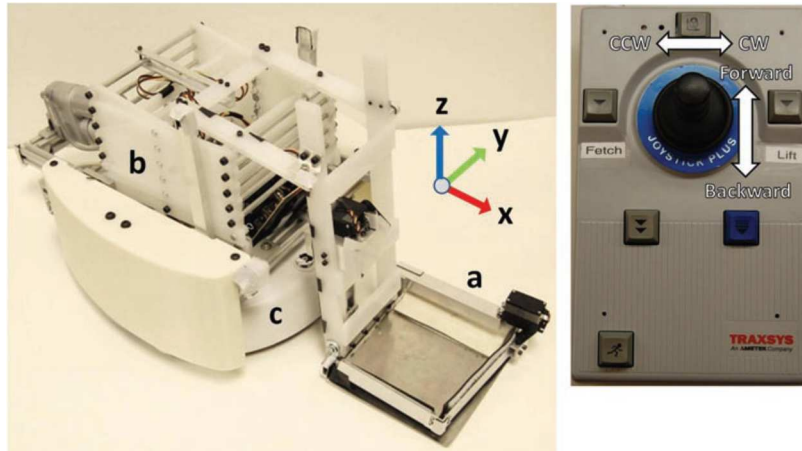


Figure 13: The Dusty robot on the left and the remote on the right, a) the end effector, b) the lift, and c) the mobile base [70].

The dusty system can be tele-operated and once an object was reached the plate (see Figure 13a above) was adjusted to the object. Then the reaching finger at the end of the plate gathers the object into the plate. The object was then placed in the plate and the user moves dusty around so it can deliver the object to the user. Finally when dusty was close to the user the plate was raised by the lift (see Figure 13b above).

This system was similar to the one described in [5, 6], but these type of assistive devices are unsuitable for the target population of this research. Keeping track of the device controls, the device itself, and the desired object would likely prove to be very challenging due to a lack of motor ability in the patients' fingers and wrist. These motion limitations can potentially discourage the targeted populations from using such devices.

1.6.1.5 Exo-skeletal Robotics and Body Bots

The robotic field took an amazing turn towards revolutionizing the industry with the introduction of Hybrid Assisted Limb [7, 71-77], HAL, often called the body bot, because these body bots are useful for not only upper or lower extremity injuries but also for the full skeleton. These body bots, or exo-skeletal robotics, were developed for future super soldiers, but have some applicability to SCI patients. Figure 14 shows the evolution of body bots over time. The full body robotics also provides the wearer with added strength comparable to that of a normal human. Several studies indicated the process by which these robots could be used for therapy [78-81]. While some of these devices help individuals recovering from stroke by allowing them to repeat a motion continuously, others support the individuals while walking or trying to regain balance.

However, daily activities remain a challenge for patients with SCI of C5 to C7 levels. Utilizing a body robot would be an extreme challenge for these patients requiring them to suit up, perform the simple task, and then take off the suit. Furthermore, these devices are extremely delicate and require help of another individual to get suited and unsuited. Such unease may discourage the user from taking advantage of this technology.

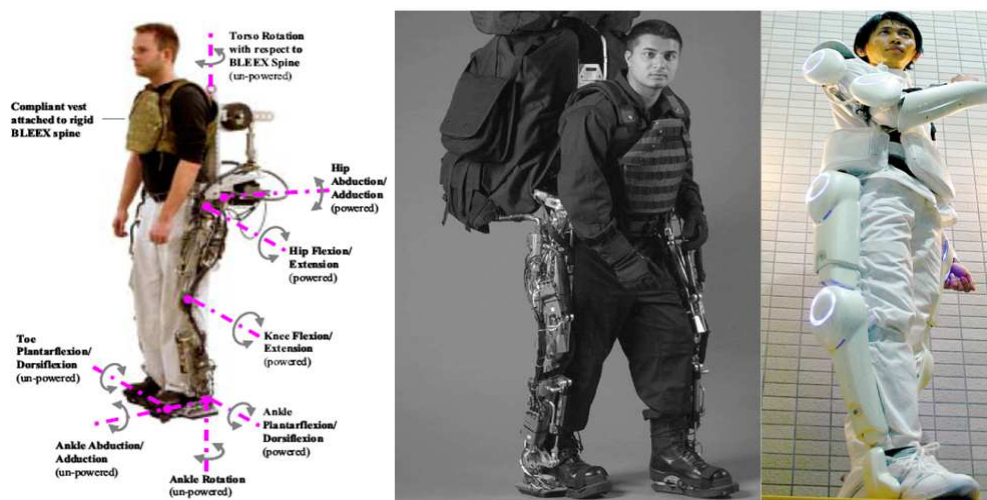


Figure 14: The Figure showing various body bots [7, 71-76, 82].

1.6.1.6 Exo-Skeletal Robotic Arms

In addition to the full body robots, some work has been done on a single exo-skeletal robotic arm [83-87]. These arms were designed to perform and enhance the mobility of a normal human. Some of these arms were designed for future space missions[83]. Although these exo-skeletal arms are very sophisticated and extremely light weight (only 5lbs), in some cases this is still too heavy for someone (e.g. SCI individual) whose maximum weight handling capacity is 2.5 pounds. In some cases the exo-skeletal arms are supported by rod that either rests on the ground or is fixed to the wearer's waist [88]. The following figures show some of these robotic arms.

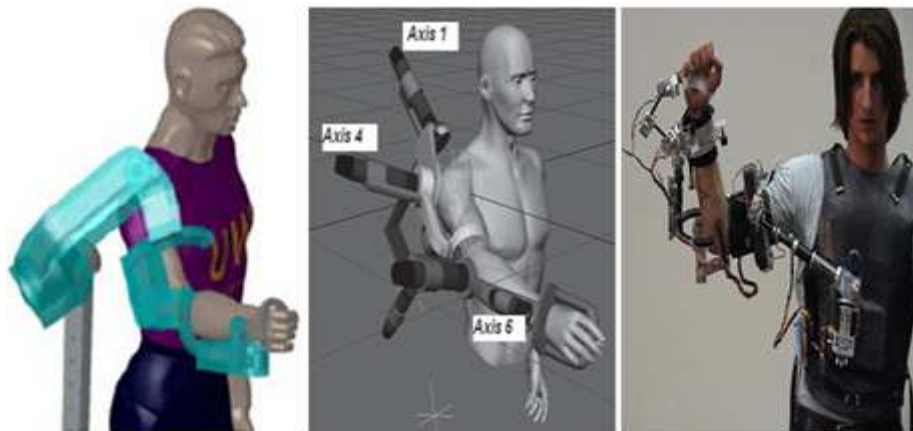


Figure 15: Variations of the modern exo-skeletal robotic arms [50-55].

Another example of an exo-skeletal arm is the SAM arm with 7 degrees of freedom (DOF) including wrist motion [89-91]. However, people with severe spinal cord injuries have very little or no voluntary wrist motions. Furthermore, the heavy back support, along with the added difficulty of taking on and off the arm, makes this device extremely difficult to use for an SCI participant. Hence the arm would be unsuitable for SCI individuals.

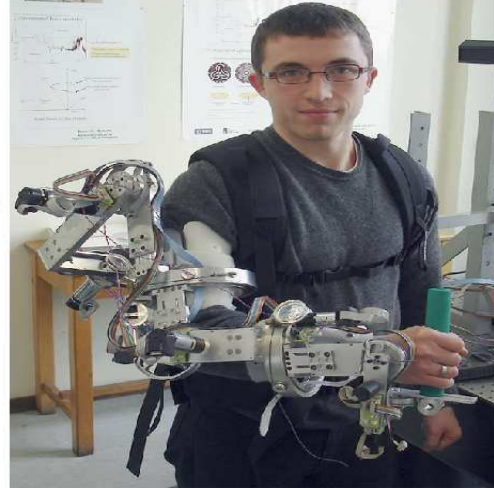
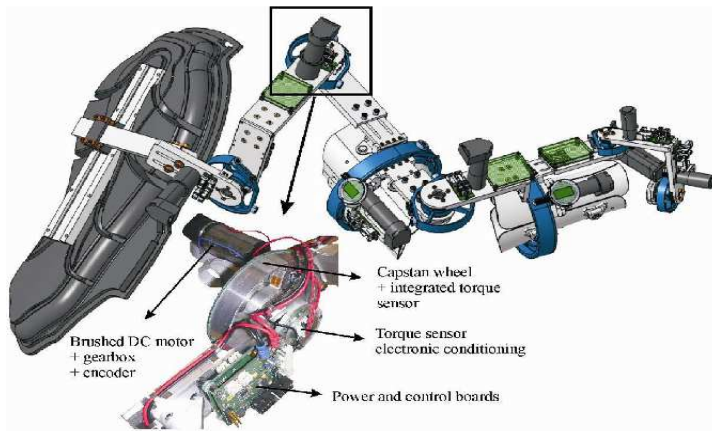


Figure 16: Proposed model and the built robotic arm with 7 degrees of freedom [89, 90].

1.6.1.7 Assistive Prosthetics

Assistive prosthetics have covered major engineering and technology milestones. For example, Touch Bionics [1] has designed an incredible prosthesis (see Figure 17) that can be connected to the nerve endings of an amputated limb and relay the strength of the grip with a feedback to the user. However, this assistive device was strictly designed for amputees and does not have advantages for individuals with residual functionality in their upper extremities.

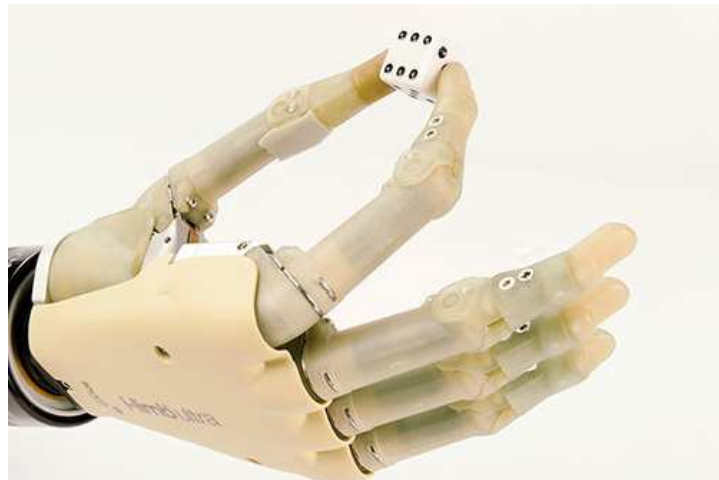


Figure 17: i-limb ultra-prosthetic hand by touch bionics [1].

One revolutionary prosthetic arm is the Luke arm created by Dean Kamen [92]. The Luke arm is modular, lightweight, agile and controllable. This arm was designed for amputated soldiers returning from the war fields. The arm gives 22 DOF and works best if attached surgically to the amputated arm. The Luke arm also provides feedback via a small motor called a tactor [93]. The tactor is worn on the user's belt so he or she can feel the vibrations generated from the device. If the end effector grips an object firmly, the tactor vibrates more vigorously indicating the intensity of the grip. The Luke arm also weighs as much as an average female arm, 8 pounds. This sophisticated arm is well adapted to the population it addresses, amputees, but not necessarily to SCI individuals.

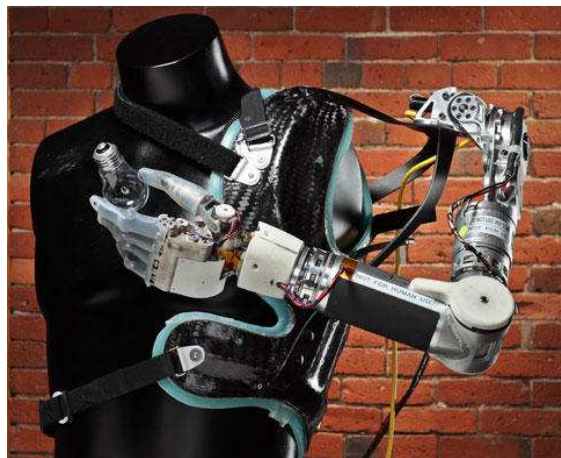


Figure 18: The Luke Arm.

1.7 Chapter Summary

This chapter provided an overall scope of the research, introduced and discussed the motivation for the research, and provided the framework being utilized for the research. Gaps in existing assistive technologies were identified by providing a brief overview of current devices.

The next chapter discusses aim/objective 1 of the research: the development of a prototype for proof of concept and feasibility. Chapter 2 provides details of the electrical, mechanical, and functional details of the device, followed by a detailed analysis of the participant study.

1.8 Organization of the Dissertation

The dissertation is divided into 5 chapters as follows:

1.8.1 Chapter 1: Introduction, Motivation, Background and Significance

The first chapter summarizes the motivation for the research by providing a brief background of existing assistive devices and identifying gaps amongst the existing technology. The chapter also discusses the novelty and significance of the research and how it can help bridge the gap for individuals with residual functionality of the upper extremities.

1.8.2 Chapter 2: Development of a Prototype for Proof of Concept and Feasibility

This chapter describes the development and testing of a voice-activated lightweight reacher to assist with upper extremity movement limitations. A case study was conducted with an SCI participant using the first generation of the Simple Assistive Reacher Arm (SARA). Experiments were conducted for reaching and grasping tasks. A second set of reaching and grasping tasks were conducted with 6 healthy participants *and* the SCI participant. The experiment was conducted to study participants' movement at three different levels: waist level, mid shin level and chest level. Statistical analysis (MANOVA) was performed on the data from the healthy individuals and was then compared with the SCI participant's data. This chapter explains the protocol, and details of the experiments with SARA. This chapter also discusses the results and conclusions from the Human Machine Interface study.

1.8.3 Chapter 3: Development and Preliminary Testing of the Exo-Skeletal Assistive Robotic Arm (eSARA)

This chapter describes the development of the second generation of the Simple Assistive Reacher Arm (SARA), called the Exo-Skeletal Assistive Robotic Arm (eSARA) platform. This chapter explains the additional features of eSARA for extension and grasping. This chapter discusses the three modalities mentioned in chapter 1, the development and implementation of the lift assist feature, and covers current consumption, battery life, force calculation and preliminary testing of the platform.

1.8.4 Chapter 4: Human Machine Interface (HMI) and Evaluation of the Exo-Skeletal Assistive Robotic Arm (eSARA)

In this chapter, two groups of healthy participants took part in experiments evaluating the eSARA platform. The first group consisted of 12 healthy, young adults, while the second group consisted of 6 Occupational Therapy students (mimicking SCI movements). These two groups and the SCI participants performed 2 experiments to study fine movement and gross movement of the individuals, respectively. Both experiments were conducted at the three different body levels mentioned above. The data from just the healthy individuals was statistically analyzed using ANOVA. The resulting data was then compared with the SCI participant's data. This chapter explains the protocol, details, and results for these experiments.

1.8.5 Chapter 5: Discussion, Conclusion, and Future Work

This chapter discusses the overall outcomes and conclusions of this thesis. It discusses the nuances of the performed experiments, the evaluation methodology, and classes of modes of control. In addition, a final case study was performed illustrating how this system of evaluation and control modes might be used to customize a system for an SCI individual. In addition, this

chapter also summarizes possible improvements to the existing generations of the assistive device including future improvements for a third generation SARA. This chapter also drives the conclusion from the results in chapter 3 and chapter 4.

Chapter 2: Voice-Activated Lightweight Reacher to Assist with Upper Extremity Movement Limitations: A Case Study

2.1 Introduction

This chapter discusses the first research objective to develop a baseline platform of a light weight, voice-activated, Simple Assistive Reacher Arm (SARA) and compare the performance of a SCI participant to normal individuals using the same device.

Mechanical reachers provide an inexpensive means of retrieving out-of-reach and dropped objects for many people with limited upper extremity and trunk function, such as those with high spinal cord injury (SCI). The frequency of dropped objects is often high; for instance, people with amyotrophic lateral sclerosis reported dropping objects an average of 5 to 6 times per day with lengthy retrieval time reported [70]. Commonly dropped objects are often ones essential for independent living including: remote controls, cell phones, prescription bottles, glasses, reading materials, and keys [53]. Currently available mechanical reachers may not benefit people with severe arm and trunk movement limitations. Reacher weight, increased torque requirements, and the need for hand and wrist movement make mechanical reachers inadequate for this population.

An extensive review of commercially available assistive devices for reaching produced no suitable low cost, lightweight, and voice-activated devices for people with high SCI. Therefore, a need exists to develop a simple, lightweight, voice-activated reacher to improve independent function for people with limited upper extremity motor skills, such as those with high SCI.

2.2 Development of Simple Assistive Reacher Arm (SARA) Platform

The current work stems from a class project designed by a student team in a medical robotics class at Wayne State University, Detroit, MI [94]. The team developed an extendable arm using air muscle technology and a voice recognition (VR) chip called VR Stamp module

[95]. A prototype of a voice-activated, ultra-lightweight mechatronic reach-assist device was designed and built. Figure 19 shows this first SARA prototype. SARA was built by modifying an inexpensive, lightweight manual reacher made by Rainbow Reacher. The device weighed 249.2 grams (0.549 lbs) with a total length 63.5 cm (25 inches). The housing of the electronics measured 7.62 cm (3 inches) by 10.16 cm (4 inches). The length of the ‘handle grip’ measured 12.7 cm (5 inches) by 2.54 cm (1 inch). The end-effectors are flexible rubber suction cups to allow for holding many different items. The manual trigger mechanism used for opening and closing the gripper was removed and replaced by an electric linear actuator linked to the band springs which are attached to the suction cup gripper. The linear actuator is voice-activated with simple phrases to open and close the gripper. The voice chip was customized for each user before using the device. To train the device for a given command a user would say the desired command twice when prompted by the VR Stamp module [95] training program with a delay each time the command was given. The voice chip then either prompts success if the two commands were similar. If the given commands were spoken differently, the VR stamp module would reject the command and the user would be required to retrain the voice chip.

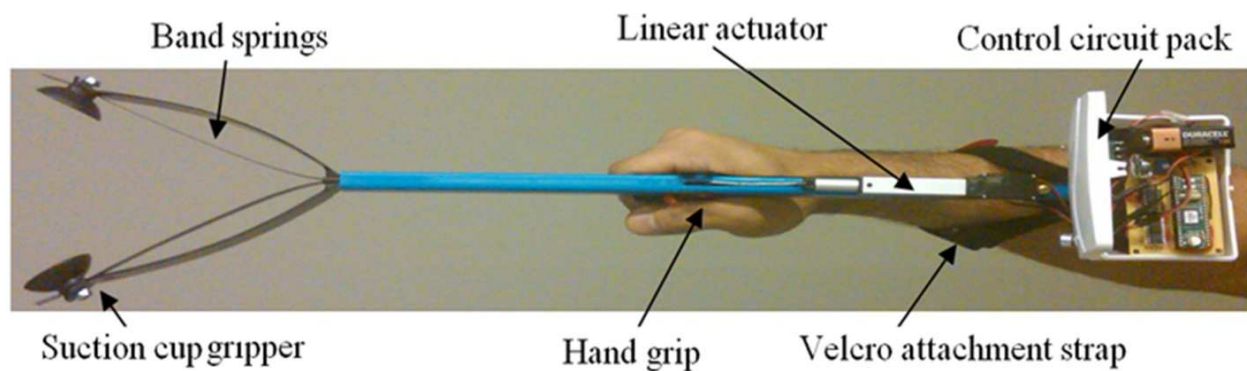


Figure 19: The Smart Assistive Reacher Arm is shown with the ‘control circuit pack’ open, showing the control circuit and dimensions of the original device (length and width of the ‘handle grip’ was by 12.7 cm by 2.54 cm).

2.3 System Hardware

Figure 20 shows the major components used in the making of the prototype including the Rainbow Reacher, the Firgelli linear actuator [96] for opening and closing the gripper, and the VR stamp module. The actuator operates on 6 Volts and can generate a back drive force of 150N. The actuator was controlled using the VR stamp module, a built-in voice recognition and microcontroller by Sensory Incorporation [95].

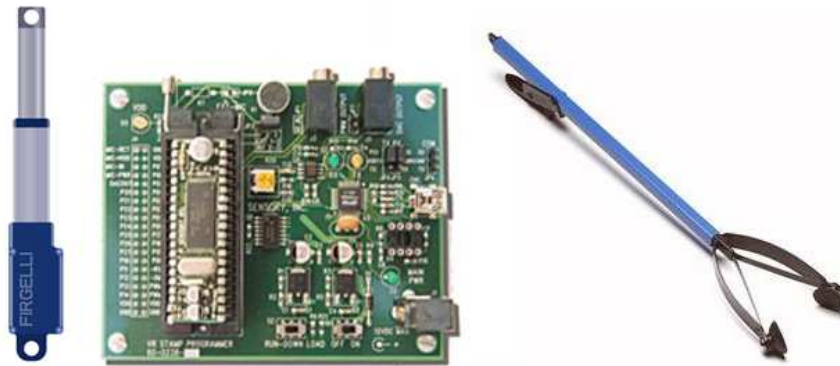


Figure 20: The L-12 linear actuator [96] (left), VR stamp module [95](center), Rainbow Reacher (right).

The mechanical reacher was selected due to its light weight of only 217grams (0.48 lbs.), and its ability to lift typical light loads (keys, cellphones, soda cans, etc.) without distortion. This is a commercially available arm which is used by many elderly and disabled people to pick up objects [42-46, 48]. The reacher requires the person to use their fingers to press the handle to close the end effectors to grip objects. Given that individuals with high SCI do not have motor control of their fingers, a voice-activated system was selected as an alternative. The mechanical assembly consists of the arm with the gripper and the linear actuator that operates the end effectors. The linear actuator causes the end-effector to grip and release the objects. When the actuator is drawn in, the gripper closes; when the actuator is drawn out, the gripper opens. The gripper is connected to the front end of the arm (Figure 20).

2.4 System Firmware and Electronics

The voice recognition chip, combined with the motor driver circuit, is connected to the linear actuator controlling the end effectors. The motor driver circuit is used to extend or contract the linear actuator for desired functionality. The microcontroller waits for a trigger word followed by a command word. Once the correct combination is received through the microphone, the linear actuator is activated, and the desired action is performed.

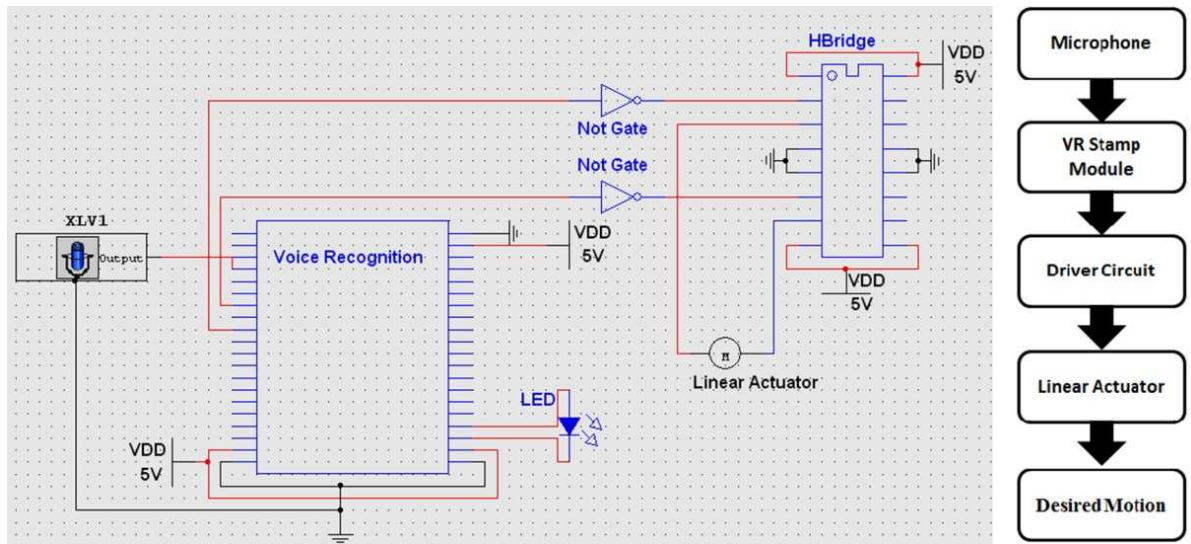


Figure 21: The driver circuit for the reacher arm (left) and the block diagram of the mechanism of operation (right).

Figure 21 shows the driver circuit which activates the linear actuator that in turn actuates the gripper. The motor driver is used to reverse the polarity of the supply to the motor. The VR Stamp Module is programmed according to the flow chart in Figure 21. When the VR module is turned on, it enters the ‘trigger mode’ waiting for the trigger word. Once the trigger word is said, it enters the ‘command mode’ and awaits the command word. Once the command word is spoken, the VR module recognizes and matches it with the two stored commands. Once the correct combination is received, the command is executed and the device waits for additional commands. The system also blinks an LED at the gripper to show the user that the system is on

and understood the said command. The device stays in the 'command mode' for 3 seconds. If additional commands are not provided within 3 seconds, the system enters the 'trigger mode' again. The voice mechanism is active only if a discrete trigger word is said followed by a specific command. If the combination is not followed then there will be no output. The system was tested with background noise. In Figure 26 there are two individuals talking in the background while the experiment was performed. The experiment was successfully repeated multiple times.

The trigger word chosen for the entire testing was 'Max'. There were two command words selected for the experiment, 'Grab' and 'Release'. Once the participant says the trigger word 'Max' followed by the command word 'Grab', the microcontroller recognizes the command issued and closes the reacher's jaws. Similarly, when the command word 'Release' is said, the microcontroller recognizes the command issued and opens the reacher's jaws.

The linear actuator is programmed in such a way that when the grab command is issued, the grip closes only half way in case of handling fragile objects. To further strengthen the grip, the command is repeated until the actuator is at its minimum position. For example, if the grab command was said once, the gripper closed half way, when the grab command was said the second time, the gripper closed fully. If the grab command was said a third time, the gripper would firmly grab onto an object. In addition, the reacher can be programmed depending on the user's needs. For instance, a 'stop' command can be implemented when the reacher is either grabbing or releasing to accommodate fragile objects.

A 170 mAh (milliamp hours) battery providing 9V (volts) was used to power the circuit.

The current drawn for a specific command is inversely proportional to the number of hours the battery will last. If the battery draws 100 mA it will last $170 \text{ mAh} / 100 \text{ mA} = 1.7$ hours. Table 3 below shows the battery life per command for the device.

Action	Current Consumption (mA)	Battery Life (hours)
Standby mode	60	2.8
Grab 1	100	1.7
Grab 2	110	1.5
Grab 3	120	1.4
Release	70	2.4

Table 3: Power consumption of the device.

Prior to research with participants, a test was conducted using various objects to determine the device's ability to grasp, lift, and move objects of various shapes and sizes. This test is shown in Figure 22.



Figure 22: This Figure shows the Pilot Test being conducted on various objects picking them from one spot and placing it on the other side.

2.5 Preparatory Assessment of the SCI Participant

One participant with high quadriplegia (incomplete level C5-6) participated in this study. In collaboration with an occupational therapist (GC), the participant's range-of-motion and lift capacity was measured. Specific movement patterns associated with reaching, lifting (average weight on a daily basis), maximum weight lifting limits (strength test), and carrying capacity (precession test) were measured. These measures provide baseline information to avoid injury to the participants.

Experiments were conducted to determine the participant's reach envelope without SARA. As the participant moved his arm in 3D, Polaris reflectors (Figure 23) captured the movements and range of motion. Based on the data obtained from the motion tracker, the work envelope of the participant was determined. Another study was conducted to determine the maximum weight that the participant could lift. These experiments informed the design of the device in terms of its reach and weight. Based on these studies, it was established that additional extension of the reacher was not necessary and that a simple grab and place reacher was enough. It was also determined from the study that the participant could lift a maximum 1150 grams (2.5 lbs.) including the load of the object being carried. It was concluded that in order to give maximum payload capacity, and be useful to the participant, the device itself should weigh less than 500grams (1.1 lbs.). The length of the reacher enabled the participant to reach objects on the floor, a table, or shelf from his wheelchair orientation. Most importantly, the reacher must enable the participant to use his available range of motion and residual functional capabilities to pick and place objects in a desired location. The reach envelope and range of motion data enabled us to select an optimal reacher length (*15 inches from the handle*).

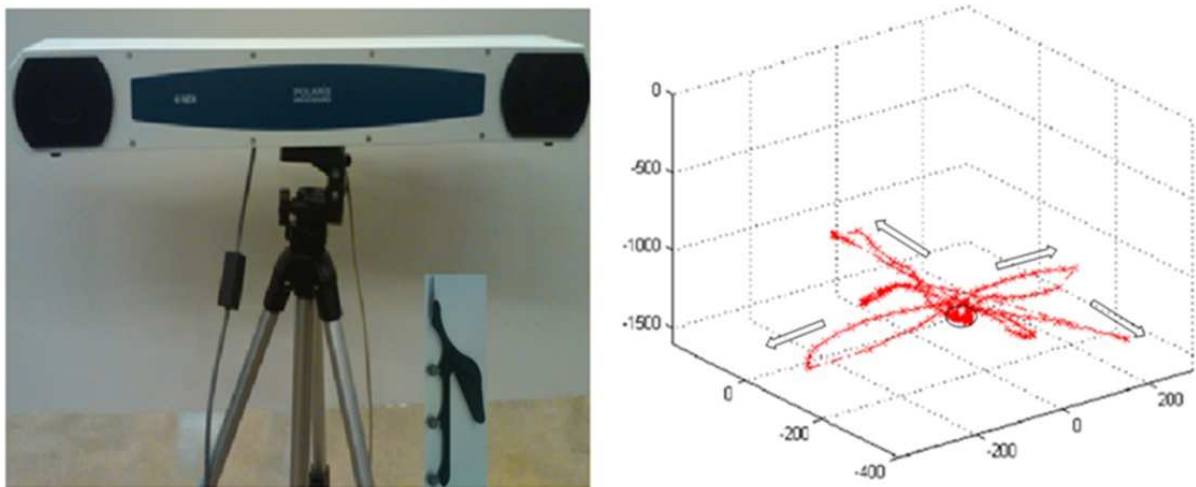


Figure 23: Polaris and the reflector unit, shown on the left, used to capture the envelope of reach of the participant which is shown in the figure on the right. The circle indicates the center point and the arrow indicates the maximum possible reach of the participant.

Figure 23 shows the Polaris and the reflector unit (left), the figure on the right shows the envelope of reach of the participant without the reacher. The center of the envelope of reach is marked by the circle and the arrows show the maximum movements of the participant with respect to the center in the specified direction. This determines the envelope of reach of the participant without the reacher. The center of movement was determined by a starting point for the individual. The individual was then asked to move his arm to the furthest position in the left, right, forward and back positions, to determine his full reach envelope. The plot shows the movement of the individual in real time.

2.6 EXPERIMENT 1: Case Study: Planar and 3D Movement by a Person with Spinal Cord Injury

2.6.1 Methods

2.6.1.1 Study Purpose

The purpose of this experiment was to determine if a person with SCI can effectively complete grasping and reaching tasks in the horizontal plane and in 3-dimensions. The study was designed, to ascertain the ability of the participant with SCI to complete reach and grasp tasks that would not be possible without the reacher. All studies were approved by the Institutional Review Board at Wayne State University.

2.6.1.2 Participants

One individual with a C5-6 spinal cord injury was the only participant in this experiment.

2.6.1.3 Materials

For the table top experiment, an area was marked to test the reach and grasp of the SCI participant. For the floor to table experiment, areas were marked on the floor and the table top to

conduct the pick and place experiments. In this experiment a pencil and a 9 volt battery were used as objects. For the second half of the floor to table experiment a cell phone was used as an object.

2.6.2 Protocol

2.6.2.1 Table Top: Case Study

The participant was asked to move an object, a 9V battery, within the white test area on the surface as shown in Figure 24. The participant was asked to grab, pick up, and move the object to three locations within the test area. The locations were selected by the test conductor. The locations were given sequentially to the participant in order to determine the ease of use as well as adaptability of the participant to the reacher. The three different locations in this test case are marked by the numbered dots in Figure 24. The locations progressively varied in difficulty as the participant's reach and gross movements were tested. This demonstrated the ability of the participant to move the object in one plane.

It was noted from the experiment that the SCI participant was able to fulfill the task completely and with ease. However, he was unable to perform any of the given tasks without the aid of the reacher.

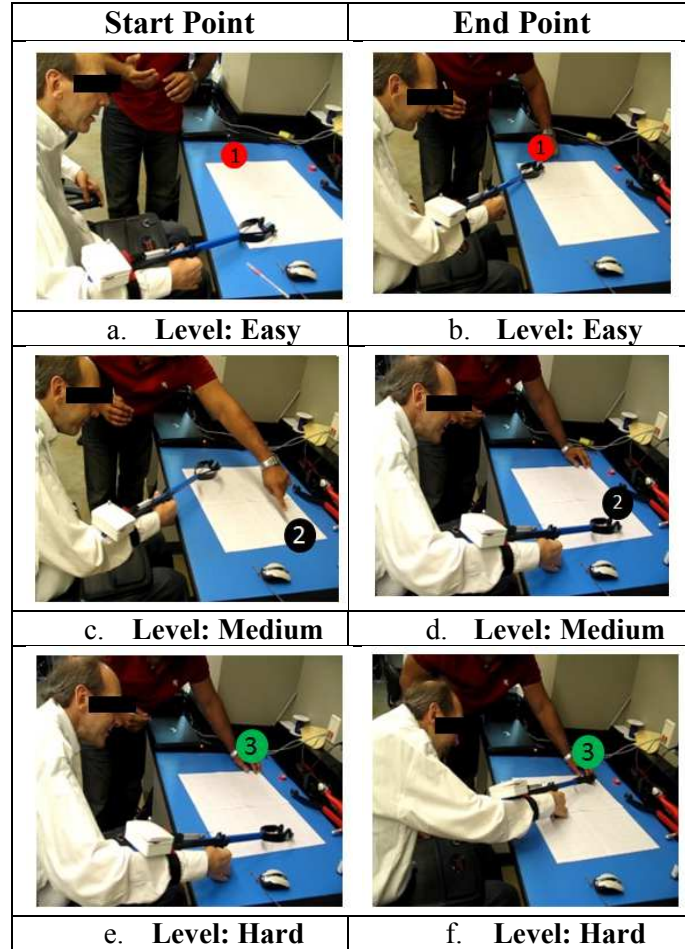


Figure 24: Participant's progress throughout the experiment. The figures show the participant moving the object in one plane on the test bench, marked with the white area. The three dots in the picture shows the points selected by the principal investigator.

2.6.2.2 Floor to Table: Case Study

In the second stage of the experiment, the SCI participant was asked to pick up objects from the floor and place them on the desk. Two objects of different shape and size were selected. The participant was expected not to drop the objects during the entire transition from the ground to the table top. Figure 25 below shows the starting and ending points of the experiment. The participant was able to successfully move both of the objects to the required positions with ease. Without the reacher, the participant was unable to pick up the objects from the floor.




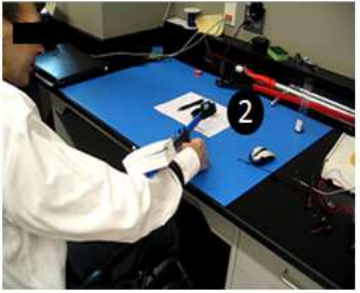
Start Point	End Point
	
a. Grabbing object (pencil) from the floor	b. Successfully transferred object to the test area
	
c. Grabbing object (battery) from the floor	d. Successfully transferred object to the test area

Figure 25: This figure shows the participant moving the object in three dimensions picking up the objects from the floor and placing them on the table within the test bench (indicated by the white area).

In a more realistic test scenario, the SCI participant was asked to pick up his dropped cellphone from the floor. The sequence of images in Figure 26 summarizes the outcome of this test.



Figure 26: (a) Cell phone falls (b) SCI participant moves to pick up the cell phone using the reacher (c) Using voice commands the SCI participant controls gripper to secure the cell phone (d) SCI participant places the cell phone on his lap and then commands the gripper to open releasing cell phone (e) Success!

2.6.3 Results

For the table top experiment (Figure 24) the SCI individual successfully completed the tasks following the given instructions. He was able to place the object accurately at the specified locations. For the floor to table top, and dropped cell phone, experiments the SCI individual accomplished the tasks successfully.

2.7 EXPERIMENT 2

2.7.1 Methods

2.7.1.1 Study Purpose

Given the lack of available reach aids for people with SCI and forearm/hand paralysis, the purpose of this experiment was to assess reach and grasp capabilities of the above designed reacher with both healthy, young adults and a person with SCI. It was hypothesized that, with the use of the reacher, the SCI individual could (1) feasibly reach and grasp objects within a newly designed test bench, (2) match movement time and errors within the limits shown by the healthy comparison group, and (3) produce these tasks in the absence of any signs or reports of fatigue or distress.

2.7.1.2 Participants

Six healthy young adults and one adult with quadriplegia (incomplete level C5-6) participated in this study. The adult with SCI was the primary person of interest in this study to evaluate the system.

2.7.1.3 Materials

A book shelf with three different levels was used as a test bench. The test bench was designed to measure the gross movements of the participant on these three different levels. The three different levels consist of level '0' (waist level), level '-1' (mid-shin level), and level '+1' (chest level) as shown in Figure 27. These levels were specified to normalize the height requirements for each participant. The Figure also shows the objects that were used in the experiment such as a small peg, a medium size peg, and a bottle weighing 227 grams (0.50 lbs.). These objects were color coded for ease of viewing. These objects were selected to represent categories of commonly used objects.



Figure 27: Left: Color coded test bench with three levels. Right: Test objects included a small peg (pink), larger peg (green), and a half pound bottle (orange).

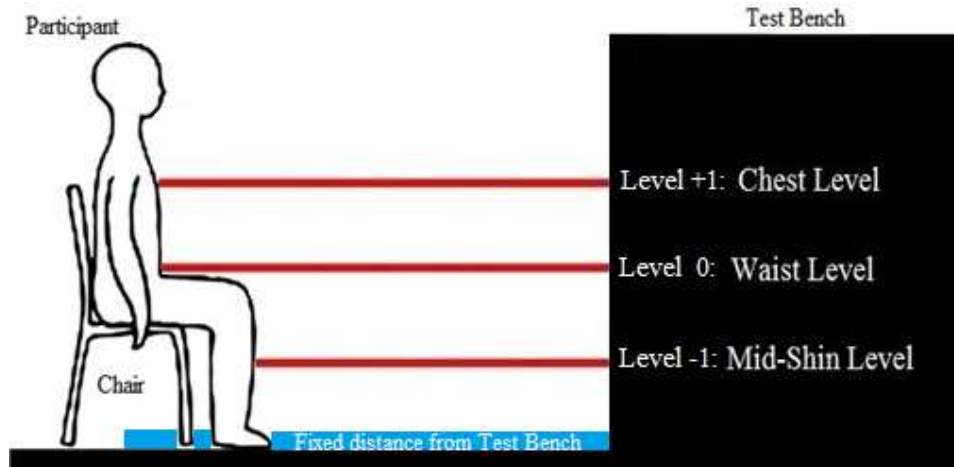


Figure 28: Test bench levels and distance from the test bench.

A chair or wheelchair was placed at a distance of 27 inches from the base of the test-bench to the chair center for all participants, as shown in Figure 28.

2.7.2 Protocol

All participants completed the reach and grasp tasks using SARA. The participants were given the reacher for 3 minutes, or 10 trials, to become familiar with the voice activation functionality. The experiment was counter balanced to reduce any possible learning effect. Three of the participants were asked to perform the experiment starting with level 0, then level -1, and then finally level +1 while the other three participants were asked to perform the experiment starting at level 0, then level +1, and then finally level -1. The goal of the experiment was to place the color coded objects from level -1 to level 0 or from level +1 to level 0. At the start of the experiment, all of the objects were placed at fixed positions within level 0 and the participants were expected to grasp each object and place them on their corresponding color coded positions. The participants were then asked to repeat the same procedure for the other levels. Figure 29 summarizes the start and expected end points of the experiment for the different levels. Two types of errors, within and outside of the test bench, were demonstrated for the

participants. These errors are shown in Figures 30a, 30b, and 30c (within the test bench) and Figures 30d and 30e (outside of the test bench). Any within-bench error required correction by the participant, while errors outside the bench were recorded as a failed attempt.





Start Point	End Point
	
a. Level: +1	
	
b. Level: 0	
	
c. Level: -1	d. Level: 0

Figure 29: Start and end points of the experiment.

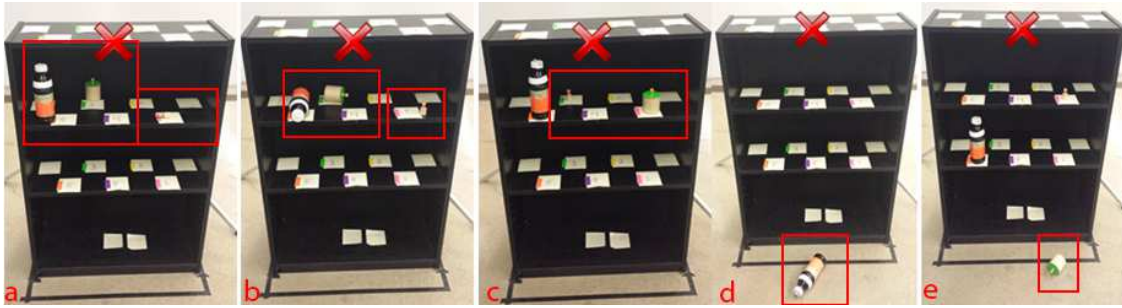


Figure 30: Errors within the test bench are shown (a-c); a) improper placement of the objects, b) wrong object position, and c) mismatched color coding of the objects. The errors outside the test bench are shown in d and e and are considered as failed attempts for those specific object for the respective level.

2.7.3 Data Analysis

Each participant's completion time and errors per level were recorded. Data were analyzed using SPSS (IBM) [97]. Descriptive data were provided for each participant. Differences in time between levels for all participants were compared using Multiple Analysis of Variance (MANOVA) with the Bonferroni correction for multiple comparisons. Significance was established at $p < 0.05$.

2.7.4 Results

Figure 31 shows each participant grasping the large peg at level +1, the chest level. All participants completed the task successfully by placing the peg in the required position on level 0. The degree of shoulder and elbow flexion was similar among all participants, as seen in Figure 31. The posture of all participants was similarly upright and relaxed.



Figure 31: This figure shows participants performance at different points in time grasping the same object. The figure also compares the posture of the participants handling the same object as level +1 with the reacher.

Figure 32 summarizes the estimated mean values with standard error at each of the three levels for data collected from the healthy participants only. Healthy participants spent the longest mean time completing tasks at the height of the mid-shin (-1), while movement times for the waist (0) and chest (+1) levels were similar.

Levels	Mean (Healthy Participants Only)	Std. Error	95% Confidence Interval	
			Lower Bound	Upper Bound
-1	1.782	.070	1.602	1.963
0	1.366	.100	1.108	1.624
+1	1.346	.099	1.092	1.601

Figure 32: Estimated mean values of the levels (in minutes) and the standard error (healthy participants only).

There was a significant main effect for level height ($F(2,10) = 54.592, p < 0.001$). Pairwise comparisons for the main effect of level were corrected using Bonferroni adjustments and are displayed in the table below. Table 4 shows that the significant main effect reflects a significant difference ($p = 0.002$) between levels -1 and 0 (lower and middle) and -1 and 1 (lower and upper) ($p < 0.001$) but not between levels 1 and 0 (upper and middle).

(I) Levels	(J) Levels	Mean Difference (I-J) (Healthy Participants Only)	Std. Error	Sig. ^b	95% Confidence Interval for Difference ^b	
					Lower Bound	Upper Bound
-1	0	.416*	.056	.002	.219	.613
	+1	.436*	.037	.000	.306	.565
0	-1	-.416*	.056	.002	-.613	-.219
	+1	.020	.047	1.000	-.146	.186
+1	-1	-.436*	.037	.000	-.565	-.306
	0	-.020	.047	1.000	-.186	.146

Table 4: MANOVA results for Experiment 2 based on estimated marginal means only for the healthy participants.

* The mean difference is significant at the 0.05 level.

^bAdjustment for multiple comparisons: Bonferroni.

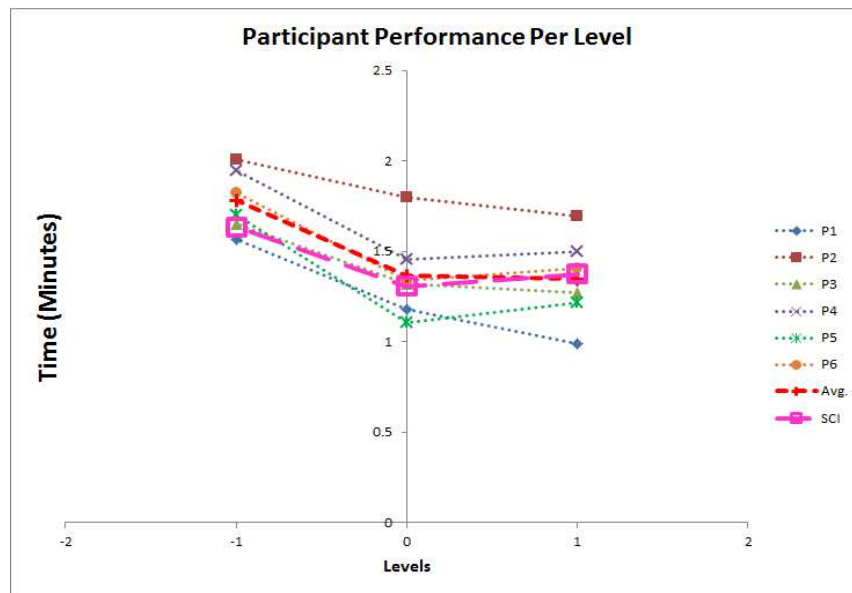


Figure 33: Individual participant performance time in minutes per level (P = healthy participant, Avg = average (healthy participants only), SCI = spinal cord injured participant).

Figure 33 shows the time performance of each participant at all three levels. Figure 34 is a box and whisker plot generated from the six healthy participants' data at each of the three levels. This plot is overlaid with the healthy (able-bodied) participants' average results (healthy participants' average time performance is represented by a thick dashed line). Figure 34 also contains the SCI participant's time performance in comparison to the healthy participant's average time performance (the SCI participant's time performance is represented by a thick dot and dash line). The data demonstrates that the SCI participant, who was unable to perform the

task of moving an object without the reacher, was able to perform the task, at all levels, in a comparable amount of time to the healthy participants. The SCI participant finished testing at levels -1 (mid-shin) and 0 (waist) faster than the average healthy participants by 8.3% and 4.2%, respectively. At level +1 (chest) the SCI participant was 2.1% slower than the average healthy individual. However, this rate was still within one standard deviation of the average. Throughout all testing, no discomfort or fatigue was observed by the investigator or reported by the SCI participant.

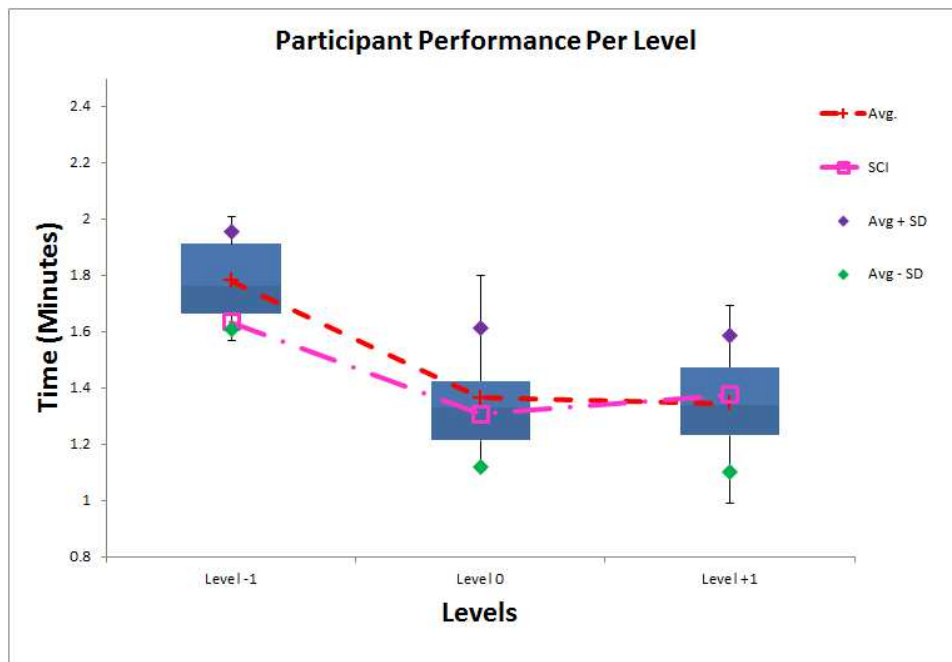


Figure 34: Box plot and average of the healthy participants' performance against the SCI participant's performance.

2.8 Discussion and Conclusion

These experiments demonstrate that this simple voice-activated reacher allowed an individual with SCI to move lightweight objects of different sizes and shapes in similar times, and with no more errors, than healthy young adults, and without reported or observed discomfort. The first experiment was designed to assess whether and to what extent the device could be used by an individual with SCI. Technical issues were identified and positively

resolved. With the use of the designed reacher, the participant was able to reach and grasp within a horizontal plane placing objects at targeted areas. In the floor to table case study, vertical movements were also successful. The hypothesis that a person with SCI would be able to complete reach and grasp tasks successfully using the voice-activated reacher was affirmed.

Experiment two required greater precision of reaching and grasping a variety of objects at three different levels. While this was not possible without the reacher, it was successful with it. These results also confirmed the hypotheses that use of the reacher would be feasible for these more rigorous movements, that movement time and errors for the SCI individual would be comparable to healthy adults, and that there would be no signs or reports of fatigue or distress for the user. These hypotheses were also confirmed. Confirming these outcomes is especially important as the movements for experiment two required more challenging and complex arm movements, within the environmental constraint of the test bench. These positive results suggests that the reacher may be useful in providing independence in placing and retrieving lightweight objects from places such as book shelves or cluttered counters.

The SARA prototype achieved previously unmet needs for the individual with high-level SCI. With this reacher, independence in reaching and grasping small, lightweight objects became possible. Errors and performance time were comparable to healthy adults, and there was no reported or apparent distress in using the device. Based on these findings, the reacher, with additional technical improvement, may provide significant and meaningful assistance to people with high level SCI.

Future work will focus on the following improvements. First, the control circuit pack can be significantly reduced in size and cost. The prototype used a proto-board and other components that can be further optimized to decrease size and weight constraints. Second, a different linear

actuator could also provide reduced weight and cost. Third, the battery pack and control circuit pack with the microphone can be designed so that they fit inside the reacher's frame making it more compact. Finally, the addition of a mechanical lift assist and reach extension will increase the value of this reacher.

Limitations of this feasibility study included the use of only one participant with SCI. In the future, more such subjects with similar disabilities should be tested to confirm broad applicability. In addition, testing should include other conditions that result in greatly decreased arm and hand function, such as people with multiple sclerosis, stroke or arthritis.

Conclusion: This specific aim provided strong proof of concept that a lightweight voice-activated reacher can be developed to enable individuals with high level SCI to reach, grasp, and accurately place lightweight objects. Movement between levels at mid-shin and mid-chest of these objects was feasible and completed with comparable movement times and errors as a control group of healthy young adults, and without observable or reported evidence of distress or fatigue.

Technical improvements for the next generation of the reacher have been identified. Improvements were made to the existing prototype before the next round of testing which will be discussed in the next chapter.

Chapter 3: Development of a Multi Modal, Exo-Skeletal Assistive Robotic Arm (eSARA) with Lift Assist

3.1 Introduction and Motivation

This chapter discusses the infrastructure development to support specific research objective 2: designing and developing a platform for reach and grasping tasks with multiple modes of control and lift assist features to be used by an individual with high-level spinal cord injury (SCI). The design and development of the new platform assumed the following objectives:

- a. Control modes matched to the functionality of SCI individuals can be created.
- b. Increased device reach extension would be beneficial and feasible for the SCI individuals.
- c. Lift assist would provide necessary additional support for moving heavy objects.
- d. The new platform must maintain no signs or reports of fatigue or distress from the SCI user.

These objectives required expanding the existing platform to develop an Exo-Skeletal Assistive Robotic Arm (eSARA) with multiple modes of control and lift assist. Furthermore, the controls modes were to be customizable for use based on the level of injury. Providing multi-modal control of an assistive device built on a range of basic human movements, easily achieved by SCI individuals, motivated the research in this chapter. The multi-modal controls were designed to control the extension and grasping abilities of the eSARA platform. The lift assist feature enabled the SCI individuals to lift objects heavier than they could otherwise handle. Once the device was completed, different measures were taken to ensure device safety before the Human Machine Interface (HMI). The HMI allowed testing different modalities and developing a methodology to fit the technology with the level of injury of the SCI individuals.

3.1.1 Classification of Modes of Control

A platform was designed and built to assist people with residual functionality in their upper extremities, specifically to expand the reaching and grasping abilities of high-level SCI individuals. An extendable robotic arm platform was developed and investigated with three modes (briefly described in chapter 1) of controlling the extension and grasping capabilities of the arm. The control modes were categorized as follows:

- (1) Ballistic modality with no extremity movement required (voice-activated)
- (2) Ballistic control mode that required minimal movement of the extremities (pushing a button)
- (3) Continuous control mode that may require major/continuous movement of the extremity (sliding a joystick)

Ballistic control mode originates from ballistic movement. A ballistic movement can be described as a short muscle contraction with maximum velocity and acceleration towards a given target. Examples include tapping a button or saying a vocal command. A continuous movement however, requires a more controlled or guided motion over a longer period of time with a rather slower velocity and acceleration towards the targeted object. For example, a sliding movement to extend or retract an actuator.

These control modes were designed such that an SCI individual could use the platform with minimal effort and a limited movement of their extremities. Depending on the level of SCI, the platform provides various ways to control the end effectors. The platform was based on a multi-modal control unit and the end effector unit. When the multi-modal control unit receives the instructions from different modalities, it commands the end-effector unit to carry out the desired instructions. Figure 35 illustrates the modality inputs to control the arm's extension/grasping units.

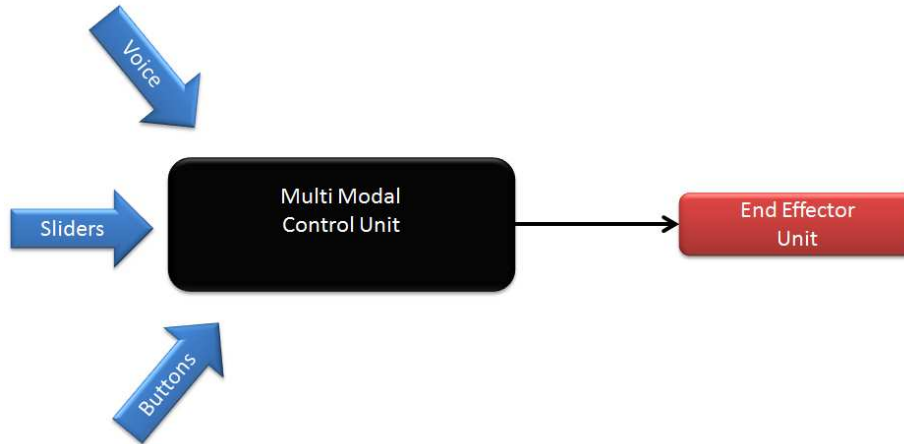


Figure 35: Multi-modal control and end effector units.

3.2 Methods for the Development of the Exo-Skeletal Assistive Robotic Arm (eSARA)

A first generation prototype, designed as SARA (Smart-Assistive Reacher Arm) [94], was discussed in chapter 2. The second generation of the reaching device, called Exo-Skeletal Assistive Robotic Arm (eSARA), was designed to improve reachability and lift-ability of the prototype. Another improvement in eSARA was to provide various ways to control the arm. To make this platform function successfully, various hardware components and software features were required. The design intent was to build a platform that can be utilized by various participants with very little or no training.

Figure 36 shows the final test platform that was built with the three modes of control. The voice control mode module, marked ‘a’ on the figure, was enclosed in a box with the speaker sticking out to receive voice commands. The slider control mode, marked ‘b’ on the figure, was housed in a clear box. The button control mode, marked ‘c’ on the figure, was also housed in a transparent box. The modality control unit and lift assist control units are marked ‘d’ and ‘e’, respectively. The pairs of biceps and triceps actuators are marked ‘g’ and ‘f’, respectively. The battery that drives both the circuits is marked ‘h’. The extension actuator is shown by ‘i’ and the

extension rail is shown by 'j'. The grabber motor and the grabber (end effector) are marked 'k' and 'm'. Pressure sensors are mounted on the handle and are shown in the figure by 'l'.

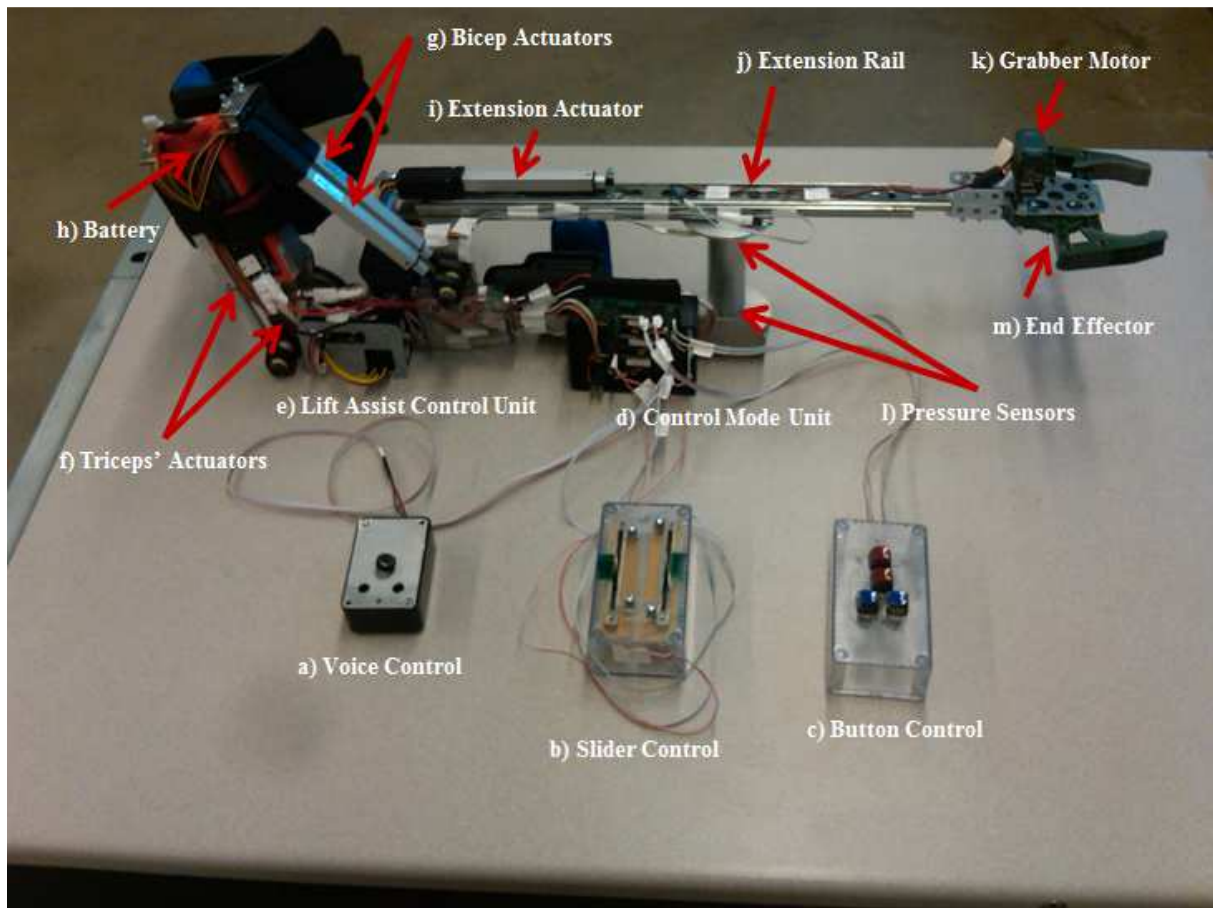


Figure 36: Final assembly of the Exo-Skeletal Assistive Robotic Arm (eSARA).

Figure 37 shows the evolution of eSARA from SARA using computer aided design (CAD) diagrams. The figure also shows the final CAD design, the final fabricated version of eSARA, and a user wearing eSARA. Throughout the design cycle, eSARA was enhanced to improve functionality, reduce weight, and increase ergonomics.

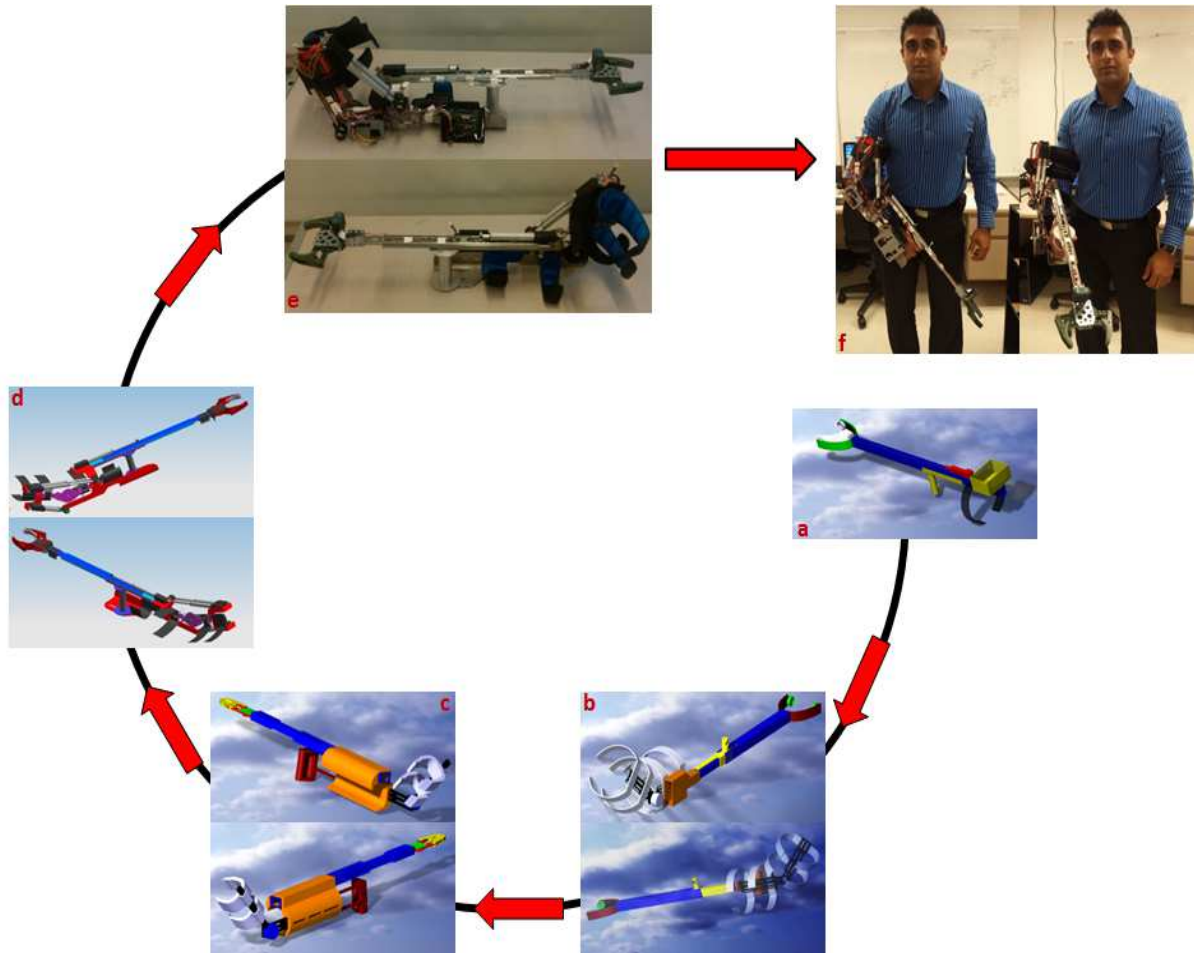


Figure 37: Evolution of eSARA, a) SARA, b) addition of arm attachment and extension to SARA, c) improved handle and design update to the device in b, d) implementation of biceps and triceps actuators and end effector finalizing the design, e) fabricated eSARA, f) user wearing eSARA.

Figure 37 above shows the evolution of eSARA from its predecessor SARA. In the figure a) represents SARA, b) shows updates to the pioneer design with added extension and arm attachments, c) shows improvement in the handle and design update, including the housing for the extendable forearm, d) shows the implementation of biceps and triceps actuators extension including adjustable handle, updated extension rails, and the end effector, finalizing the design, e) shows the completed eSARA, and f) shows a user displaying eSARA.

In the figure above the user donned eSARA while standing, this was only for demonstration purposes. For the experimental study and HMI analysis, the eSARA platform was suspended by

a weight countering device called The Zeiss S21[98]. This suspension allowed the participants free movement of their extremity, zeroing out the additional weight of eSARA (7.42lbs.), along with their own arm.



Figure 38: (a) Zeiss S21 [98] stand used to support eSARA's weight (b) user operating the Zeiss S21 system.

The Zeiss S21 stands are generally used to support surgical microscopes. Figure 38 shows how a participant was able to move freely and weightlessly with the help of the Zeiss S21 stand. Prior to the start of the experiment the flexibility of Zeiss S21 was adjusted for each participant. These adjustments were kept the same until the experiments were completed. The purpose of the Zeiss S21 system was to provide the participants with a zero-gravity device to counter the weight of the arm.

3.2.1 System Hardware

Multiple hardware components were used to develop this platform. The hardware used for eSARA, along with a description of its integration into the platform, is described in this section.

3.2.1.1 Actuators

The L16 actuators are complete, self-contained linear motion devices with position feedback capable of sophisticated position control, end of stroke limit switches for simple two position automation, or Radio Control (RC) servo. Several gear ratios are available providing various speed/force configurations. One Firgelli actuator (L16-P, 140 mm length, 150:1 gear ratio, Force) was used for extension, 2 for biceps (100 mm length, 150:1 gear ratio, Force), and 2 for triceps (50 mm length, 150:1 gear ratio, Force) [96]. These actuators have axial design utilizing powerful Permanent Magnet Direct Current (PMDC) motors with a rectangular cross section for increased strength. The “P” type series of actuators was selected because they offer an analog position feedback signal that can be inputted to an external controller. Figure 39 shows the 12 volt L16-P actuators.

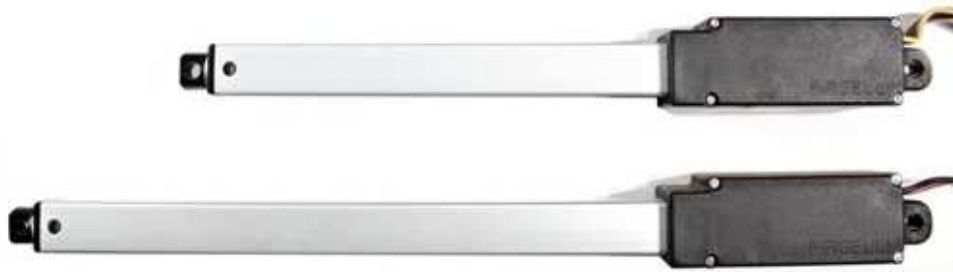


Figure 39: Firgelli L16-P actuators. The actuator on the top (50mm) was used for the triceps and the actuator at the bottom (100mm) used for the biceps[96].

The load versus force and current versus force curves of the actuator re shown in Figure 40. The plot shows the gear ratios available for all the L-16 actuators (35:1, 63:1, and 150:1). When power was removed, the actuator held its position unless the load applied was greater than the back driving force. The higher the gear ratio the greater load the actuator can withstand. Therefore, the gear ratio selected for all actuators was 150:1. Due to an increased number of

moving gears, the speed of the actuator was slower compared to the actuators with lower gear ratios. Figure 40 shows the load curves.

Figure 40 also provides current versus force plots, showing that the actuators handling a force of 50 or 100 Newtons (N) require a larger current (approximately 550mA) compared to the actuator handling a force of 200 N (approximately 450mA). From the plots, higher currents were proportional to the speed of the actuators.

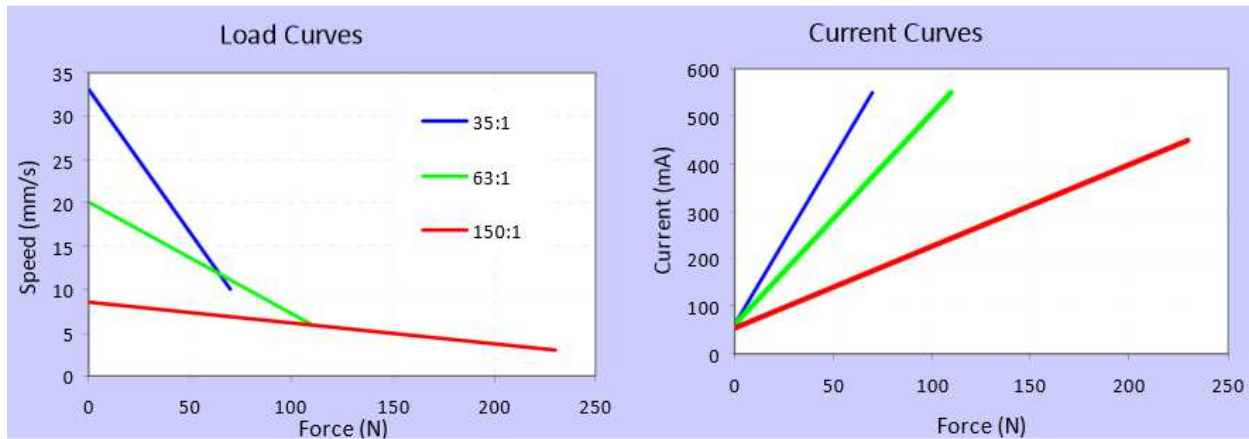


Figure 40: L16-P actuator load vs. force (left) and current vs. force plots (right) [96].

Table 5 below summarizes available options for the L-16 actuators including the gear ratio options, stroke options, and the force. From the table, the 150:1 gear ratio was able to drive a maximum lift force (200N). This actuator was selected as a precaution due to the uncertainty in the final weight of the platform. An actuator with greater lift force was preferred in case the platform itself weighed more than the expected 7lbs. The SARA prototype used a similar actuator (L-12) without any reliability or durability issues. The variety of lengths, gear ratio/speed, weight and durability (from previous experience) of the actuators proved to be a vital part in their selection for the eSARA platform.

Gear Option	35:1	63:1	150:1
Peak Power Point	50N @16mm/s	75N @10mm/s	175N @4mm/s
Peak Efficiency Point	24N @24mm/s	38N @15mm/s	75N @7mm/s
Max Speed (no load)	32mm/s	20mm/s	8mm/s
Max Force (lifted)	50N	100N	200N
Back Drive Force	31N	46N	102N
Stroke Options	50mm	100mm	140mm
Mass	56g	74g	84g
Positional Accuracy	0.3mm	0.4mm	0.5mm
Max Side Load (extended)	40N	30N	20N
Feedback Potentiometer	9k Ω ±30%	18k Ω ±30%	25k Ω ±30%
Electrical Stroke	48mm	98mm	138mm
Input Voltage	0-15 VDC. Rated at 12VDC.		
Stall Current	650mA @ 12V		
Operating Temperature	-10°C to +50°C		
Audible Noise	60dB @ 45cm		
Ingress Protection	IP-54		
Mechanical Backlash	0.2mm		
Limit Switches	Max. Current Leakage: 8uA		

Table 5: Available features for the L-16 actuators [96].

3.2.1.2 Elbow Brace

The innovator X[®] elbow brace by Össur (Americas) [99] was used as a starting point for making the eSARA platform wearable. The brace's arm grips were used but not the elbow angle constraints. This elbow brace was selected due to its light weight and secure/easy attachment to the arm. The elbow brace, shown in Figure 41, provided an easy attachment of the eSARA platform to the user. The strapping mechanism provided convenience when taking on and off eSARA while the open structure provided ease of movement for the SCI individuals.



Figure 41: The innovator X[®] elbow brace by Össur [99].

3.2.1.3 End Effector

The claw kit and 2-Wire Motor 393 from VEX Robotics [100] was used for the end effector due to its ability to hold and grasp various objects. The rubber coating inside the claw prevented objects from slipping. The gap between the claws allowed for a tighter grip on various objects. With the use of the servo, the position of the grabber could be monitored at all times. Figure 42 shows both the motor and servo.

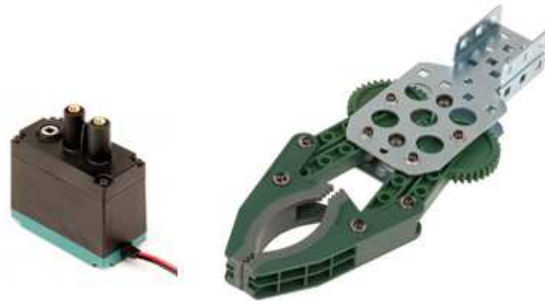


Figure 42: Claw kit and 2-wire motor 393 from VEX Robotics [100].

3.2.1.4 Machined Parts

A top plate and base plate were machined from stainless steel forming a sturdy frame for the exo-skeletal boundary of the arm. Stainless steel was chosen to prevent the exo-skeletal structure from collapsing during experiments. A floating handle (between the two plates) was machined from aluminum. Aluminum was selected due to its light weight and durability and also because the handle would not be subjected to intense movements or force. Two brackets to hold the biceps and triceps actuators were also machined from stainless steel for strength and durability as the biceps and triceps actuators were to mount directly to the brackets. Stainless steel provided durability against any unexpected weight on the platform. Stainless steel was also a first choice due to low cost and availability. Figure 43 shows the machined parts of eSARA. The forearm top and bottom support rails are shown in 'a' and 'b', respectively. The triceps and biceps brackets to

attach the actuators are shown in ‘c’ and ‘d’, respectively. The parts and assembled handle are shown in ‘e’ and ‘f’.



Figure 43: Machined parts of eSARA a) Top of the arm used to hold the extension rail, b) Bottom plate to hold the floating handle, c) Bracket to hold triceps actuator, d) Bracket to hold biceps actuator, e) Floating handle components, f) Assembled floating handle.

3.2.1.5 Microprocessor (Arduino)

The Arduino Duemilanove [101] is a microcontroller board based on the ATmega328 [102]. The hardware consists of an open-source hardware board designed around an 8-bit Atmel AVR microcontroller. It has fourteen digital input/output pins. Six can be used as pulse width modulation (PWM) pins marked by ‘~’ and six analog inputs. This Arduino also consists of 16 MHz crystal oscillator, a USB connection, a power jack, an ICSP header, and a reset button. Table 6 summarizes the Arduino Duemilanove’s characteristics. Arduino provides an easy to use, open source electronic platform.

Hardware	Specification
Microcontroller	ATmega328
Operating Voltage	5V
Input Voltage	7-12V
Input Voltage	6-20V
Digital I/O Pins	14 (of which 6 provide PWM output)
Analog Input Pins	6
DC Current per I/O Pin	40 mA
DC Current for 3.3V Pin	50 mA
Flash Memory	32 KB (ATmega328) (2 KB used by boot-loader)
SRAM	2 KB (ATmega328)
EEPROM	1 KB (ATmega328)
Clock Speed	16 Hz

Table 6: Summary of the Arduino Duemilanove microcontroller board.

3.2.1.5.1 Power

This board can be powered from a USB connector or an external power supply of 6 to 20 volts. The power source was selected automatically. If the external power was less than 7 volts the five volt pin may provide power less than 5 volts on the board. Supplying more than 12 volts can overheat and damage the board. A pin named 'V_{IN}' provided input voltage to the Arduino board when an external power source was used. The pin name '5V' provided 5 volts once the Arduino was powered. Similarly the 3.3V and GND pins provided 3.3 volts and ground, respectively.

3.2.1.5.2 Memory

The ATmega328 has 32 KB of flash memory for storing code (of which 2 KB is used for the boot-loader), 2 KB of SRAM, and 1 KB of EEPROM.

3.2.1.5.3 Input and Output

From the 14 available pins, each can be used as an input or output. This board has 6 analog inputs, each of which provide 10 bits of resolution (i.e. 1024 different values). By default they measure from ground to 5 volts.

3.2.1.5.4 Communication

The Arduino Duemilanove is capable of communicating with a computer, another Arduino, or other microcontrollers. The ATmega168 and ATmega328 provide UART TTL (5V) serial communication available on digital pins 0 (RX) and 1 (TX). An FTDI FT232RL on the board channels this serial communication over USB and the FTDI drivers (included with Windows version of the Arduino software) providing a virtual com port to software on the computer. The Arduino software includes a serial monitor which allows simple textual data to be sent to and from the Arduino board. The RX and TX LEDs on the board flashed when data was being transmitted via the FTDI chip and USB connection to the computer (but not for serial communication on pins 0 and 1). The software serial library allows for serial communication on any of the Duemilanove's digital pins. The ATmega328 also support I2C (TWI) and SPI communication. Arduino Duemilanove board, [101] using Integrated Developmental Environment (IDE) was used to upload the programs to the Atmega 328p microprocessor chip by Amtel [102]. The handshake between the voice recognition module and Arduino was achieved without third party software or licenses. Figure 44 shows the Arduino Duemilanove board with the Atmega chip.

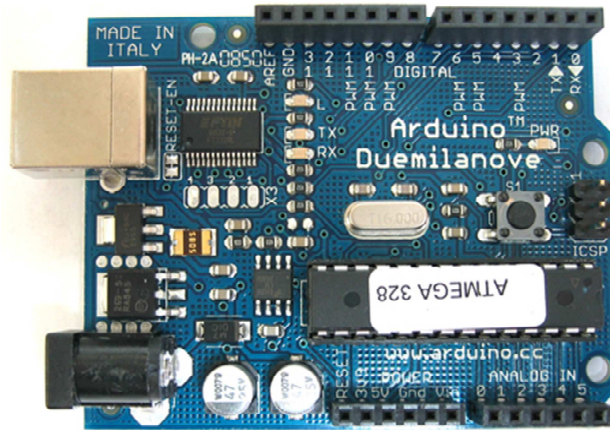


Figure 44: Arduino Duemilanove board with Atmel Atmega 328 chip [101, 102].

3.2.1.6 Push Buttons

Push buttons were used as one mode of controlling the extension and grasping of the device. The buttons were color coded for extension of the arm (blue) and for grasping (red). The buttons were placed in the orientation shown in the figure below for ease of use. The extension buttons were in one line and grasp/release buttons were perpendicular to them. This divided the two distinct functions (extension/contraction and grasping/releasing) needed into two different sections. In the future, the size and spacing requirements for these buttons could be optimized. Figure 45 shows the buttons used for this control mode.



Figure 45: Examples of the color coded push buttons used in the device.

3.2.1.7 Slider

Figure 46 shows a sliding resistor. This resistor served to provide a slide-able controlling mode for the device. Two of these resistors were used; one controlled the extension/contraction of the arm while the other controlled the grasping releasing of the end effector. The sliders were housed in a clear box as show in Figure 36.



Figure 46: Slider used to control extension and grasping.

3.2.1.8 Voice Control Module

The speech recognition module, VRbot by Veear, was used for voice recognition mode [103]. This VRbot was selected due to high robustness and user recognition through training. The VRbot was able to record the command words in any accent or language. These abilities, combined with the cost, made VRbot the first choice for the eSARA platform. Figure 47 shows the VRbot that was used for the eSARA voice control.



Figure 47: VRbot by Veear [103].

3.2.1.9 Force (Pressure) Sensor

The Force Sensing Resistor (FSR) from Interlink Electronics [104] was used in the handle for the lift assist part of the device. The FSR shows a decrease in resistance when there is an increase in the force applied. This feature allows the sensor to detect force or pressure with sensitivity ranging from a few grams to a few kilograms. This sensor, designed for human touch control applications, is shown in Figure 48.

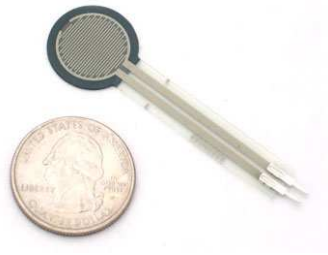


Figure 48: The FSR sensor by Interlink Electronics [104].

3.2.1.10 Battery

A lithium polymer battery by SMC Lightning Volts was used. This battery was rated at 11.1 volts and 55.5Wh with 5000mAh. This battery was sufficient to drive all of the actuators, control modes, and the lift assist simultaneously. The chosen battery is shown in Figure 49.



Figure 49: Lithium polymer battery: 11.1V, 55.5Wh with 5000mAh.

3.2.1.11 Safety (Emergency Stop)

Safety switches were used to control power to individual circuits and the main power. The overall system of eSARA was designed such that the main power supply was routed through a safety ‘Main Power’ switch. Beyond this main power switch, the lift assist and the modality control units have individual power switches. Once the main power switch is turned on, the user has the flexibility to turn on either the modality control switch, or the lift assist switch, or both, depending on his or her needs. The switches are shown in Figure 50.

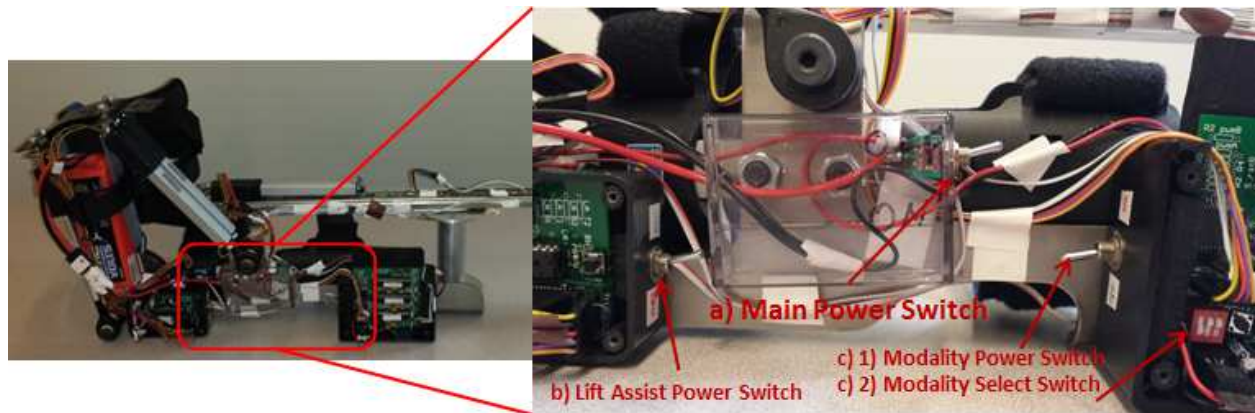


Figure 50: Safety and power switches: a) Main power switch, b) Lift assist power switch, c) Modality control power and modality selection switches.

When the main power and lift assist switches are turned on, lift assist is activated and ready for use. Once power is supplied to the modality control unit, the user then has the ability to select from the 3 given modes of control (button mode, slider mode, or voice mode). Once the control mode is selected the device is ready for use. Turning off the main switch cuts power to both the modality and lift assist control units even if their individual power switches are turned on. Once the main power is turned back on, the modality and lift assist settings are retained.

3.2.2 System Architecture

The eSARA platform was divided into two separate control units, the modality control unit and the lift assist control unit. Figure 51 shows the hierarchy of the system and illustrates how the various modes were isolated for their specific purpose.

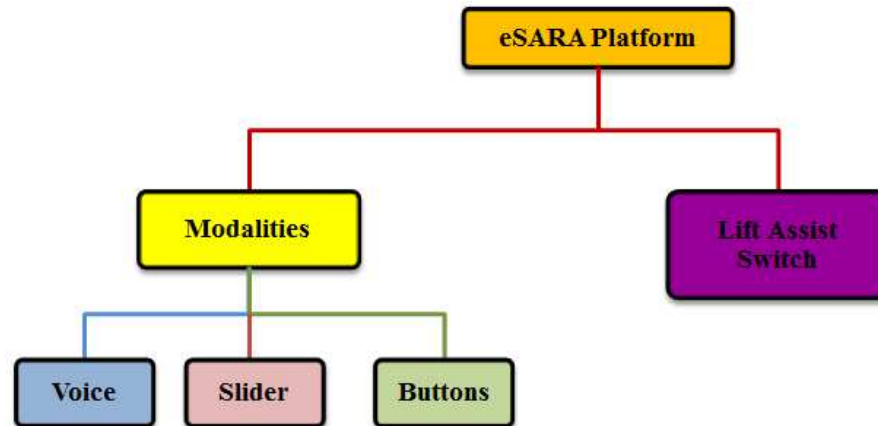


Figure 51: Hierarchy of the system firmware.

When the lift assist unit is powered on, the biceps and triceps actuators rely on two pressure sensors on the top and bottom of the device's handle. When the modality control unit is powered on, a modality must be selected to control the extension and grasping of the eSARA platform. When selecting voice mode, the protocol described in the previous chapter is followed. Briefly, a trigger word activates the system, followed by the command word to enable the desired action. The system was designed so that once the trigger word is said the system waits for the command word. Once the command word is detected, the respective command is carried out. When selecting slider mode, the extension and grasping sliders are activated. One slider controls the extension of the arm and the other controls the grasping of the end effector. When selecting the button modality, the four buttons responsible for extension and grasping are activated. Each

button is connected to a specific action: extension, contraction, grasping, or releasing. This mechanism is summarized in Figure 52 below.

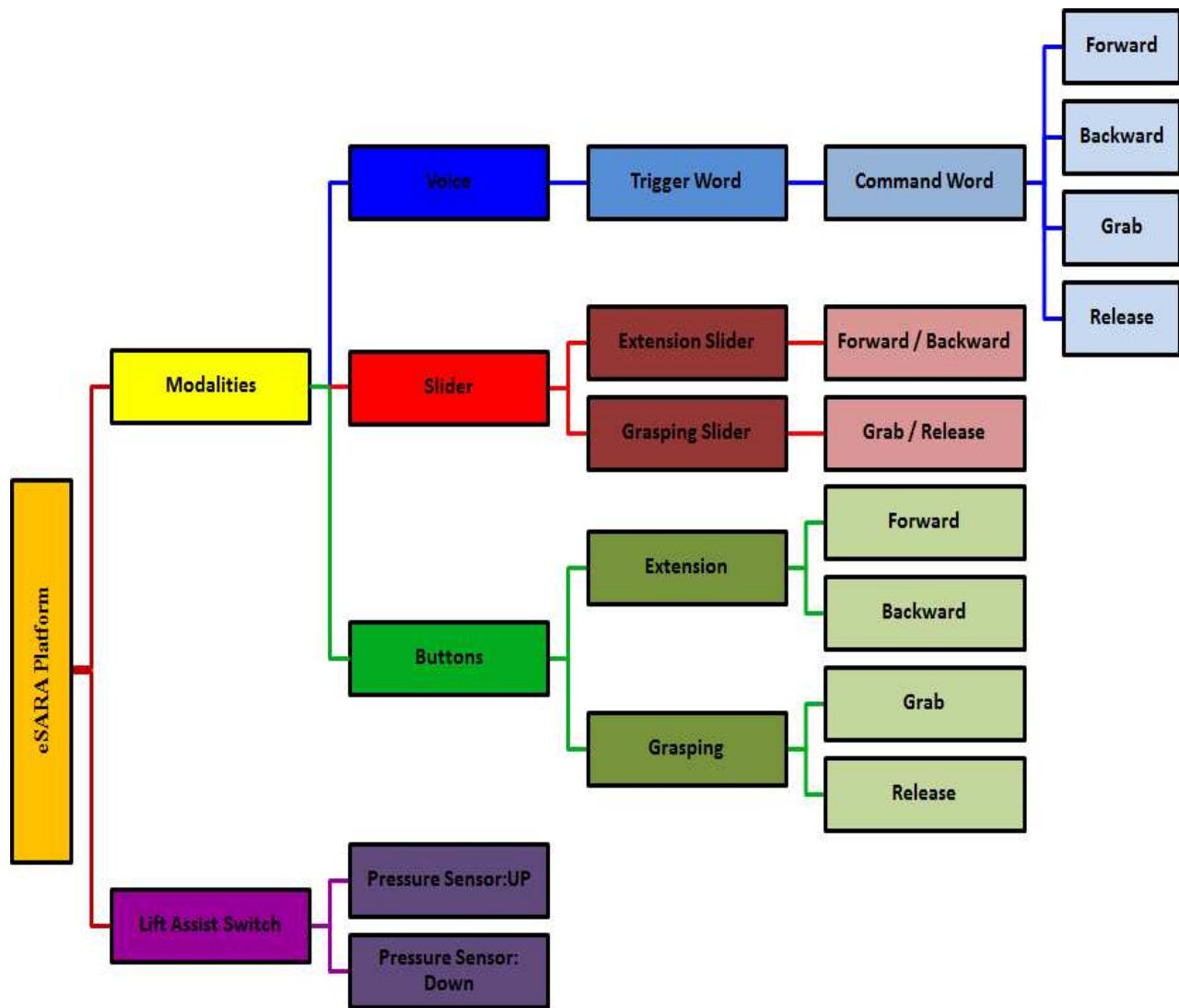


Figure 52: Flow chart of the control mode and lift assist processes.

3.2.2.1 Voice Control (Ballistic Control Mode with Minimal Movement of the Extremities)

The voice command was divided into a trigger word and command word, similar to SARA in chapter 2. In addition to the original command words, grab and release, two new command words were added. These command words, forward and backward, were added so that

the participants could control the extension of the arm. The voice control unit was capable of recording the voice of the participant in order to associate the appropriate trigger and command words. This feature makes the voice controls highly customizable and user friendly. Table 7 summarizes the entire trigger and command words used during the participant study showing flexibility and customizability of the voice module.

Trigger Word	Command Word			
	Extension	Contraction	Grasping	Releasing
Max	Forward	Backward	Grab	Release
Joe	Go	Back	Close	Open
Robot	Move Forward	Move Backward	Hold	Drop

Table 7: Trigger and command words used in the voice control modality.

Table 7 shows the various trigger and command word combinations that were used by the different participants during the experiment. Following the voice modality structure, when a participant says the trigger word, 'Joe', once, the system was activated. The participant then says the command word, 'go', 'back', 'close', or 'open', to perform the desired function. The voice mode was customized for each participant as various participants were comfortable using different trigger and command words.

Figure 53 below shows the voice recognition module used in this research. The programmable user interface of the VRbot allowed multiple customizable options. This Figure shows the VRbot and the housing for the VRbot that was used for the participant study. The Graphical User Interface (GUI) is also shown in the figure. This GUI enabled the participants to record custom word combinations from Table 7.

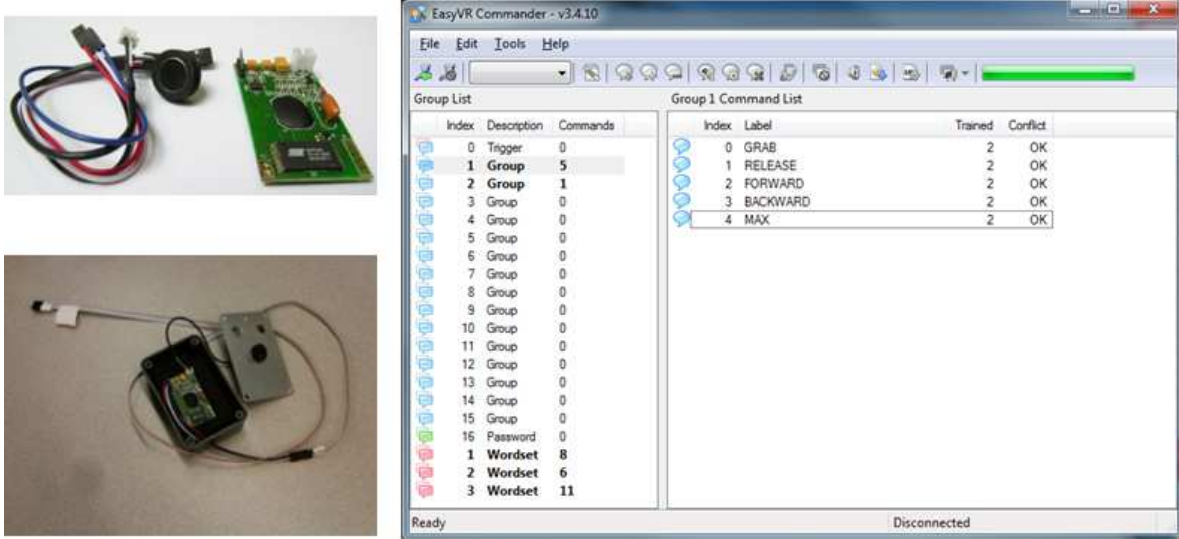


Figure 53: Voice control mode showing VRbot and the Graphic User Interface (GUI) for VRbot [103].

3.2.2.2 Button Control Mode (Ballistic Control Mode with Minimal Movement of the Extremities)

Four separate buttons, each responsible for a unique task, were connected to the control board. The red set of buttons, shown in the figure below, were moment on-off buttons attached to the grabber motor. Once a button was pressed the grabber opened or closed depending on the button pressed. The blue set of buttons, shown in figure below, were on-off buttons connected to the extension unit of the arm. Once a button was pressed, the arm extended and kept extending until the button was pressed again. Pressing the button the second time stopped the extension. This enables the participants to extend the arm and position/orient it in a direction of choice and to utilize the grabber at the same time. For instance, if a participant was trying to reach something on the far end of the table, the participant can extend the arm and while the arm was extending open the grabber unit to make it ready for grasping the object. Once the desired position was reached, the participant can stop the extension, by pressing the blue button again, and grab the object desired. Then during the retrieval of the arm the participant can move the arm to the next desirable position without holding the button until the arm was fully collapsed.

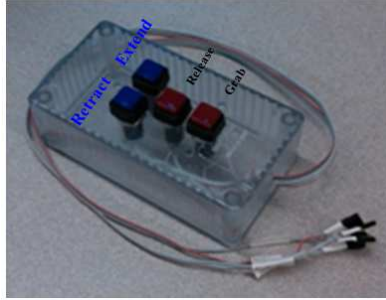


Figure 54: Button Control mode.

3.2.2.3 Slider controlled (Continuous Control Mode with Major/Continuous Movement of the Extremity)

This mode of control consists of a pair of sliders that allow participants to extend the arm of the device to a desired length with a light pushing motion. When the slider is pushed forward, the actuator extends. The actuator continues extending until the slider is brought back to a central green marked area- the dead zone. To retract the arm, the slider is pushed backwards until the appropriate length is achieved and then the slider should be returned to the dead zone.

A second slider provides the ability to open or close the gripper. To grab an object, the slider is pushed forward. If the grabbed object slipped this grabber unit was powered constantly by moving the slider out of the dead zone. Participants were advised to keep the slider inside the dead zone. If the slider was outside of the dead zone for a prolonged period of time, the grabber motor and the circuit could overheat. To release an object the slider is pushed backwards allowing the grabber to open. The two sliders for continuous control mode are shown in Figure 55.

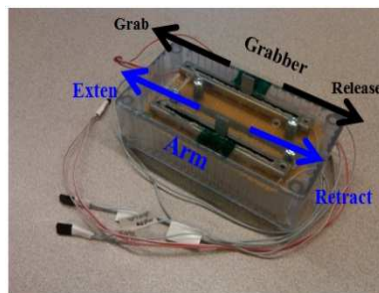


Figure 55: Slider Control Mode.

3.2.2.4 Proportional Integral Derivative (PID) Control and Tuning

Filtering out the tremors and achieving smooth transition in both upward and downward directions were critical aspects of the platform. Therefore, a feedback mechanism was needed to control the biceps and triceps actuators of the eSARA platform. A proportional-integral-derivative (PID) controller was used as a control loop feedback mechanism. This controller calculates ‘error’ as the difference between the set point and the feedback (Error = Set point – Feedback). The digital controller tries to minimize the error by adjusting the ‘process’ control inputs. PID is named for three distinct parameters: the Proportional (P), the Integral (I), and the Derivative (D) values. These values are computed in terms of time where P depends on the present error, I depends on accumulation of past errors, and D is a prediction of future errors, based on current rate of change. The subjective sums of these three quantities were used to fine-tune the process by a control element. For example the position of a control valve, another example can be controlling the power supplied to a heater. Another example can be in which the set point was equal to the Required Temperature of the water. Feedback was given by the skin and error was equal to the difference. The controller was the brain and the output was a function of the error.

The controller can provide the desired action by tuning the three parameters of the PID algorithm. The system proved to be more robust when the response of the controller to the error was the shortest, meaning the degree to which the controller overshoot the set point and the system oscillation were minimized. However, the PID algorithm does not assure system stability. In some cases only one or two parameters provides appropriate control of the system, accomplished by setting other parameters to zero. The control can then be called a PI, PD, P, or I controller with respect to the absence of the zeroed parameter(s). Derivative action generally

measures noise and leads to frequent use of the PI algorithm, where the absence of the integral term may prevent the system to reach the targeted value due to control action.

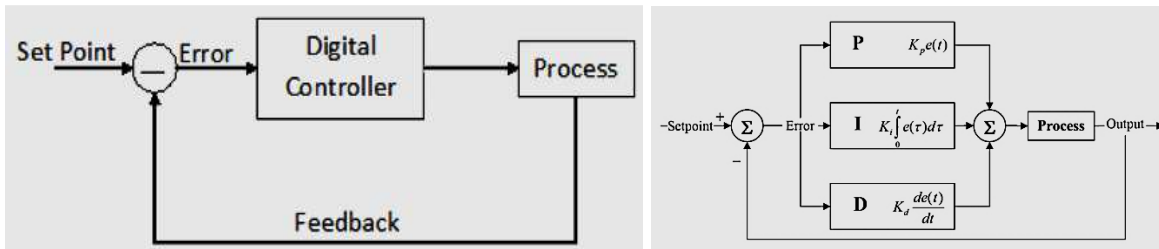


Figure 56: The PID controller concept (left) and the PID algorithm (right).

The algorithm does not know the correct output to bring the process to the set point, but rather adjusts the output so that the process moves towards the set point (refer to Figure 57).

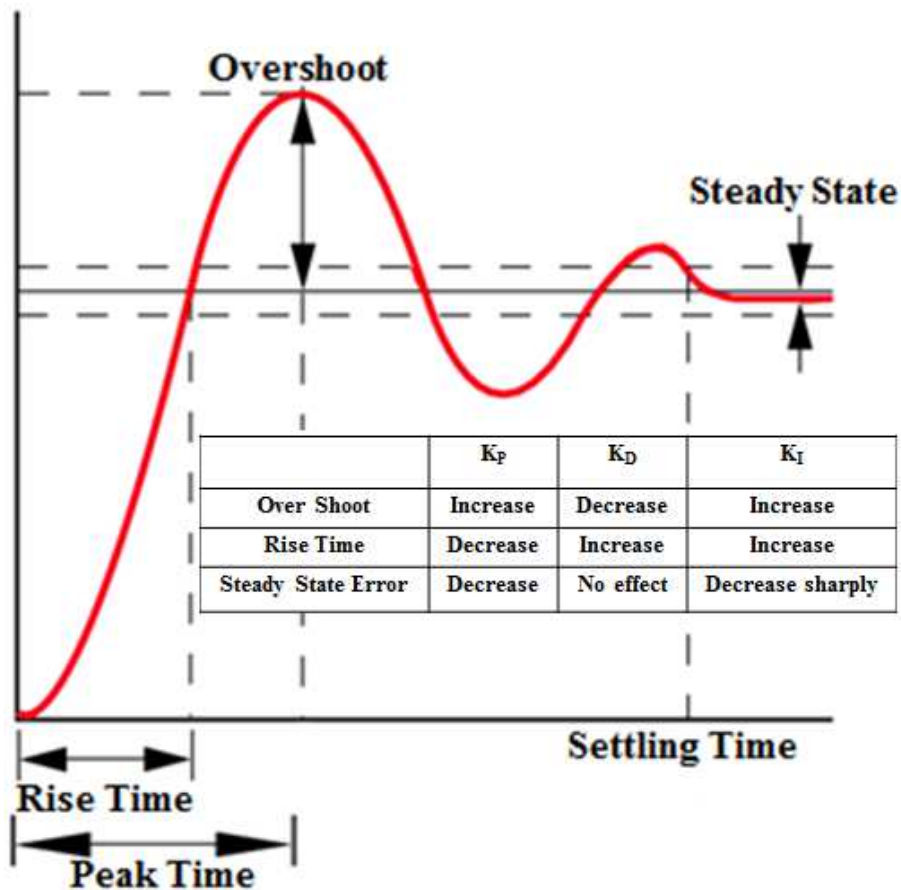


Figure 57: PID Tuning

3.2.2.5 Tracking Biceps and Triceps Actuators as an Antagonistic System

Parallel PID controllers were used to tune the eSARA lift assist. An equation was used to calculate a ratio of distance travelled by the biceps actuator (BA) to that of the triceps actuator (TA) as these two actuators differed in their lengths. The biceps actuator was marked at quarter inch intervals along its entire length. The respective potentiometer position feedback from the actuator counts were noted through the serial monitor. At every point the bicep actuator's readings were taken, the triceps actuator was marked and its position feedback from the serial monitor was noted. The markings from the triceps actuator were measured in inches. Figure 58 shows the marked biceps and triceps actuators.

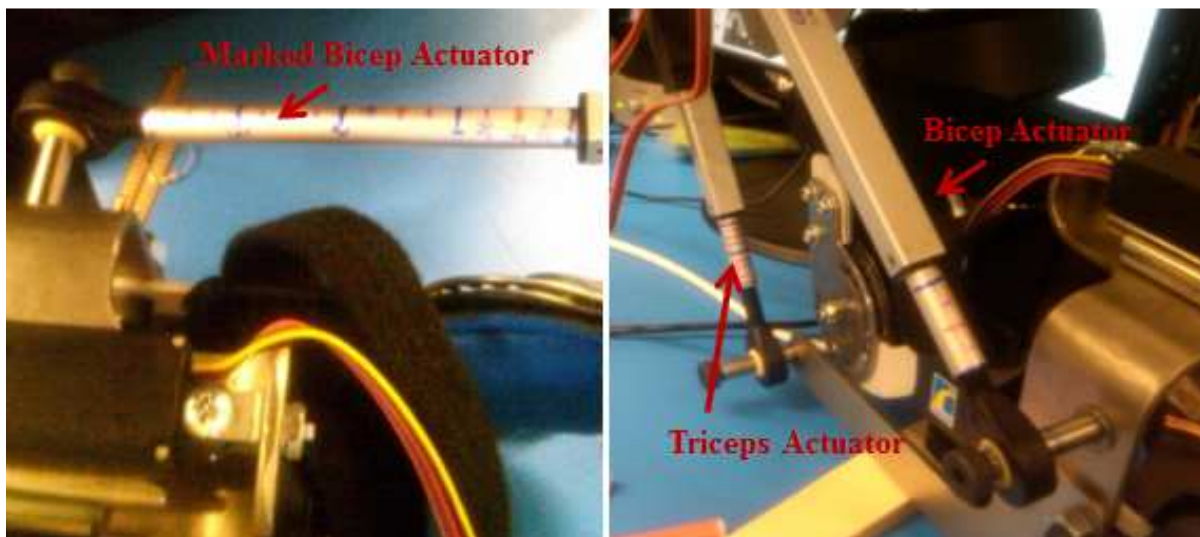


Figure 58: The calibrated BA (left) and the calibrated TA using BA as the primary actuator.

Measured lengths of the marked BA vs. measured lengths of the TA are plotted in Figure 59 along with a plot of the biceps actuator position feedback vs. the triceps position feedback.

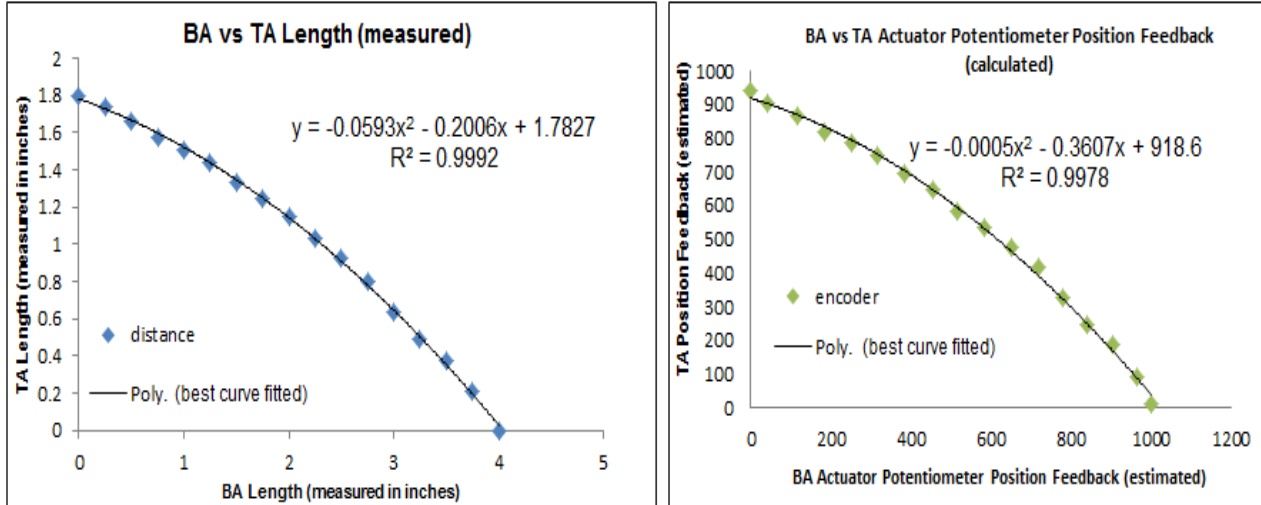


Figure 59: Distance travelled by biceps actuator vs. triceps actuator (left). Potentiometer position feedback from the biceps actuator vs. the triceps actuator.

From the position feedback an equation of best fit was determined as follows:

$$Output = y = -0.0005x^2 - 0.3607x + 918.6 \quad \text{Equation 1}$$

This equation provided a start point for the PID parameter tuning. The parameters were tuned according to the following equations:

PID parameters:

$$pwm1 = k_{p1} \times Error1 + k_{d1} \times (Error1 - LastError1) \quad \text{Equation 2}$$

$$pwm2 = k_{p2} \times Error2 + k_{d2} \times (Error2 - LastError2) \quad \text{Equation 3}$$

Where *Error1* and *Error2* are given by:

$$Error1 = SetPoint1 - Actuator1Value \quad \text{Equation 4}$$

$$Error2 = SetPoint2 - Actuator2Value \quad \text{Equation 5}$$

The sensed position, called the actuator value, was considered the process variable. The desired position was called the set point. The input to the processes was the position of the actuator and the output of the PID controller was called the manipulated variable or the control variable. The difference between the measured actuator position and the set-point was the ‘error’.

The ‘error’ quantifies whether the actuator position was higher or lower and by how much. The

PID controller sets the actuator position after measuring the process variable and calculating the error. The proportional control method (P) sets the actuator position in proportion to the current error. The derivative control method considers the rate of change of position of the actuator the position in adjusting the error. Finally, the integral action method uses the average position in the past to detect whether the position of the actuator was set too high or too low and sets the position proportional to the current error. Over time the steps add up (with the discrete time equivalent to the integration) the past errors. If a change was made that was too large when the error was too small lead to over-shooting the position. If the controller were to repeatedly make changes that were too large and constantly over shoots the target. The output oscillated around the set-point in a growing sinusoid. In this case the parameters were heavily tuned until the output oscillated around the set point. Fine tuning was done afterwards to minimize or eliminate any oscillations or jittering of the system. After the parameters were tuned, the position feedback serial readout of the biceps actuators vs. the triceps actuators was plotted and the outcome is shown in Figure 60.

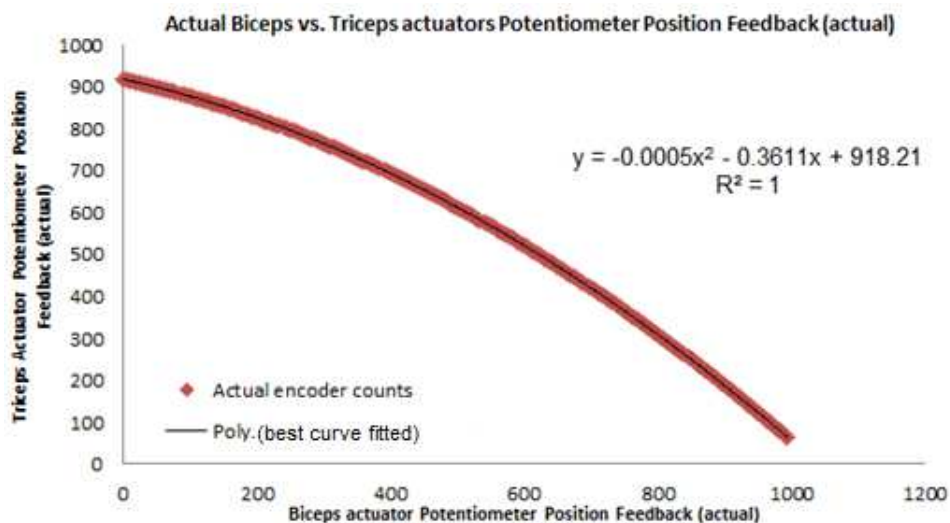


Figure 60: Actual BA vs. TA potentiometer position feedback from the actuator counts. An equation for the curve of best fit was obtained.

grabber motor pins were connected to the 16, 17, 11, and 12 pins of the Atmega 328 microprocessor, respectively. These pins were declared as output pins. It was written in the code that if, for example, the user presses the contraction button while the extension button is already pressed, no changes would take place. This type of code was applied to the grabber button controls as well. However, the extension actuator and the grabber motor can work simultaneously.

3.2.3.2 Slider Modality

For the slider control mode, the extension/contraction and grab/release sliders were connected to pins 24 and 25 of the Atmega 328 microprocessor, respectively. These pins were declared as input pins. The enable pins (both A and B) were connected to 5 volts. The extension and grabber motor pins were connected to 16, 17, 11 and 12 pins of the Atmega 328 microprocessor, respectively. These pins were declared as output pins. A variable, 'Current Value', was declared to hold the current values of the sliding potentiometers and the initial value was set to zero. The sliding potentiometer was positioned in a neutral zone. Once the slider moved from the neutral position, the potentiometer limit set in the code was exceeded and the extension or grasping motors of the arm became active. The extension slider (ES) and grabber slider (GS) values are read from the analog pins with extension and grasping being adjusted by changing the settings for the extension motor pins (EMPin1, EMPin2) and the grabber motor pins (GMPin1, GMPin2).

3.2.3.3 Voice Modality

For the voice mode, Arduino had to interface with the VRbot. This interface required a handshake protocol between the two hardware modules which was achieved by processing

information via software serial ports that transmitted and received information between the modules. The ports were connected to pins 18 (receiving pin) and 19 (transmitting pin) of the Atmega 328 microprocessor. The enable pins (both A and B) were connected to 5 volts. The extension motor and the grabber motor pins were connected to 16, 17, 11 and 12 pins of the Atmega 328 microprocessor respectively. An LED was added to pin 7 to provide feedback to the user for the successful handshake between the Arduino board and the VRbot.

To establish a successful protocol, certain parameters had to be sent and received between the Arduino and the VRbot. Figure 62 explains this process. Once the protocol was established, Arduino transmits the character 'b' and receives the character 'o' from the VRbot. Once the expected character was received, the VRbot was active (awake) shown in part (a) of the figure.

<pre>tx.print('b'); for(i=0; i<100; i++){ if (rx.read()=='o'){ Serial.println("awake"); break; } }</pre> <p style="text-align: right;">a</p>	<pre>tx.println('x'); for (i=0; i<100; i++){ if (rx.read()=='x'){ Serial.println("x received"); break; } }</pre> <p style="text-align: right;">b</p>	<pre>tx.println(' '); for(i=0; i<100; i++){ if(rx.read()=='A'){ Serial.println("firmware good"); break; } }</pre> <p style="text-align: right;">c</p>
<pre>tx.print('l'); tx.println('A'); for (i=0; i<100; i++){ if(rx.read()=='o'){ Serial.println("language set"); break; } }</pre> <p style="text-align: right;">d</p>	<pre>tx.print('o'); tx.println('A'); for (i=0; i<100; i++){ if(rx.read()=='o'){ Serial.println("Infinite Timeout"); break; } }</pre> <p style="text-align: right;">e</p>	<pre>tx.print('d'); tx.print('B'); Serial.println("Say Trigger Word ");</pre> <p style="text-align: right;">f</p>

Figure 62: Handshake protocol between Arduino and VRbot.

The Arduino then sends a character 'x' and expects to receive the character 'x' from the VRbot. Once that was confirmed, Arduino registers the character 'x' as being received (Figure 62b). For the next step Arduino sends a space (' ') and expects to read the character 'A' from the VRbot. This step confirms that the firmware is functioning (Figure 62c). The language was set to English by sending the letter 'A' to the VRbot. Arduino receives the letter 'o' confirming that the language has been set to English (Figure 62d). Multiple timeouts can be selected; in this case infinite timeout was selected by send the character 'A' (Figure 62e). Finally, the handshake was

completed and the VRbot was ready to accept the trigger word for the voice chip to and to start controlling eSARA (Figure 62f). This entire process takes less than one second.

The next step was to set up the command words following receipt of the trigger word. Once the trigger word was received, the VRbot expected the command words from the allocated group slots. Figure 63a shows that after receiving the trigger word (in this case ‘Max’) the reader was active for 1000 milliseconds during which the VRbot expects to receive commands.

```

Serial.println(" : MAX Received");
reset();
Serial.println("Say Command Word ");
while (true)
{
  reader = rx.read();
  if(reader=='r')
  {
    Serial.print(reader);
    delay(1000);
    tx.print(' ');
  }
}

```

a

<pre> if(reader=='A') { Serial.print(reader); Serial.println(" : Grab"); digitalWrite(LED, HIGH); delay (20); digitalWrite(LED, LOW); digitalWrite(GMpin1, HIGH); digitalWrite(GMpin2, LOW); delay(1000); digitalWrite(GMpin1, LOW); digitalWrite(GMpin2, LOW); break; } </pre> <p style="text-align: right;">b</p>	<pre> if(reader=='B') { Serial.print(reader); Serial.println(" : Release"); digitalWrite(LED, HIGH); delay (20); digitalWrite(LED, LOW); digitalWrite(GMpin1, LOW); digitalWrite(GMpin2, HIGH); delay(1000); digitalWrite(GMpin2, LOW); digitalWrite(GMpin1, LOW); break; } </pre> <p style="text-align: right;">c</p>	<pre> if(reader=='C') { Serial.print(reader); Serial.println(" : Forward"); digitalWrite(LED, HIGH); delay (20); digitalWrite(LED, LOW); digitalWrite(EMpin1, HIGH); digitalWrite(EMpin2, LOW); delay(5000); digitalWrite(EMpin2, LOW); digitalWrite(EMpin1, LOW); break; } </pre> <p style="text-align: right;">d</p>	<pre> if(reader=='D') { Serial.print(reader); Serial.println(" : Backward"); digitalWrite(LED, HIGH); delay (20); digitalWrite(LED, LOW); digitalWrite(EMpin1, LOW); digitalWrite(EMpin2, HIGH); delay(5000); digitalWrite(EMpin2, LOW); digitalWrite(EMpin1, LOW); break; } </pre> <p style="text-align: right;">e</p>
--	---	---	--

```

Serial.println(" Command Word Received");
reset();
Serial.println("Say Trigger word");

```

f

Figure 63: Allocated command words for the VRbot.

In this sample figure the four commands: grab, release, forward, and backward, are denoted by the letters ‘A’, ‘B’, ‘C’ and ‘D’ as shown in Figure 63b-e. Once the desired command was received, the VRbot was updated and the process continued. The users only had to speak and record their voice using the Graphic User Interface of the VRbot shown earlier in Figure 53 but if more commands were needed, then the code would require additional updates.

3.2.3.4 Lift Assist

The lift assist of the eSARA platform was controlled by using the Proportional Integral Derivative (PID) system. The PID calculates an ‘error’ value as the difference between a measured variable and a set-point. The PID minimizes the error using an iterative process to adjust the initial output of the PID (manipulated variable). This control method was used because it allows a fast and improved adjustment that can be made to the system. PID provides three forms of tuning controls that were relatively easier to tune and accomplish the required task quickly and accurately.

The beginning of the program not only defines with pins but also defines the PID variables including: set-point, max-set-point, min-set-point, error-threshold, step-size, K_p , K_i , K_d , error, and last error. Equation 1 was used as the second set-point, with the first set point being the analog readout from the positional feedback of the biceps actuator. The PWMs were defined using equation 2 and equation 3. The errors were defined by equation 4 and equation 5. Figure 64a shows these equations being used in the code, while Figure 64b shows various functions being called based on the error state. The extend and contract functions, to extend or contract the actuators accordingly, lead to the rotation in the elbow joint of eSARA. The stop function stops the motion of the actuators.

<pre> if(initFlag == 0) { setPoint1 = analogRead(actuator1Analog); x = setPoint1; setPoint2 = (int)(-0.0005*x*x - 0.3607*x + 918.6); initFlag = 1; } actuator1Val = analogRead(actuator1Analog); actuator2Val = analogRead(actuator2Analog); error1 = setPoint1 - actuator1Val; Serial.print("\t"); Serial.println(error1); error2 = setPoint2 - actuator2Val; Serial.print("\t"); Serial.print("\t"); Serial.println(error2); pwm1 = kp1*error1 + kd1*(error1 - lasterror1); pwm2 = kp2*error2 + kd2*(error2 - lasterror2); </pre> <p style="text-align: right;">a</p>	<pre> if(error1 > 0) { Extend1(); } else if(error1 < 0) { Contract1(); } else { Stop1(); } if(abs(pwm1) >= 255) { pwm1 = 255; } if(error2 > 0) { Contract2(); } else if(error2 < 0) { Extend2(); } else { Stop2(); } if(abs(pwm2) >= 255) { pwm2 = 255; } </pre> <p style="text-align: right;">b</p>
--	---

Figure 64: (a) Equations used to define variables in the code (b) Functions being called based on the error state.

3.2.4 Electrical Design

The electrical design for eSARA was divided into two categories. Category 1 was the electrical design for the three control modes. Each of the three control modes were designed to control the extension/contraction and the grasping ability of the device. Category 2 was designed solely to control the two pressure sensors that were responsible for the lift assist portion of the device.

3.2.4.1 Electrical Design for Control Modalities and Extension

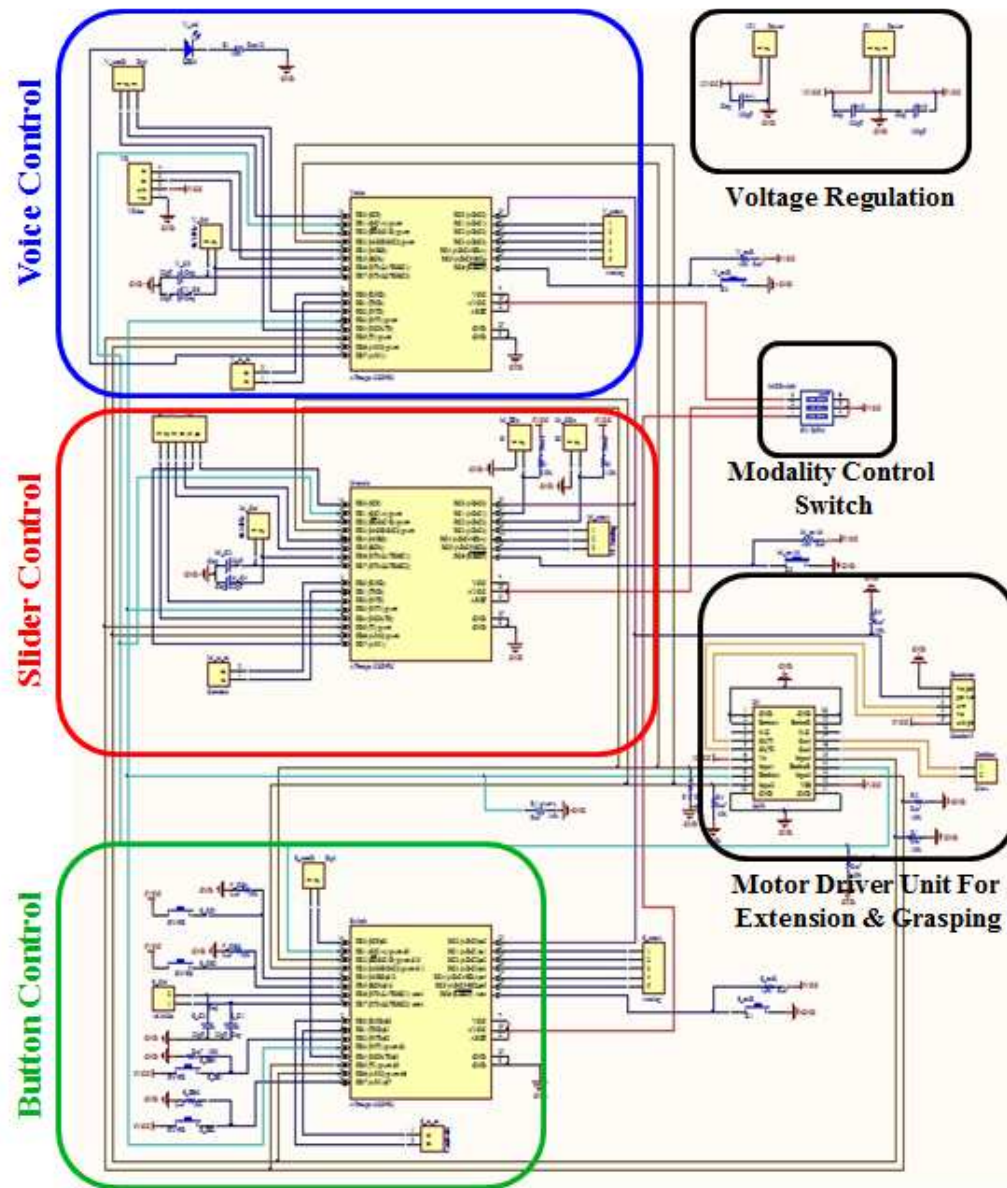


Figure 65: Full circuit diagram interfacing all the control modes for extension and grasping.

Figure 65 above shows the three Atmega 328p microprocessor chips used [102], one to connect each control mode separately. One motor driver was responsible for controlling the extension actuator and the grasping servo motors. The circuit was divided into two segments, a high voltage (11.1 volts) and a low voltage (5 volts) segment. The high voltage circuit

contained the motor driver unit for extension and grasping. The low voltage circuit consisted of the microprocessors, sensors, and feedback LEDs. The voltage regulation was used to convert 11.1 volts to 5 volts. A 28 pin motor drive, L298P, was used to drive the extension and grabber motors because this motor driver was able to control two actuators simultaneously (in this case the extension actuator and the grabber motor). Figures 66 to 70 below show detailed views of each part of the circuitry from Figure 65.

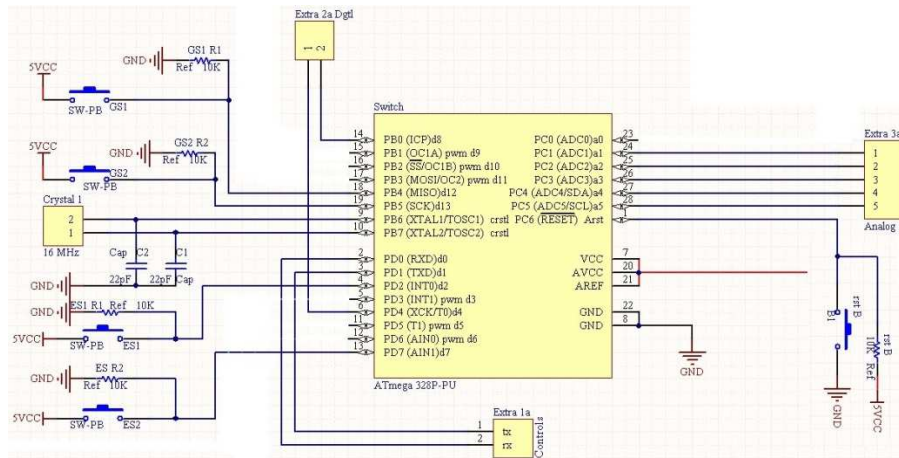


Figure 66: Atmega328 micro controller used for the button modality.

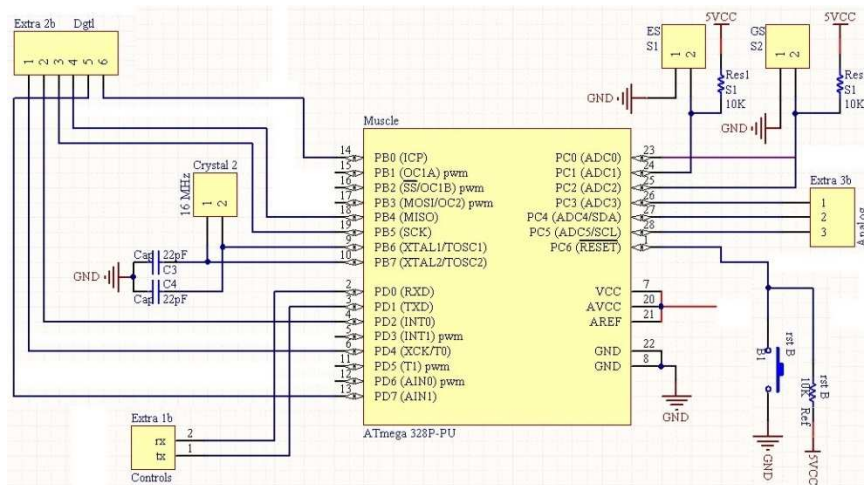


Figure 67: Atmega328 micro controller used for the slider modality.

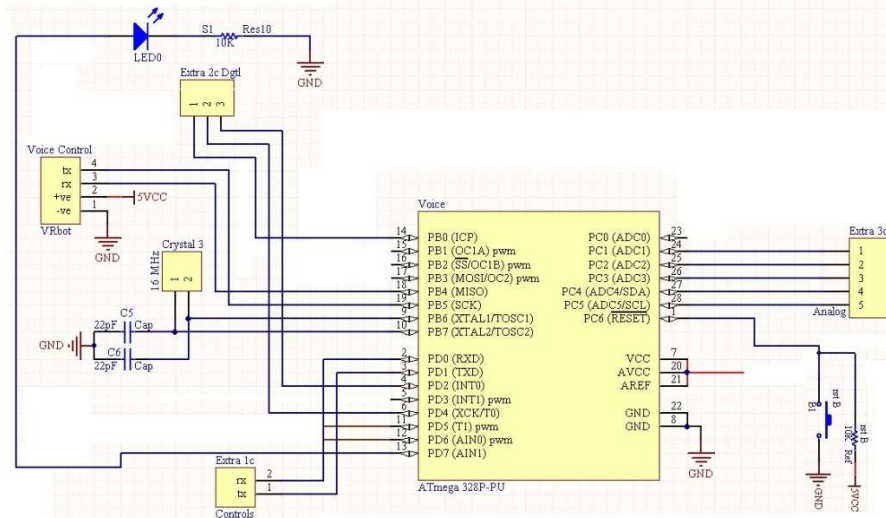


Figure 68: Atmega328 micro controller used for the voice modality.

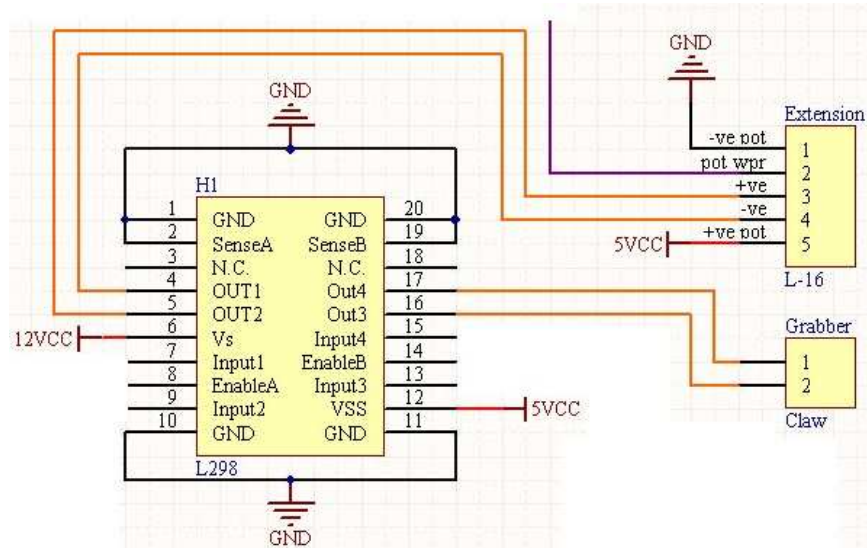


Figure 69: L298P motor-driver controlling the extension and grasping motors.

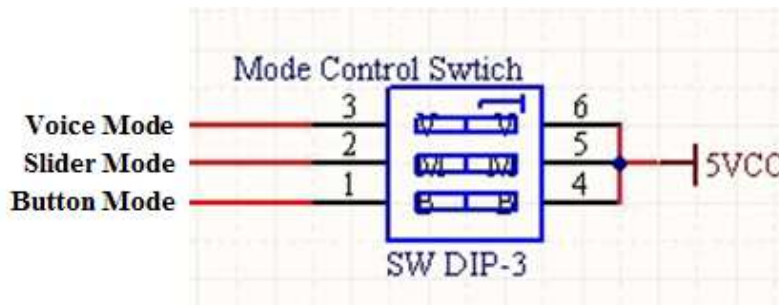


Figure 70: Modality control switch.

3.2.4.2 Electrical Design for Lift Assist Mechanism

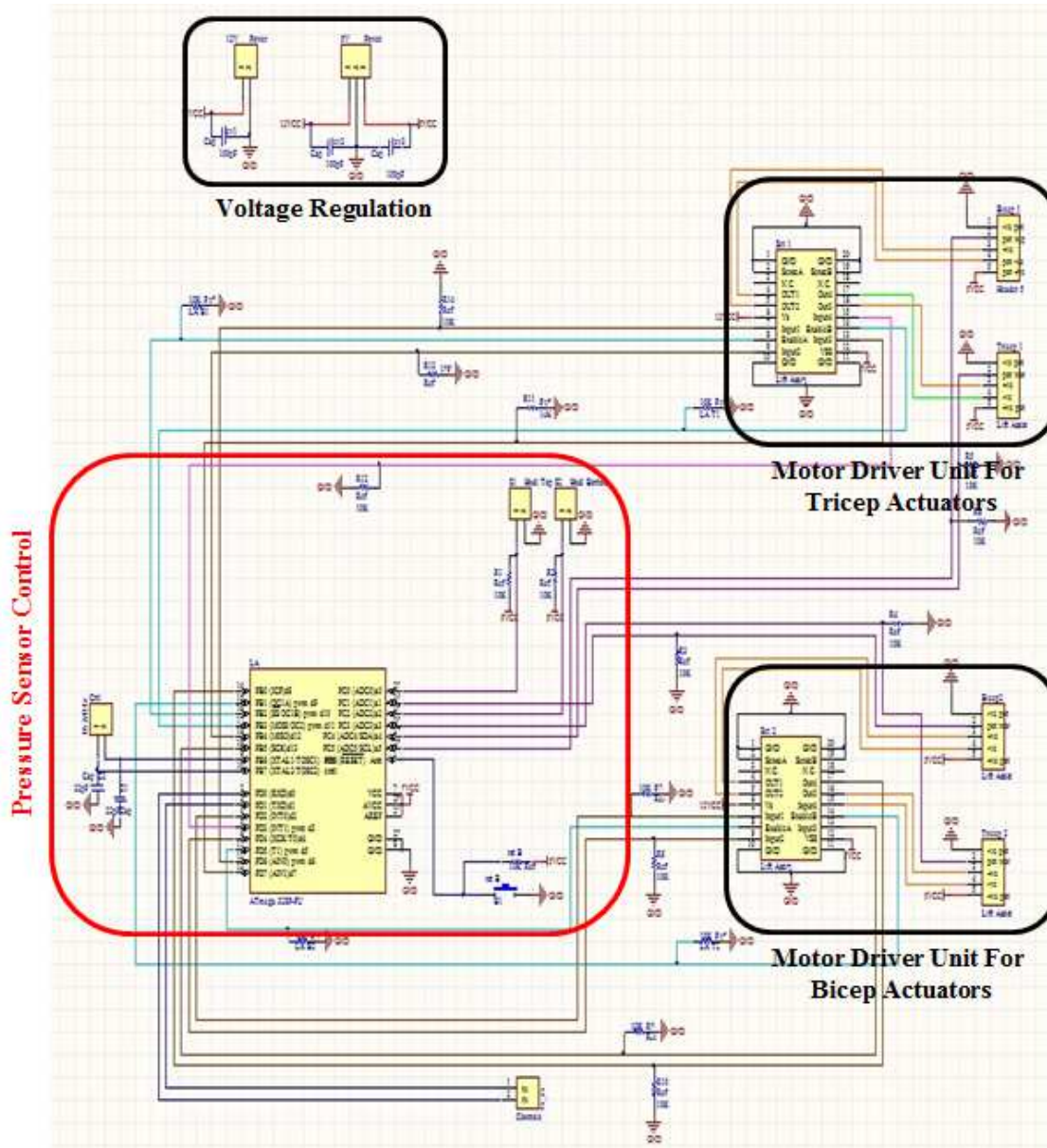


Figure 71: Full circuit diagram interfacing both of the pressure sensors for the lift assist feature.

Figure 71 shows the electrical circuit for the lift assist feature of the arm which also utilized an Atmega 328p [102] microprocessor chip. The pressure sensors provided an analog input to the microprocessor and, based on the threshold pressure, the microprocessor controlled the biceps and triceps actuators. The threshold pressure was customized for each user via a variable resistor.

The variable resistor controlled the pulse with modulation (pwm) signal and thereby changed the threshold frequency for the pressure sensors. This feature allowed participants to customize their force exerted on the pressure sensors. The PID system was used to control the rate at which the actuators moved based on the input from the pressure sensors. This process was controlled by the ‘Pressure Sensor Control’ shown in Figure 71. Here two motor driver units control the biceps actuators and triceps actuators separately. Figure 72 to Figure 75 below show detailed views of each section of the circuitry from Figure 71.

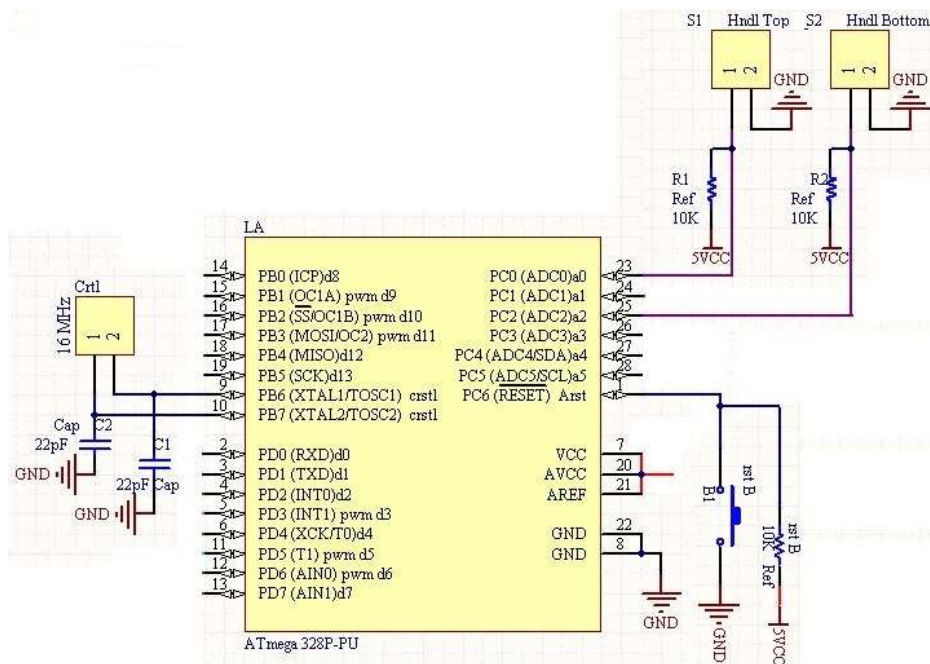


Figure 72: Atmega328 micro controller used for the lift assist pressure sensors.

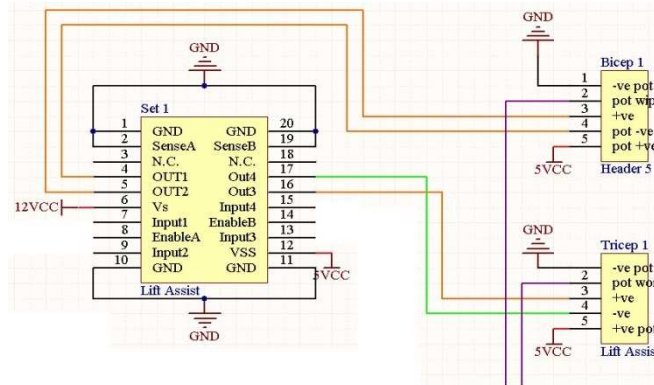


Figure 73: L298P motor-driver controlling the first set of biceps and triceps actuators.

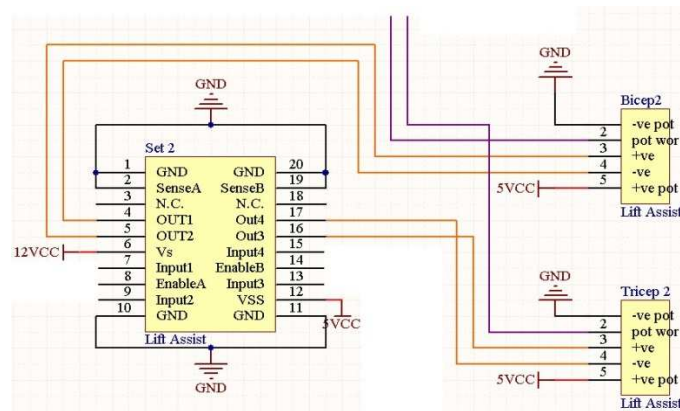


Figure 74: L298P motor-driver controlling the second set of biceps and triceps actuators.

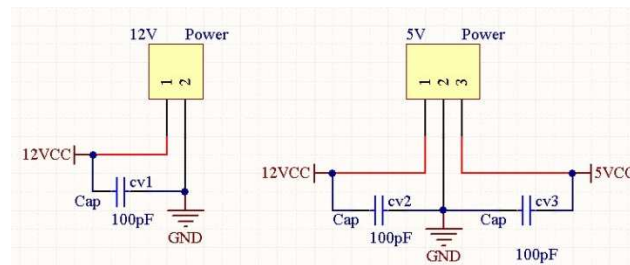


Figure 75: Voltage regulation circuit.

Both of the electrical circuits were then converted into a Printed Circuit Board (PCB) and populated with the components. Figure 76 shows the stages of the PCB for modalities, from the breadboard tests, to the plain PCB, and finally the populated PCB.

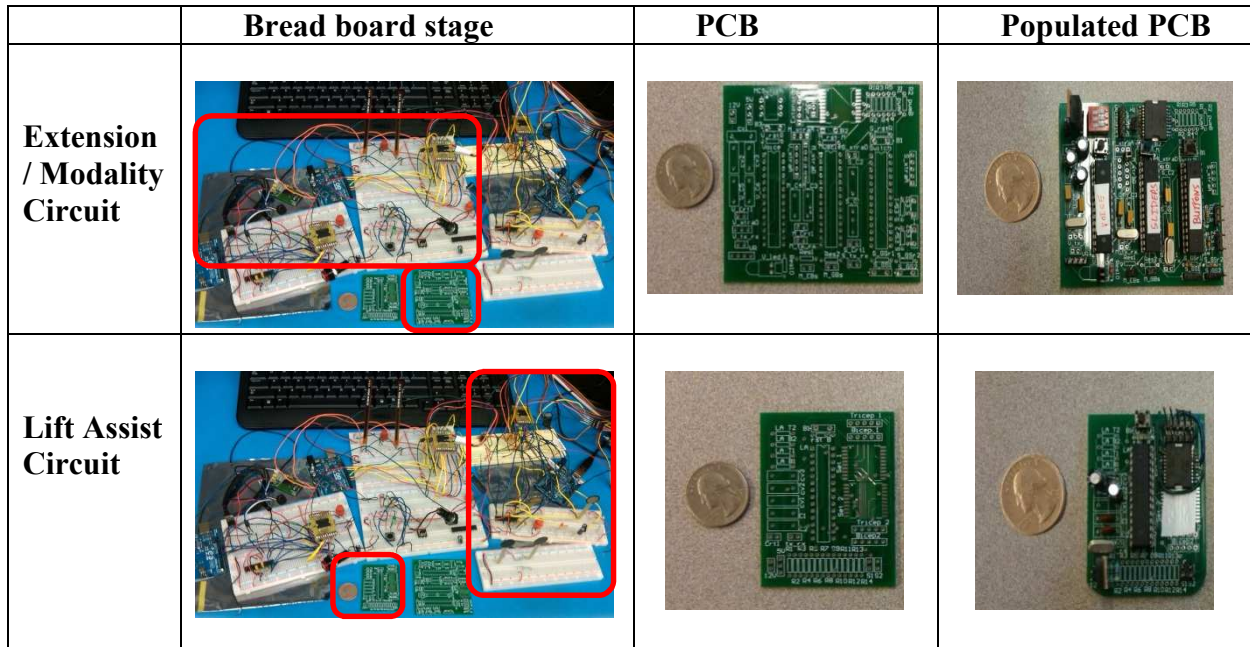


Figure 76: This Figure shows stages of the Printed Circuit Board (PCB) for the modalities from design to building and populating the PCB.

3.2.5 *Preliminary Testing of the Exo-Skeletal Assistive Robotic Arm (eSARA) Platform*

Various aspects of eSARA were tested prior to the Human Machine Interface (HMI). First, the extension and grasping units were tested with each of the modalities independently. Then the lift assist unit was tested individually. Finally, the combination of the modalities for extension and grasping were tested simultaneously and rigorously to confirm usability before HMI and the participant studies.

3.2.5.1 Extension

The length of the arm was 4 inches when fully collapsed and 15 inches when fully extended, giving the arm an extension range of 11 inches. This full range of extension was controllable by any of the modalities. The extension actuator is triggered by the control modality and keeps extending until the maximum length is reached. Figure 77 shows the fully collapsed and fully extended arm.

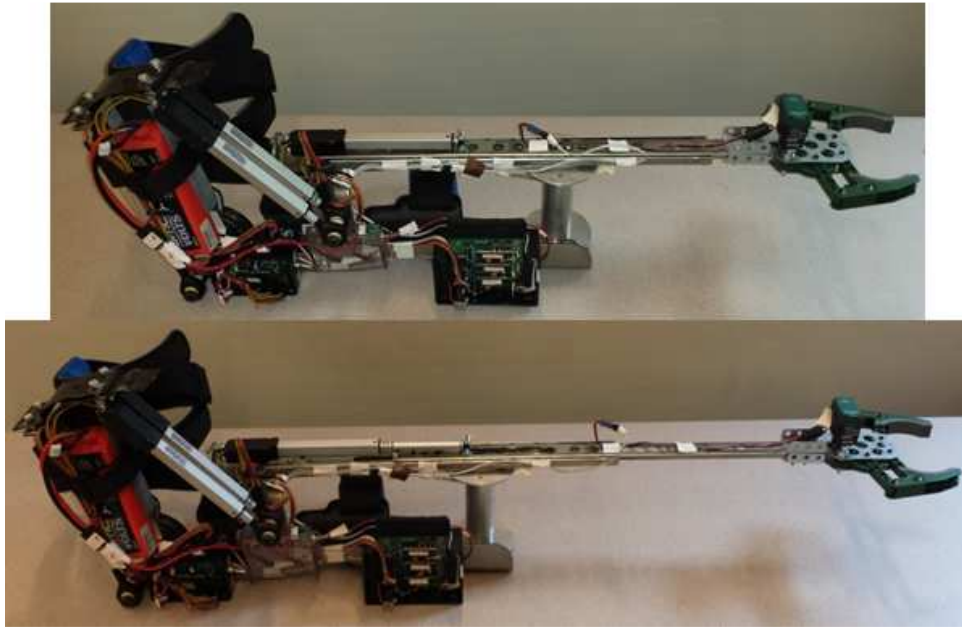


Figure 77: Figure showing eSARA with minimum and maximum extension.

Extension and grasping were first tested independently using each control modality. Then a test combining extension and grasping was conducted with each modality. Finally, all the modalities were activated at the same time with the modality selection switch. The arm was extended using one modality and retracted using the other modalities. Similarly, the grabber was opened with one mode and closed with another mode. These tests were done extensively to prevent any unexpected behavior during the participant testing.

3.2.5.2 Lift Assist

Pressure sensors were mounted in the handle of eSARA such that the user of the arm was able to control the lift assist feature with these pressure sensors. The sensors were placed so that if a participant presses down on the handle the system unfolds (arm stretches) and the system folds (arm flexes) when the participant exerts pressure on the top of the handle. Haptic feedback was added with an LED connected to the pressure sensors. The LED would light up when the pressure sensors were engaged. The biceps and triceps actuators were designed to provide lift

assist for the users. These actuators move antagonistically. The biceps actuator was longer and moved faster whereas the triceps actuator was smaller and moved slower. This antagonism produces a force couple (pure moment) creating rotation without translation or acceleration of the center of mass of the arm. The system acts like a rigid body with the pivot point being the elbow joint. The force couple acts as free vectors creating a resultant moment (torque). The calculations of these vector forces are shown in the next section. These actuators can be activated any time by turning on the main power supply and the lift assist unit. The lift assist was designed to be used frequently when retrieving the objects from the floor or above the chest.

There were two ways to control the sensitivity of the pressure sensor. First, a potentiometer was attached to the device and adjusting the resistance of the potentiometer increased or decreased the pressure sensitivity. Alternatively, the pressure threshold could be changed within the software and uploaded to the micro-processor for a specified participant. The device was capable of adapting to a user desired threshold in both of these ways in order to prevent undesired movement of the arm when the user presses on the handle. When the user presses down on the handle the pressure sensor reads the force being applied by the user. An adjustable threshold, set by the user, allows the system to move only when the force, exerted by the user on the handle, exceeds this threshold. This additional assistive feature was designed to provide the user with flexibility in choosing from a broader spectrum of objects with fewer weight constraints.

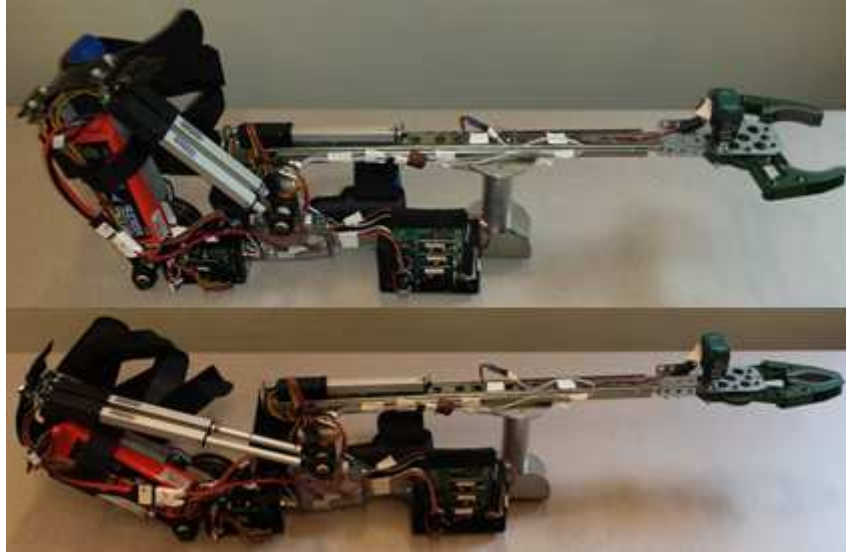


Figure 78: Figure showing eSARA minimum and maximum lift assist angles

Figure 78 shows the minimum (95°) and maximum (155°) lift assist angles. The maximum lift assist angle occurs when the biceps actuator is at its maximum extension. The platform was tested initially by isolating the lift assist feature. The arm was repeatedly tested by taking the lift assist from its minimum lift angle to its maximum lift angle. Once the lift assist functionality was successfully confirmed, a combination of extension, grasping, and lifting was tested with various objects. This preliminary pilot testing was done to assure no malfunctioning of the eSARA platform during the Human Machine Interface (HMI).

3.2.5.3 Force Evaluation/Calculations

Due to the fact that eSARA is a dynamic device with irregular shape and a shifting center of mass (depending on its position), force limitations were calculated at 9 different positions. These positions were chosen based eSARA's range of extension and flexion between the forearm and the biceps. The extension of the forearm was measured from the handle to the tip of the grabber and three points were considered: no extension (14 inches), mid-point extension (17.5 inches) and full extension (21 inches). When the biceps actuator was at its maximum length and the

triceps actuator was at its minimum length the bend angle between the bicep and the forearm of the device was 155° and the arm was considered to be in no-flex (stretched) position. When the biceps and triceps actuators were both at mid-point lengths, the bend angle was 125° and the arm was considered to be in a mid-point flex position. When the bicep actuator was at its minimum length and the triceps actuator was at its maximum length the bend angle was 95° and the arm was considered to be in a full-flex position. Figure 79 shows these three bend angles.

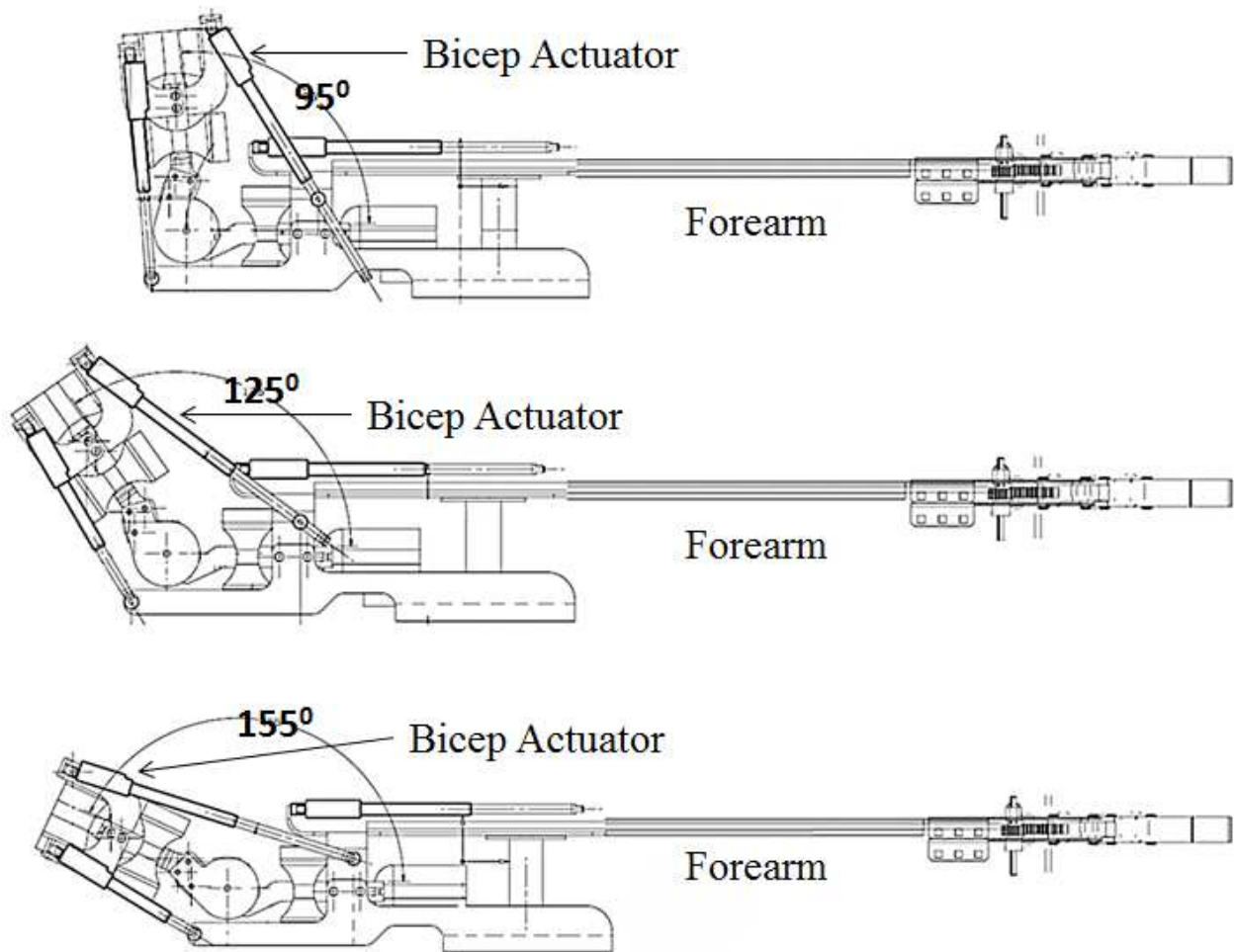


Figure 79: Side view of eSARA showing three flex angles for force calculations.

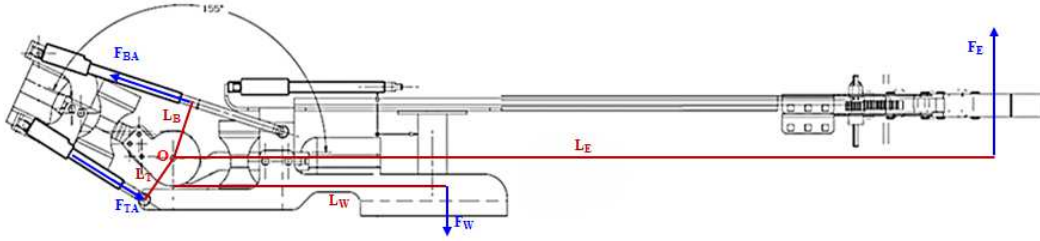


Figure 80: Calculations based on the measurements from Computer Aided Design (CAD) diagram.

Figure 80 above shows how the force at the end-effector (F_E) was to be calculated. The following steps were taken to calculate the force at the end-effector based on the torque produced at the elbow joint 'O'. Force generated by the bicep actuator and triceps actuator was denoted by F_{BA} and F_{TA} , respectively. The perpendicular distances from the point of rotation ('O') to the line of direction of the force for the bicep and triceps actuators were denoted by L_B and L_T , respectively. The torque produced by each set of actuators was multiplied by 2 because the device contains two biceps and two triceps actuators. The weight of the forearm only was denoted by F_W and its distance from the point of rotation ('O') was denoted by L_W . Similarly, the force at the end-effector was denoted by F_E and its distance from the point of rotation ('O') was denoted by L_E .

Given: $F_{BA} = F_{TA} = 44.96179$ lbs., $F_W = 4.4167$ lbs., $L_B = 2.5$ inches, $L_T = 2.126$ inches,

$L_W = 8.213$ inches. F_E was the only unknown.

Torque produced by the bicep actuators at 'O'

$$\tau_{BA} = L_{BA} * F_{BA} \quad \text{Equation 6}$$

Torque produced by the triceps actuator at 'O'

$$\tau_{TA} = (-L_{TA}) * (-F_{TA}) = L_{TA} * F_{TA} \quad \text{Equation 7}$$

Torque produced by the weight

$$\tau_W = L_W * F_W \quad \text{Equation 8}$$

Torque produced by the end-effector

$$\tau_E = L_E * (-F_E) \quad \text{Equation 9}$$

The torque produced by the actuators was equal to the torque produced by the weight and the force at the end-effector. Therefore, the following equation was generated.

$$2\tau_{BA} + 2\tau_{TA} = \tau_W - (-\tau_E) = \tau_W + \tau_E \quad \text{Equation 10}$$

From the equation above:

$$F_E = \frac{2\tau_{BA} + 2\tau_{TA} - \tau_W}{L_E}$$

The above calculations were repeated for all 9 positions described earlier based on the flex angle of the arm Figure 79.

Actuator	Flex Angle (deg)	Distance (inches)		Force (lbs.)	Torque (inc. lbs.)	Actuator count	Total Torque (inc. lbs.)	Fore-Arm Ext. Pos	LCG (inches)	FW (lbs.)	W Torq. (inc. lbs.)	LE (inches)	FE (lbs.)
		LB	LT										
Bicep	155	2.51	-	44.96	112.67	2	225.35	Contracted	10.21	4.42	45.11	24.70	15.04
Tricep	155	-	2.13	44.96	95.59	2	191.18	Mid-Way	10.72	4.42	47.35	27.70	13.33
								Extended	11.22	4.42	49.55	30.70	11.95
Average Force at Arm Fully Flexed													13.44
Bicep	125	3.75	-	44.96	168.52	2	337.03	Contracted	10.21	4.42	45.11	24.70	18.91
Tricep	125	-	1.95	44.96	87.59	2	175.17	Mid-Way	10.72	4.42	47.35	27.70	16.78
								Extended	11.22	4.42	49.55	30.70	15.07
Average Force at Arm Mid-Point Flexed													16.92
Bicep	95	4.64	-	44.96	208.40	2	416.80	Contracted	10.21	4.42	45.11	24.70	20.14
Tricep	95	-	1.40	44.96	62.86	2	125.71	Mid-Way	10.72	4.42	47.35	27.70	17.88
								Extended	11.22	4.42	49.55	30.70	16.06
Average Force at Arm Not Flexed													18.02
Overall Average													16.13

Table 8: Summary of the maximum force at the end effector resulting from the change in the extension and the flexion of the arm.

Table 8 shows the force at the end-effector in relation to the flex angle of the actuators and the change in length of the end-effector from the point of rotation. The first few columns calculate the torques for the bicep and triceps actuators. For each bicep flex angle, end-effector

force was calculated at the three forearm positions. From the table, the maximum force at the end-effector was calculated to be 20.14 lbs.

The eSARA platform was tested physically with a weight of 17.85 lbs suspended at the end-effector. Figure 81 shows this weight being lifted using the eSARA platform. This weight was tested with ‘contracted’ forearm extension and the position between the bicep and triceps flex angle of 125° to 155° . The calculated weights at positions mentioned earlier were 18.91lbs. and 20.14 lbs. Although the eSARA platform was fully capable to lift greater weight at the end-effector, it was not subjected to any additional weights. This was done as a precaution against any damages that may have occurred.



Figure 81: 17.85lb weight start and end point when moved with the eSARA platform.

3.2.5.4 Current Consumption and Battery Life Calculations

An important and critical aspect of any device is the actual time the device can be utilized (runtime). The run time is based on the power source available and the amount of power being consumed by the system. The power consumption may vary depending on the activity and duration of the individual components. Current consumption and battery life calculations were done to create a profile for the runtime of eSARA.

Table 9 shows the current usage and the battery life of all the possible commands for eSARA. The same command was repeated ten times and the current drawn was measured with a multi-meter. Then combinations of commands were repeated ten times and the current drawn was measured. This process was repeated for all the three modalities, the button control mode, slider control mode, and the voice control mode. The setup of the experiment and the multi-meter are shown in



Figure 82.



Figure 82: Current measuring experiment showing all the three modes, button, slider and voice control mode.

After measuring the current consumption, the battery life was calculated for each command set. The battery was rated 500mAh (milliamp hours) providing 11.1V (volts) and 55.5Wh (watt hours). The current drawn for a specific command was inversely proportional to the number of hours the battery lasted. If the battery draws 37.1mA it lasted for $500\text{mAh} / 37.1\text{mA} = 134.77\text{h}$. The table below shows device battery life per command as well as different command sets.

Extension Position	Grabber Position	Lift Assist Position	Button Mode Average Current	Button Mode Battery Life	Slider Mode Current	Slider Mode Battery Life	Voice Mode Current	Voice Mode Battery Life
Status	Status	Status	Average	h	Average	h	Average	h
ON	OFF	ON	i' mA		i' mA		i' mA	
Forward	-	Up	37.1	134.77	39.4	126.9	41.2	121.36
Forward	-	Down	41.1	121.65	41.9	119.33	39.2	127.55
Backward	-	Up	38.8	128.87	31.7	157.73	42.3	118.2
Backward	-	Down	42.3	118.2	44.6	112.11	52.9	94.52
Grab	-	Up	65.8	75.99	54.8	91.24	64.7	77.28
Grab	-	Down	63	79.37	57.9	86.36	58.1	86.06
Release	-	Up	82.6	60.53	67.8	73.75	81.5	61.35
Release	-	Down	84.6	59.1	77.3	64.68	83.6	59.81
ON	ON	ON	-	-	-	-	-	-
Forward	Grab	Up	70.6	70.82	60.8	82.24	-	-
Forward	Grab	Down	76	65.79	76.8	65.1	-	-
Forward	Release	Up	89.8	55.68	77.1	64.85	-	-
Forward	Release	Down	82.1	60.9	77.4	64.6	-	-
Backward	Grab	Up	70	71.43	72.8	68.68	-	-
Backward	Grab	Down	67.5	74.07	69.8	71.63	-	-
Backward	Release	Up	76.2	65.62	83.3	60.02	-	-
Backward	Release	Down	87.6	57.08	78.5	63.69	-	-
ON	OFF	OFF	-	-	-	-	-	-
Forward	-	-	9.8	510.2	10.5	476.19	11	454.55
Backward	-	-	10.2	490.2	10.2	490.2	11	454.55
Grab	-	-	43.8	114.16	36.3	137.74	44.6	112.11
Release	-	-	65.4	76.45	46.7	107.07	66.5	75.19
ON	ON	OFF	-	-	-	-	-	-
Forward	Grab	-	53	94.34	43.8	114.16	-	-
Forward	Release	-	66.5	75.19	65.2	76.69	-	-
Backward	Grab	-	42.7	117.1	38.3	130.55	-	-
Backward	Release	-	64.5	77.52	59.2	84.46	-	-
OFF	OFF	ON	-	-	-	-	-	-
-	-	Up	24.8	201.61	25.8	193.8	37.6	132.98
-	-	Down	29.3	170.65	38.8	128.87	30.8	162.34

Table 9: Current consumption and battery life for all the three modalities and lift assist.

Table 9 includes results for all the possible positions and orientations of the arm. For each modality, the current was measured and noted 10 times for a specific configuration, and then it was averaged. Table 9 also captures results for basic movements, such as opening and closing the gripper, and complex movements, such as moving forward with the lift assist going up and grasping all at the same time. From Table 9 there were three columns for extension position, grabber position, and lift assist position. The independent average currents driven by each were stored in separate columns for the three modalities. Then the current consumption from the combination of extension, grabber, and lift assist positions were measured and the average was reported in corresponding modality column. The resulting battery life from the measured current was calculated and reported in the columns for each modality. This creates a complete profile of the current consumed for a specific movement indicating the potential usage that can be achieved from a fully charged battery.

3.3 Discussion and Conclusion

This chapter described the design and construction of an extendable, exo-skeletal, multimodal robotic arm with lift assist. The functionality of the arm was designed to facilitate reaching and grasping tasks for people with residual functionality or limited movement of their upper extremities. This platform was developed especially to extend the reach envelope of high-level SCI individuals. The platform provided an additional 11 inches of reach length beyond the original length (4 inches). Furthermore, the end effector of the device was able to grasp various objects with ease.

Three different modalities were designed for controlling the platform. The button modality, slider modality, and voice modality could be used individually or in combination depending on

the user's needs. Switching between the modalities was made easier by the mode selection switch.

Participant safety was an important consideration achieved through the use of three separate switches. A main switch powered both the modality control unit and the lift assist unit, while each of these units also had individual power switches.

The platform provided lift assist for users who were unable to lift objects heavier than 2.5lbs extending their ability to include easy handling of objects up to 38 lbs. (subjected to limitations). Based on the results of force calculations and preliminary testing, eSARA demonstrates significant endurance and durability.

The device's battery life was sufficient to support intensive reaching, grasping, and lifting tasks before needing to be recharged. The current consumption matrix provides the battery-life of eSARA.

Conclusion: The hypothesis, that a platform robotic reaching and grasping arm with multiple modes of control and lift assisting features could be created, was confirmed. A system has been created with the needed functionality for testing. The safety of the participant was given high priority and was assured with the 'emergency stop' system of the platform. The current and power consumption matrix provides feasibility of use on a daily basis. The force calculation and the actual force that eSARA was subjected in the preliminary testing meet the standards set for Human Machine Interface.

The next chapter describes utilizing the eSARA platform to study HMI in detail. Chapter 4 describes two experiments with various reaching, grasping, and lifting tasks. The platform developed in this chapter was used extensively with 19 different participants. The experimental protocol, results, and discussions for these experiments are also found in the next chapter.

Chapter 4: Evaluation of Control Modes

4.1 Introduction and Motivation

This chapter discusses the third research objective to conduct an extensive Human Machine Interface (HMI) study to evaluate the control modes and lift assist of the eSARA device. This HMI study was conducted to evaluate which modality of control was best matched to the capability of SCI participants and to associate that modality with the level of injury. This chapter describes the purpose, methods, and protocols of the experiments conducted. The main objective of these experiments was to create an evaluation methodology for a range of user interface movement modalities. The methodology devised was expected to be useful for the evaluation of SCI patients with short or long term upper extremity limitations.

Given the lack of available reaching aids for people with SCI and forearm/hand paralysis, and the purpose of the HMI experiments was to assess the utility of the eSARA design (chapter 3) for completing reaching and grasping tasks by both healthy, young adults and a person with SCI. Figure 83 shows the fully developed eSARA platform from chapter 3. The figure shows the three modalities (voice, slider, and buttons) connected to the modality control unit. The biceps and triceps actuators are connected to the lift assist control unit and were successfully operated by pressure sensors in the device handle. The extension actuator, extension rail, grabber motor, and claw (end effector) are also shown. Controlling the extension actuator and the grabber motor was successfully achieved with all the three modalities.

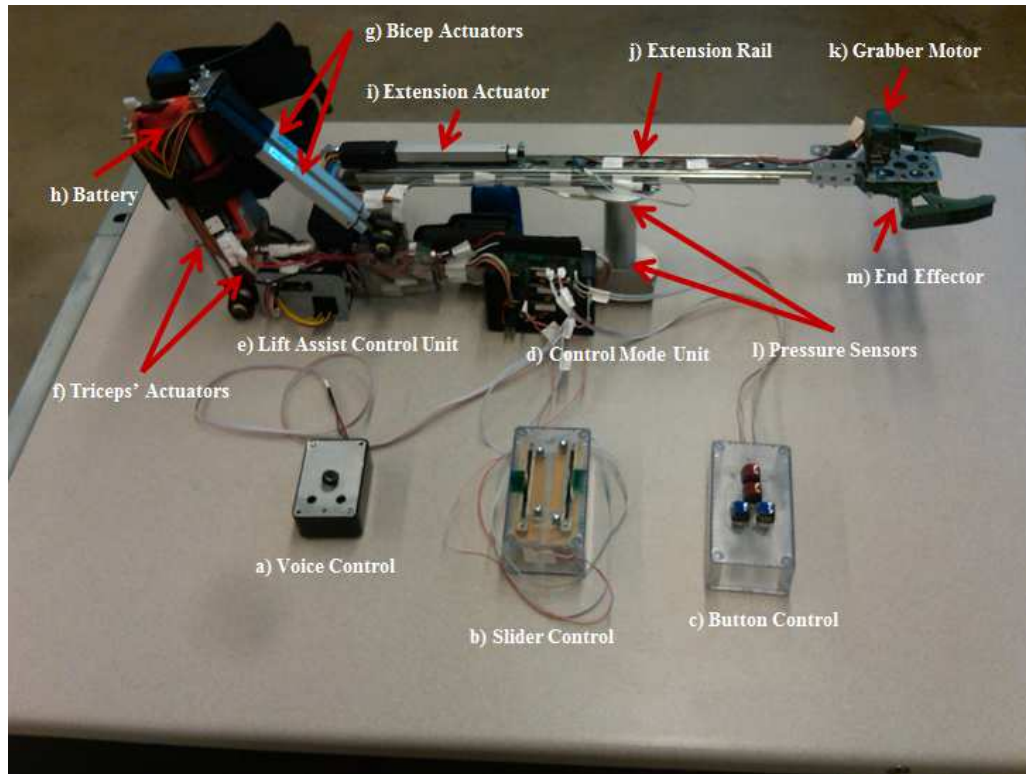


Figure 83: The final assembly of the Exo-Skeletal Assistive Robotic Arm.

The hypotheses (from chapter 1) for the third objective were that:

- (3) A methodology to evaluate multiple modes of operating a device can be created.
 - a. Multi-modal control would provide devise customization.
 - b. The key metric of success was that movement time and errors of the SCI participant would be within the limits set by a healthy, adult group using the same device for both ‘fine movement’ and ‘gross movement’ experiments.

This section provides detailed criteria for the experiments regarding the participants, experimental setup, test-bench, materials used, and error tracking.

4.2 Human Machine Interface (HMI) Structure and Process

Two experiments were conducted to test the HMI structure using the eSARA platform and 3-level test-bench. These experiments were characterized based on the level of precision and

accuracy required for the assigned task and the handling of the weight of the object. Figure 84 summarizes the structure and process flow of the HMI study.

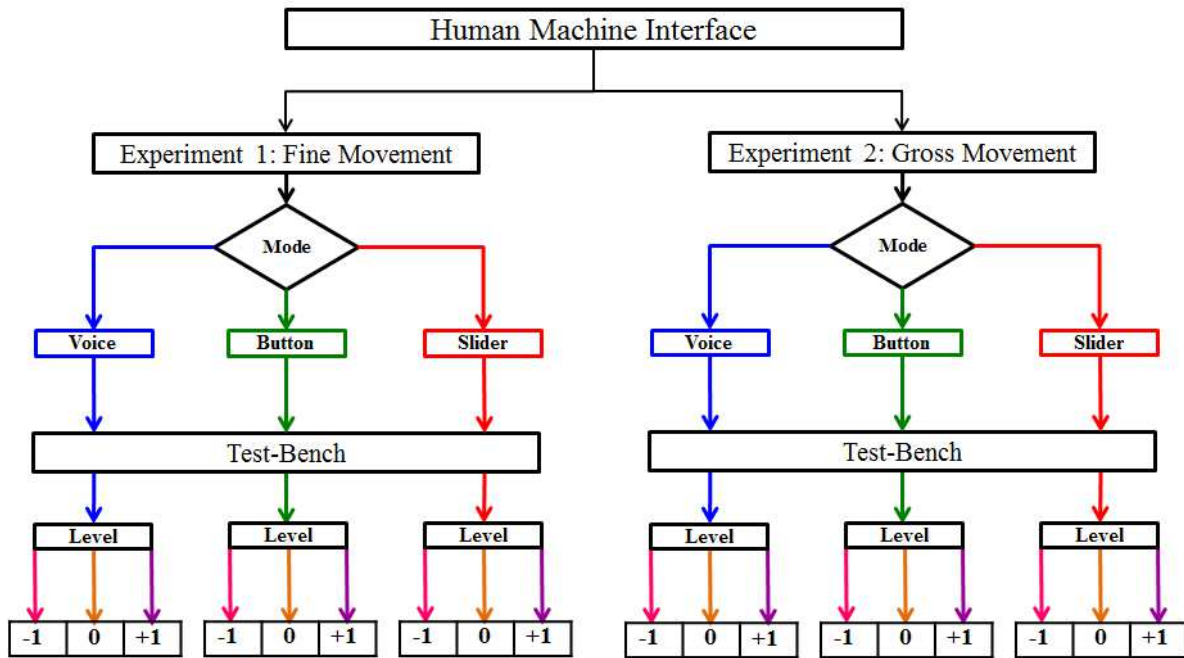


Figure 84: HMI structure and process flow.

The HMI was divided into two experiments. Experiment 1 was defined as a ‘fine movement’ experiment, where the participants were required to perform light weight precision and accuracy tasks. Experiment 2 was defined as a ‘gross movement’ experiment, where the participants were required to perform an accuracy task with a heavier weight. Both of the experiments were repeated on all three levels of the test-bench and using all three available control modalities. In both of the experiments, time performance of the participants was measured and the number of errors produced during the course of the experiment was noted. The details and protocols of these experiments are discussed individually in the respective sections. After completing both experiments, participants were asked to complete a task load index assessment, also discussed below.

4.3 Test-Bench for Human Machine Interface (HMI)

A book shelf with three different levels was used as a test-Bench shown in Figure 85. **Error! Reference source not found.** The dimensions for the test-bench were 627mm (length) x 237mm (width) x 900mm (height) (24.7in x 9.3in x 35.4in). The three different levels consist of level '0' (waist level), level '-1' (mid-shin level), and level '+1' (chest level) as shown in Figure 85b. These levels were based on the average height of a person while sitting on a chair. For the entire course of the experiment the participants sat at a fixed distance from the test bench. A chair or wheelchair was placed at a distance of 27 inches from the base of the test-bench to the chair center for all participants, as shown in Figure 85.

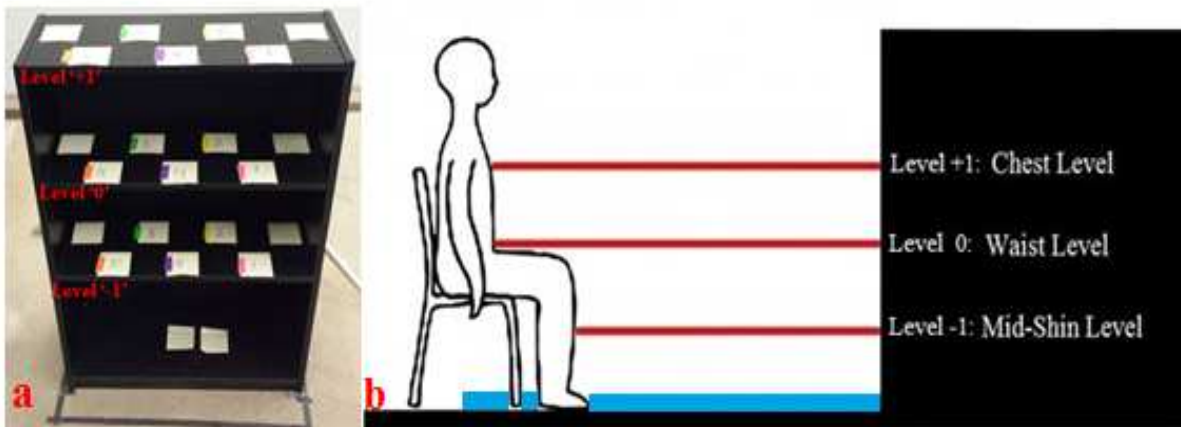


Figure 85: (a) Color coded Test bench with three levels to be used for the experiment (b) Test bench levels and distance from the test bench shown.

This test-bench (chapter 2) was designed with three height levels in order to test the use of the eSARA platform (chapter 3) for similar reaching and grasping tasks but at altered heights. The three modes of controls (voice, buttons, and slider) were used independently during the course of the HMI. The HMI was designed to measure time performances of participants based on reaching and grasping tasks on the three levels.

4.4 National Aeronautics and Space Administration (NASA) Task Load Index (TLX)

NASA-TLX is a subjective workload assessment tool used to evaluate the workload on operators using various human machine systems. This multi-dimensional rating procedure derives an overall workload score based on a weighted average of ratings on six subscales. These subscales include Mental Demands (MD), Physical Demands (PD), Temporal Demands (TD), Performance (PF), Effort (EF) and Frustration (FR). The ‘Scores’ represent the ‘Weighted Mean Workload’. NASA utilizes this tool to assess workload in various human-machine environments including: aircraft cockpits, command, control, and communication workstations; supervisory and process control environments; simulations and laboratory tests [105]. The NASA-TLX was used for this research to assess the workload participants were subjected to when using the Exo-Skeletal Robotic Arm (eSARA). All participants were required to complete the NASA-TLX assessment after finishing both the fine movement and gross movement experiments. Figure 86 shows the structure of the NASA-TLX model used for the two experiments. The two experiments were treated as conditions, and each test-bench level was treated as a trial. The structure below was applied to all the participants.

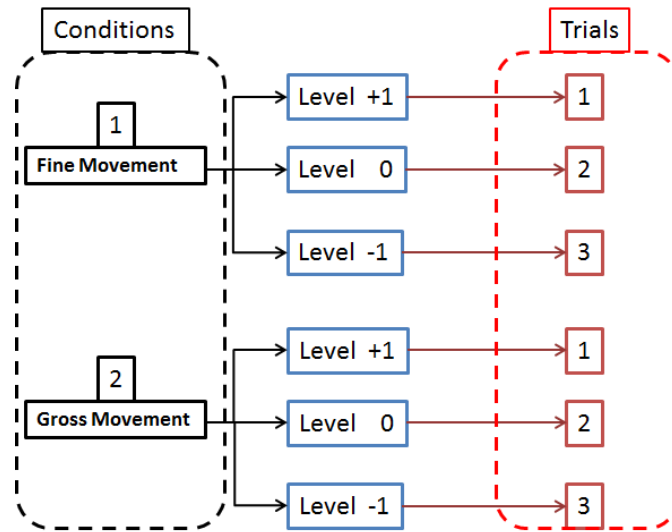


Figure 86: Structure of the NASA TLX for the fine movement and gross movement experiment showing the relationship between the conditions and trials.

4.4.1 Participants and Inclusion / Exclusion Criterion

Inclusion criteria: Male and female, ages 18-60, any race or ethnicity, complete or incomplete spinal cord injury levels C5 through C7, able to reach and extend their extremity for simple movements.

Exclusion criteria: People with extensive contractures, thoracic braces, or additional physical impairments that limit their ability to move. People who cannot speak, understand, or follow simple three step commands due to their injury were also excluded.

Participants were divided into 3 groups:

- Group 1: Healthy participants (General Population)
 - 12 participants
- Group 2: Healthy participants mimicking movements of a C5-6 individual (Occupational Therapy Students)
 - 6 participants
- Group 3: Spinal Cord Injury (SCI) Individual
 - 1 participant (incomplete quadriplegia level C5-6)

4.5 EXPERIMENT 1: Fine Movement Experiment

4.5.1 Methods

4.5.1.1 Materials

To test the fine movements of the participants a peg block was used with the test-bench. The test-bench and the peg-blocks are shown in Figure 87a and 87b, respectively. The pegs and the slots were color-coded. The participants were tasked with matching the color coded peg to the corresponding color coded slot. The pegs that were selected for this experiment loosely fitted in the slots, providing a flexible fit for the participants

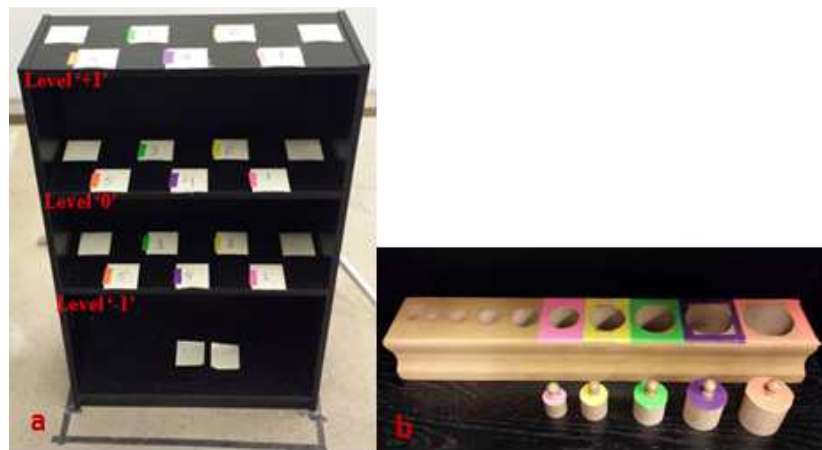


Figure 87: (a) Test-bench (b) Color-coded pegs for the fine movement experiment.

4.5.1.2 Protocol

For fine movements, the participants were required to perform a peg transfer task. The participants were to pick up the pegs from color coded areas and put them in corresponding colored peg slots. The experiment was to be repeated with five colored pegs, at the three different levels, and with the three modalities. The experiment was conducted with five colored pegs at level 0 (waist level), then the task was repeated with the pegs placed at level -1 (mid-shin level), and finally the task was repeated with the pegs placed at level +1 (chest level). This completed one modality (e.g. buttons). The same experiment was repeated with the remaining

two modalities. The five pegs used were of different shapes and sizes. Figure 88 below shows the start point and expected end point of the experiment for the three levels.

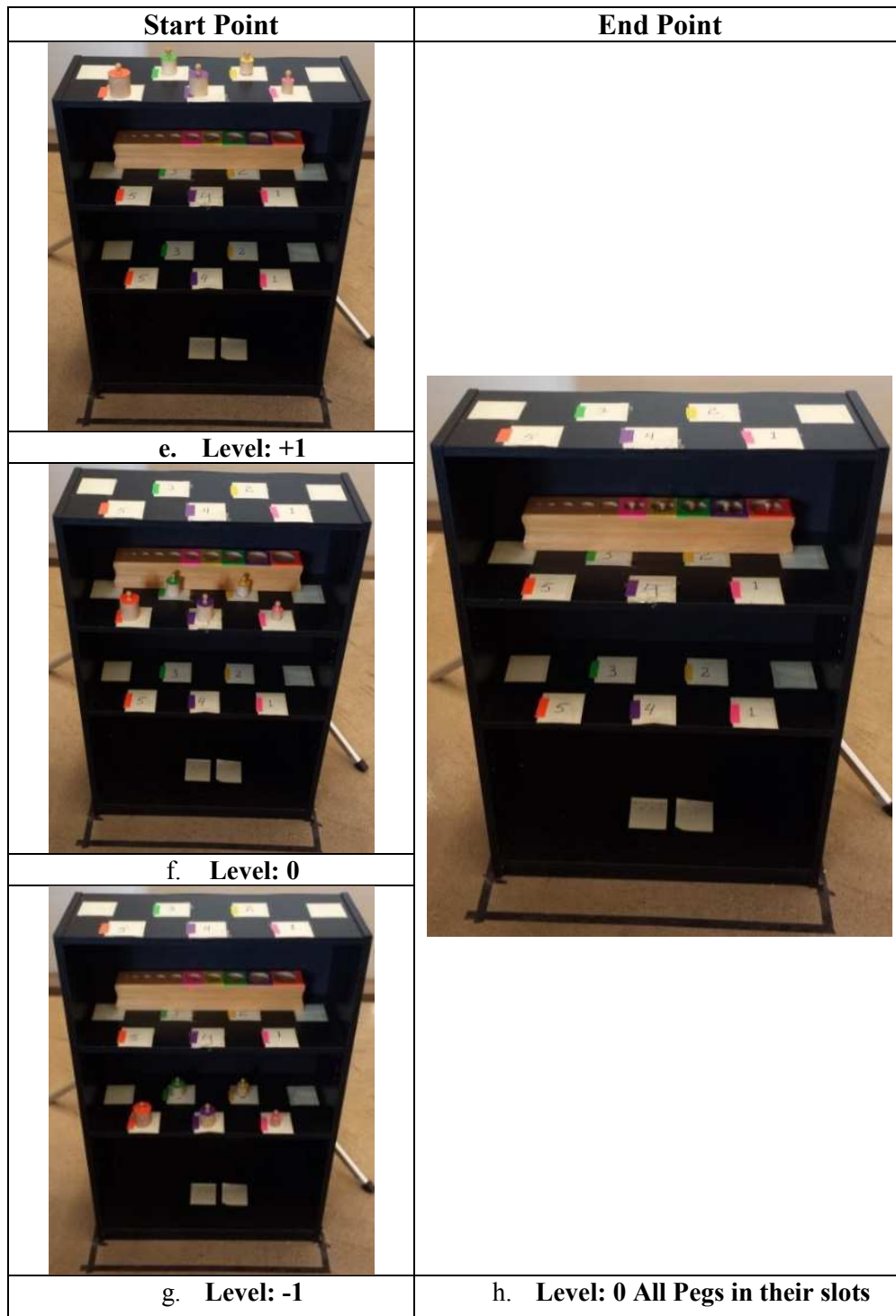


Figure 88: Start and end points of the fine movement experiment.

To avoid fatigue, participants were allowed to take breaks during testing. Breaks within levels were 3 minutes and breaks between modalities were 5 minutes. The number of breaks taken was subject to the individual participant's desire. Participants who required even more rest due to excessive fatigue were allowed to rest after completing each level. An option was also given to all the participants to complete the test over the course of one or two days if preferred. The total time to take the test without any breaks was approximately 45 minutes.

4.5.1.3 Error Tracking

For the fine movement experiments, participants were required to place the color-coded pegs into their corresponding slots such that the peg was fully descended into the slot. Figure 89(a-d) shows examples of errors within the test bench that participants were required to rectify before moving on. Figure 89e shows an error outside of the test bench that did not have to be rectified. The number of errors per level and the color of the peg with the error were documented manually. No additional penalties were added to the experiment time.

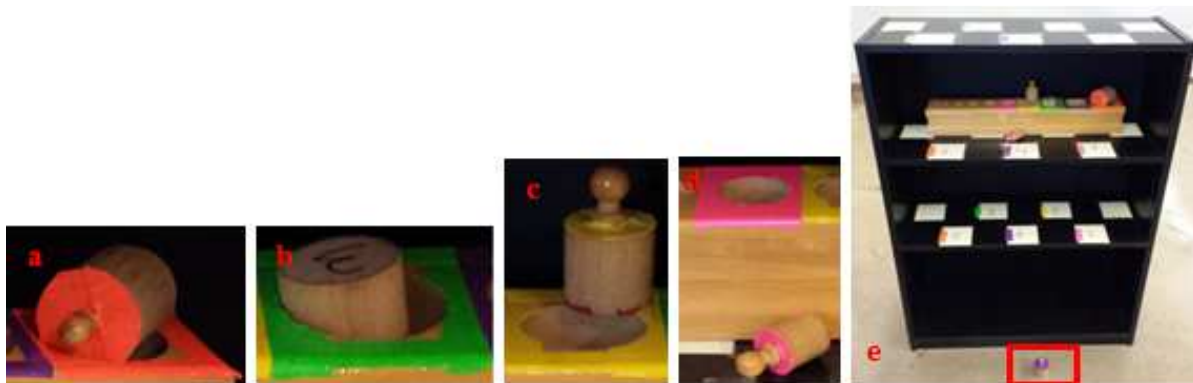


Figure 89: (a-d) Errors counted within the testbench that must be rectified (e) error outside testbench considered a failed peg transfer.

Placing a peg incorrectly would increase the time for that particular level as participants were required to fix the error before moving onto the next level. The participants were informed before the start of each experiment about the errors and their consequence. The participants were also informed of correct, acceptable placement of the pegs. The lift assist feature was actively/

automatically available for those participants who required it. When a participant moved from one level to the next (level -1, 0, or +1) the pegs were quickly reset and the experiment resumed.

4.5.2 Data Analysis

For the entire series of experiments the mean estimation and Analysis Of Variance (ANOVA) were calculated for able-bodied participants only. This compiled control data was then compared with the time performance of the SCI participant. Data was analyzed using SPSS (IBM) [97] statistical software. Descriptive data were provided for each participant. Differences in time between levels for all participants were compared using Analysis of Variance (ANOVA) with the Bonferroni correction for multiple comparisons. Significance was established at $p < 0.05$. Overlaying the plots was the average time of the healthy participants took to complete the experiment in each level. This average time of the healthy participants was represented by a thick dashed line, the SCI participant was represented by a thick dot and dash line. The plots also indicate the upper limits (marked with a dot) and lower limits (marked with a dot) for standard deviations. Participants did not report experiencing any discomfort or fatigue, and the principal investigator did not observe any signs of discomfort or fatigue over the course of the experiments.

Figure 90 shows how participants performed tasks for a given mode on all three levels. The time the participant took to complete each level was recorded in order to study the effect of change in height in relation to the modality. Level 0 represented natural working position in contrast to out of reach positions (level +1 and level -1).

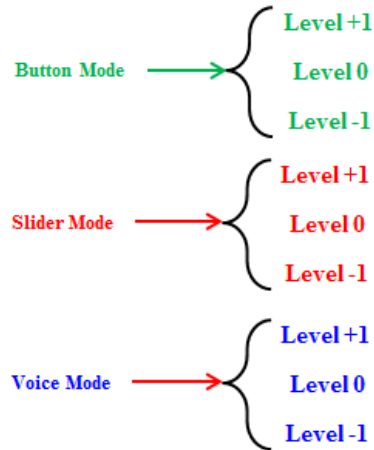


Figure 90: One mode, all levels for fine movement.

Figure 91 shows how participants were asked to perform tasks using all three control modalities on each of the height levels. For a given level, the participant completed the tasks using all three modalities. The time the participant took to complete each level was recorded in order to study the effect of change in the control mode at a given height (level). Level 0 represented a natural working position in contrast to out of reach positions (level +1 and level -1).

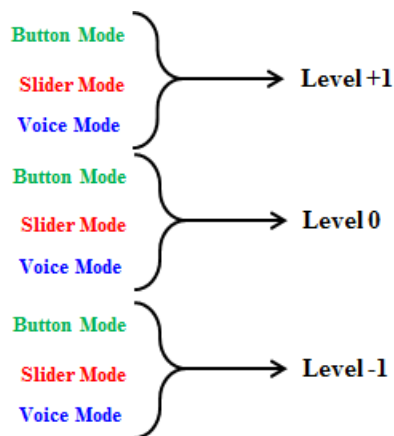


Figure 91: All modes, one level for fine movement.

4.5.3 Results

4.5.3.1 Healthy Participants in Comparison with SCI Participant

Figure 92 provides a box and whisker plot summarizing the time performance of the participants during the ‘fine movement’ experiment using the ‘button’ mode. The SCI participant finished testing at levels -1 (mid-shin) and +1 (chest), faster than the average healthy participants by 9.6% and 19.9%, respectively. At level 0 (waist) the SCI participant was 22.0% slower than the average healthy individual. However, this outcome was still within one standard deviation (SD) of the healthy participants’ average.

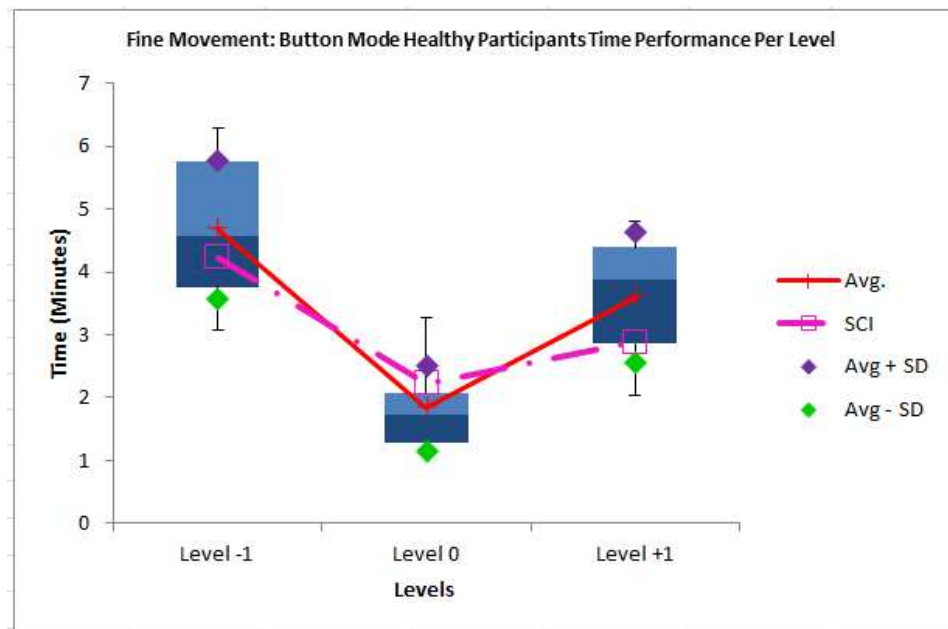


Figure 92: Time performance of healthy participants during the fine movement experiment using the button modality on the three levels.

Each healthy participant’s completion time and errors per level were recorded for the button mode for the fine movement experiment.

Levels	Mean	Std. Error	95% Confidence Interval	
			Lower Bound	Upper Bound
-1	4.676	.318	3.976	5.375
0	1.827	.197	1.394	2.259
+1	3.591	.299	2.932	4.249

Table 10: Estimated marginal mean of time (minutes) values of the levels and the standard error for the fine movement experiment. These estimated marginal means were calculated only for the healthy participants using the button mode.

There was a significant main effect for level height ($F(2, 22) = 53.891, p < 0.001$) in the fine movement experiment for the healthy participants using button mode. The pairwise comparisons for the main effect of level were corrected using Bonferroni adjustments and are displayed in the following table. Table 11 shows that the significant main effect reflects a significant difference ($p < 0.001$) between levels -1 and 0 (lower and middle), between levels -1 and 1 (lower and upper; $p = 0.010$), and between levels 1 and 0 (upper and middle; $p < 0.001$).

(I) Levels	(J) Levels	Mean Difference (I-J)	Std. Error	Sig. ^b	95% Confidence Interval for Difference ^b	
					Lower Bound	Upper Bound
-1	0	2.849*	.301	.000	2.002	3.697
	+1	1.085*	.292	.010	.261	1.909
0	-1	-2.849*	.301	.000	-3.697	-2.002
	+1	-1.764*	.233	.000	-2.423	-1.106
+1	-1	-1.085*	.292	.010	-1.909	-.261
	0	1.764*	.233	.000	1.106	2.423

Table 11: ANOVA analysis for the fine movement experiment of healthy participants using the button mode, based on estimated marginal means. * The mean difference was significant at the 0.05 level. ^b Bonferroni adjustment for multiple comparisons.

The box and whisker plot in Figure 93 below, summarizes the results of the fine movement experiment for the healthy participants using the slider control mode. The SCI participant finished testing at levels -1 (mid-shin), 0 (waist), and +1 (chest), slower than the average healthy participants by 14.7, 5.4 and 3.3%, respectively. However, his performance still falls within one standard deviation of the healthy participant average.

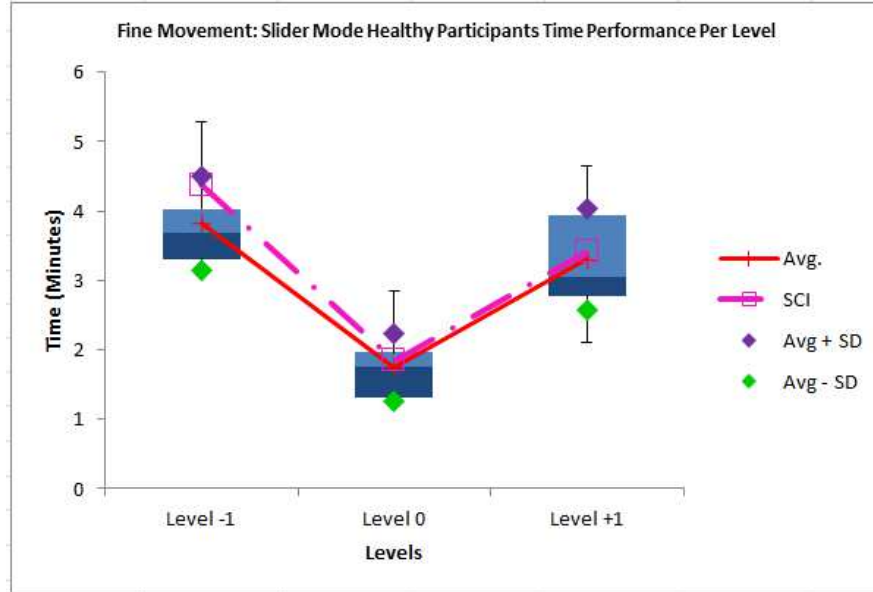


Figure 93: Box and whisker plot of the time performance of healthy participants during the fine movement experiment using the slider modality on all three height levels.

Each healthy participant's completion time and errors per level were recorded for the slider mode for the fine movement experiment.

Levels	Mean	Std. Error	95% Confidence Interval	
			Lower Bound	Upper Bound
-1	3.819	.196	3.388	4.249
0	1.754	.141	1.445	2.064
+1	3.302	.211	2.838	3.766

Table 12: Estimated marginal mean of time (minutes) values and standard error for the different height levels during the fine movement experiment, calculated from healthy participant data only.

There was a significant main effect for level height ($F(2, 22) = 104.331, p < 0.001$) in the fine movement experiment for the healthy participants using the slider control mode. The pairwise comparisons for the main effect of level were corrected using Bonferroni adjustments and are displayed in the table below. Table 13 shows that the main effect for level height reveals a significant difference ($p < 0.001$) between levels -1 and 0 (lower and middle), between levels -1 and 1 (lower and upper; $p = 0.012$), and between levels 1 and 0 (upper and middle; $p < 0.001$).

(I) Levels	(J) Levels	Mean Difference (I-J)	Std. Error	Sig. ^b	95% Confidence Interval for Difference ^a	
					Lower Bound	Upper Bound
-1	0	2.065*	.152	.000	1.636	2.494
	+1	.517*	.142	.012	.117	.916
0	-1	-2.065*	.152	.000	-2.494	-1.636
	+1	-1.548*	.152	.000	-1.977	-1.119
+1	-1	-.517*	.142	.012	-.916	-.117
	0	1.548*	.152	.000	1.119	1.977

Table 13: ANOVA results for the fine movement experiment with healthy participants using the slider mode, based on estimated marginal means *The mean difference was significant at the 0.05 level. ^b Bonferroni adjustment for multiple comparisons.

Figure 94 shows a similar plot to those presented in figures 92 and 93, but contains the results of the fine movement experiment for the healthy participants using the voice control mode. The SCI participant finished testing at both the -1 (mid-shin) and +1 (chest) levels 1.5% slower than the average healthy participants. This result, however, was still within one standard deviation of average. At waist level 0, the SCI participant was 8.6% faster than the average healthy individual.

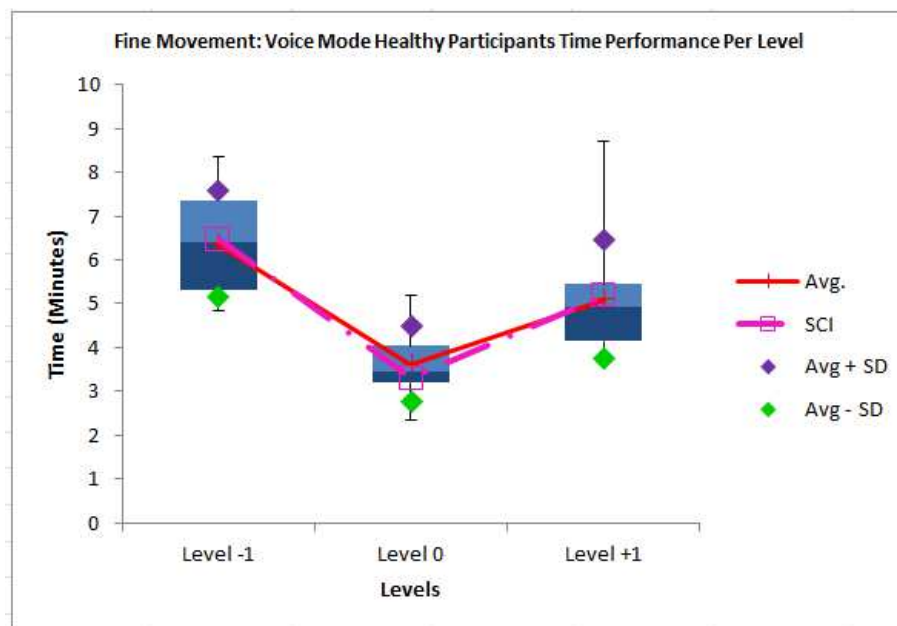


Figure 94: Box and whisker plot of the time performance of healthy participants during the fine movement experiment using the voice control modality on all three height levels.

Each healthy participant's completion time and errors per level were recorded for the voice mode for the fine movement experiment.

Levels	Mean	Std. Error	95% Confidence Interval	
			Lower Bound	Upper Bound
-1	6.369	.353	5.591	7.146
0	3.618	.248	3.072	4.164
+1	5.101	.391	4.240	5.963

Table 14: Estimated marginal mean of time (minutes) values and standard error for the fine movement experiment at each of the three height level, calculated only for the healthy participants using the voice mode.

There was a significant main effect for level height ($F(2, 22) = 39.692, p < 0.001$) in the fine movement experiment for healthy participants using the voice control mode. The pairwise comparisons for the main effect of level were corrected using Bonferroni adjustments and are displayed in the table below. Results of the statistical analyses in Table 15 show that a significant difference exists between levels -1 and 0 (lower and middle; $p < 0.001$), between levels -1 and 1 (lower and upper; $p = 0.004$), and between levels 1 and 0 (upper and middle; $p = 0.001$).

(I) Levels	(J) Levels	Mean Difference (I-J)	Std. Error	Sig. ^b	95% Confidence Interval for Difference ^b	
					Lower Bound	Upper Bound
-1	0	2.750*	.332	.000	1.814	3.686
	+1	1.267*	.297	.004	.429	2.106
0	-1	-2.750*	.332	.000	-3.686	-1.814
	+1	-1.483*	.296	.001	-2.319	-.647
+1	-1	-1.267*	.297	.004	-2.106	-.429
	0	1.483*	.296	.001	.647	2.319

Table 15: ANOVA results for the fine movement experiment of healthy participants using the voice mode, based on estimated marginal means. *The mean difference was significant at the 0.05 level. ^b Bonferroni adjustment for multiple comparisons.

4.5.3.1.1 Time Performance of the SCI Participant vs. Healthy Participants Using One Mode at All Levels

Figure 95 below shows the individual time performance of each healthy participant completing the fine movement experiment at all three height levels while using the button modality.

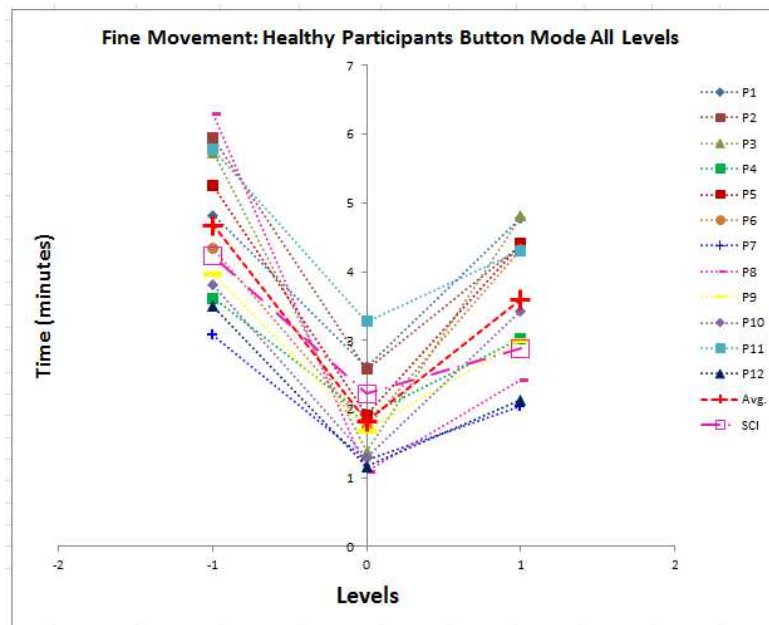


Figure 95: Individual time performance of healthy participants, their average, and the SCI participant's performance during the fine movement experiment using the button modality at all three height levels.

Figure 96 below shows the individual time performance of each healthy participant completing the fine movement experiment at all three height levels while using the slider modality.

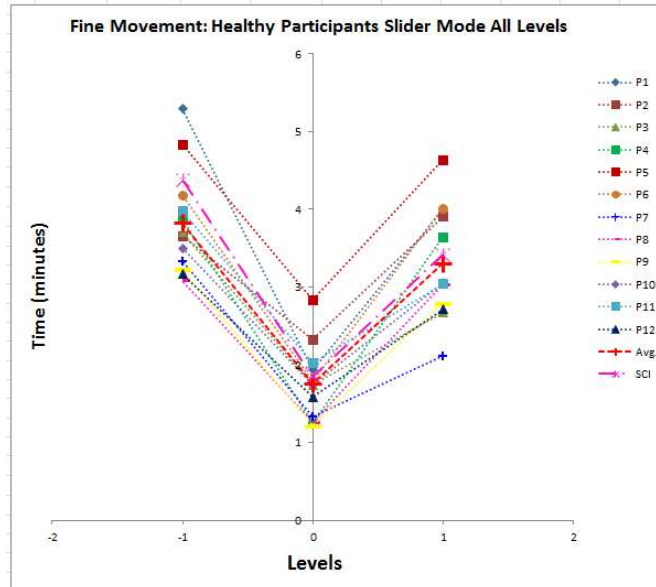


Figure 96: Individual time performance of healthy participants, their average, and the SCI participant's performance during the fine movement experiment using the slider modality at all three height levels.

Figure 967 below shows the individual time performance of each healthy participant completing the fine movement experiment at all three height levels while using the voice modality.

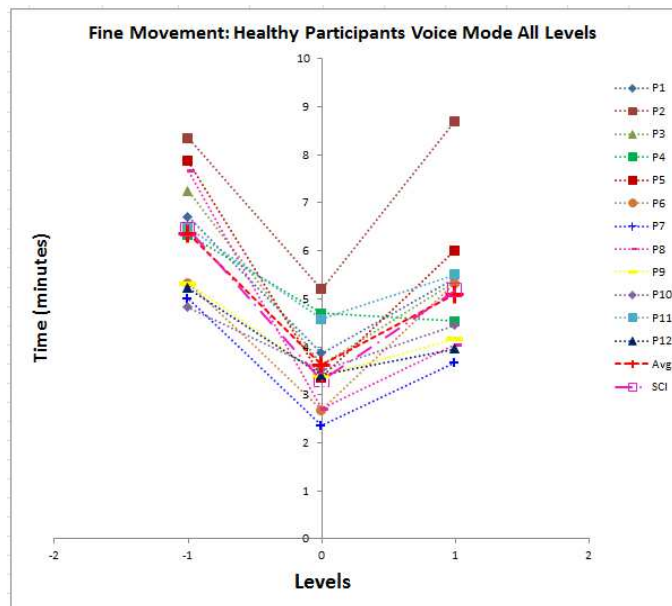


Figure 97: Individual time performance of healthy participants, their average, and the SCI participant's performance during the fine movement experiment using the voice modality at all three height levels.

4.5.3.1.2 Time Performance of the SCI Participant vs. Healthy Participants using All Modes at One Level

Figure 98 below shows the time performance of each healthy participant for the fine movement experiment at level +1 using all three control modalities.

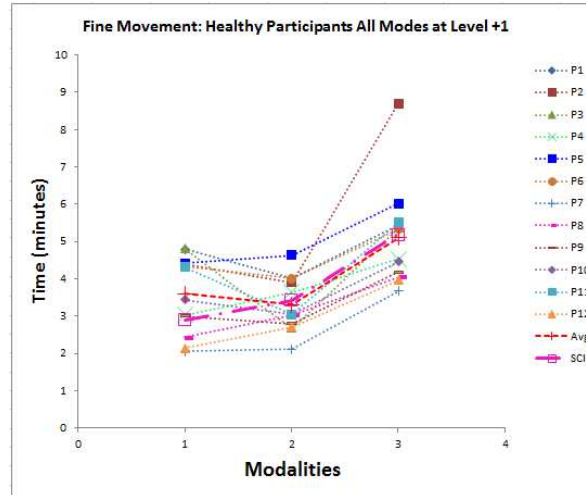


Figure 98: Individual time performance of healthy participants, their average, and the SCI participant's performance during the fine movement experiment on level +1 (chest) using all the three control modalities; (1=button, 2=Slider, 3=Voice).

Figure 99 below shows the time performance of each healthy participant for the fine movement experiment at level 0 using all three control modalities.

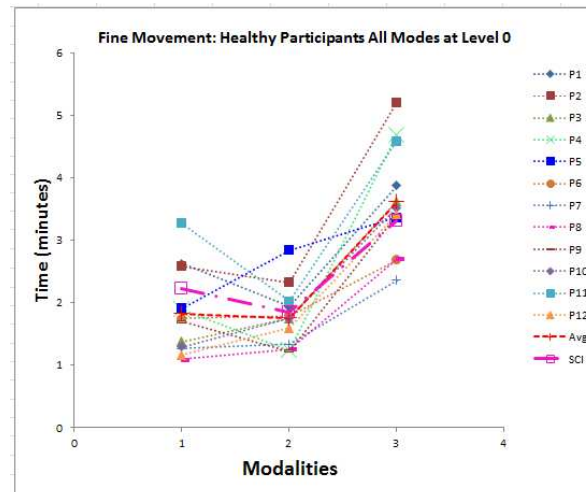


Figure 99: Individual time performance of healthy participants, their average, and the SCI participant's performance during the fine movement experiment on level 0 (waist) using all the three control modalities; (1=button, 2=Slider, 3=Voice).

Figure 100 below shows the time performance of each healthy participant for the fine movement experiment at level -1 using all three control modalities.

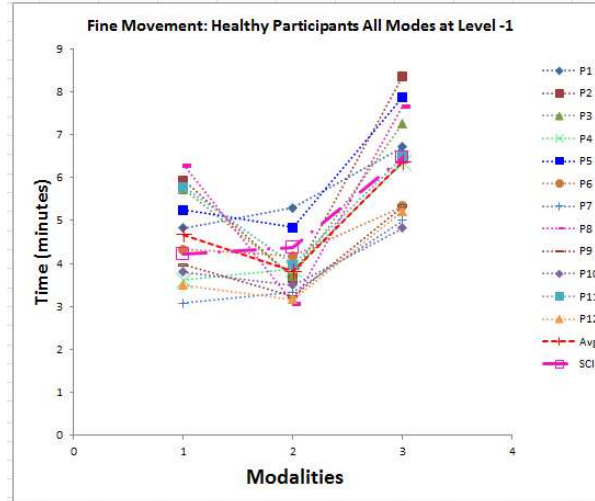


Figure 100: Individual time performance of healthy participants, their average, and the SCI participant's performance during the fine movement experiment on level -1 (mid-shin) using all the three control modalities; (1=button, 2=Slider, 3=Voice).

4.5.3.2 Healthy Restricted Participants (Occupational Therapy Students) in Comparison with an SCI Participant

For each of the experiments conducted, summary statistics (e.g. mean and analysis of variance) were computed for the able-bodied participants only and this compiled data was then compared with that of the SCI participant. In the above sections, the performance of the healthy participants (group 1) was averaged and compared to that of the SCI individual. In the following sections, time performance results of the occupational therapy participants (group 2) will be compared to that of the SCI individual.

The box and whisker plot in Figure 101 summarizes the performance of the occupational therapy students during the fine movement experiment using the button control modality. The SCI participant finished testing at levels -1 (mid-shin), 0 (waist), and +1 (chest), faster than the average of the occupational therapy participants by 14.6, 35.9, and 24.6%, respectively. His performance times were within two standard deviations of group 2's means for levels -1 and +1. However, at level 0, the SCI participant's performance significantly exceeded (indicated by a faster completion time) the average from the occupational therapy participants.

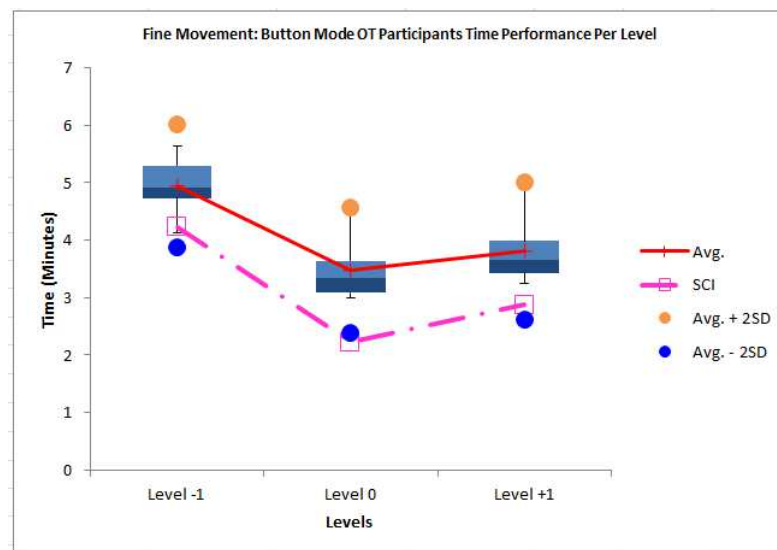


Figure 101: Box and whisker plot of the time performance of the occupational therapy participants during the fine movement experiment using the button modality at all three height levels.

Each occupational therapy participant's completion time and errors per level were recorded for the button mode for the fine movement experiment.

Levels	Mean	Std. Error	95% Confidence Interval	
			Lower Bound	Upper Bound
-1	4.949	.218	4.389	5.509
0	3.476	.222	2.905	4.047
+1	3.817	.243	3.192	4.441

Table 16: Estimated marginal mean of time (minutes) values and the standard error are reported for the fine movement experiment at each of the three levels using the button control mode. Values are calculated using data from the occupational therapy participants only.

There was a significant main effect for level height ($F(2, 10) = 62.632, p < 0.001$) in the fine movement experiment for the occupational therapy participants using the button control mode. The pairwise comparisons for the main effect of level were corrected using Bonferroni adjustments and are displayed in the table below. Table 17 indicates a significant difference in main effect between levels -1 and 0 (lower and middle; $p < 0.001$) and between levels -1 and 1 (lower and upper; $p = 0.006$). However, there was no significant difference between levels 1 and 0 (upper and middle; $p = 0.065$).

(I) Levels	(J) Levels	Mean Difference (I-J)	Std. Error	Sig. ^b	95% Confidence Interval for Difference ^b	
					Lower Bound	Upper Bound
-1	0	1.473*	.102	.000	1.111	1.835
	+1	1.132*	.189	.006	.464	1.800
0	-1	-1.473*	.102	.000	-1.835	-1.111
	+1	-.341	.104	.065	-.707	.026
+1	-1	-1.132*	.189	.006	-1.800	-.464
	0	.341	.104	.065	-.026	.707

Table 17: ANOVA results for fine movement experiment of occupational therapy participants using the button mode, based on estimated marginal means. *The mean difference was significant at the 0.05 level. ^b Bonferroni adjustment for multiple comparisons.

Figure 102 summarizes the results of the fine movement experiment for the occupational therapy participants using the slider control mode. The SCI participant finished testing at levels -1 (mid-

shin), 0 (waist), and +1 (chest), faster than the average of the occupational therapy participants by 11.2, 42.5, and 12.7%, respectively. His performance for levels -1 and +1 were within one standard deviation of this average, and within two standard deviations of the average for level 0.

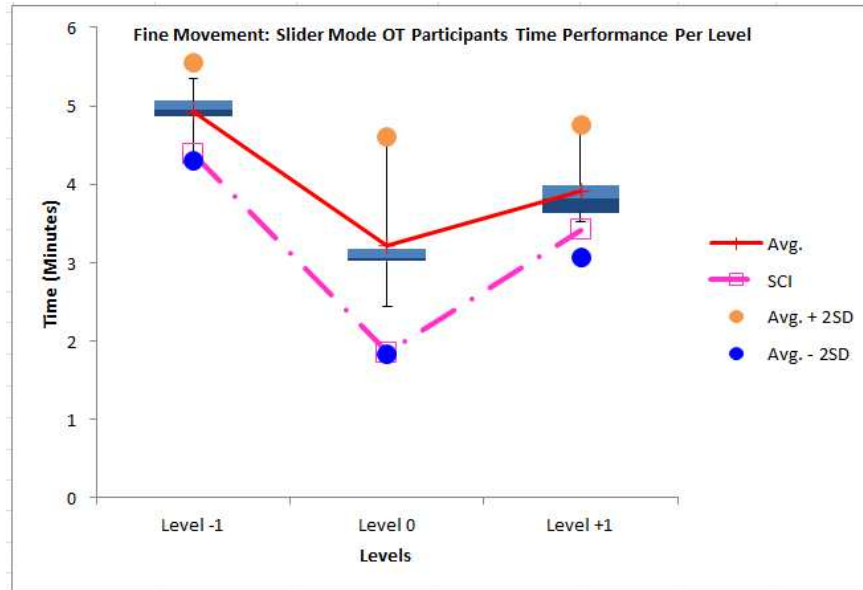


Figure 102: Box and whisker plot of the time performance of occupational therapy participants during the fine movement experiment using the slider modality at all three height levels.

Each occupational therapy participant's completion time and errors per level were recorded for the slider mode for the fine movement experiment.

Levels	Mean	Std. Error	95% Confidence Interval	
			Lower Bound	Upper Bound
-1	4.931	.128	4.601	5.261
0	3.215	.284	2.486	3.945
+1	3.910	.172	3.468	4.353

Table 18: Estimated marginal mean of time (minutes) values and the standard error are reported for the fine movement experiment at each of the three levels using the slider control mode. Values are calculated using data from the occupational therapy participants only.

There was a significant main effect for level height ($F(2, 10) = 23.123, p < 0.001$) in the fine movement experiment for the occupational therapy participants using the slider control modality.

Table 19 shows this significant main effect using Bonferroni adjustments to correct the pairwise comparisons. A significant difference was observed between levels -1 and 0 (lower and middle; $p = 0.013$), between levels -1 and 1 (lower and upper; $p = 0.009$), and between levels 1 and 0 (upper and middle; $p = 0.046$).

(I) Levels	(J) Levels	Mean Difference (I-J)	Std. Error	Sig. ^b	95% Confidence Interval for Difference ^b	
					Lower Bound	Upper Bound
-1	0	1.716*	.347	.013	.490	2.941
	+1	1.021*	.189	.009	.351	1.690
0	-1	-1.716*	.347	.013	-2.941	-.490
	+1	-.695*	.193	.046	-1.376	-.014
+1	-1	-1.021*	.189	.009	-1.690	-.351
	0	.695*	.193	.046	.014	1.376

Table 19: ANOVA results for fine movement experiment of occupational therapy participants using the slider mode, based on estimated marginal means. *The mean difference was significant at the 0.05 level. ^b Bonferroni adjustment for multiple comparisons.

Figure 102 summarizes the results of the fine movement experiment for the occupational therapy participants using the voice control mode. The SCI participant finished testing at levels -1 (mid-shin) and +1 (chest), slower than the average occupational therapy participant by 16.2% and 23.4%, respectively. At level 0 (waist), the SCI participant was 23.4% faster than the average healthy individual but still within one standard deviation of the average). At levels -1 and 0, the SCI participant's performance fell within two standard deviations of the healthy participant averages.

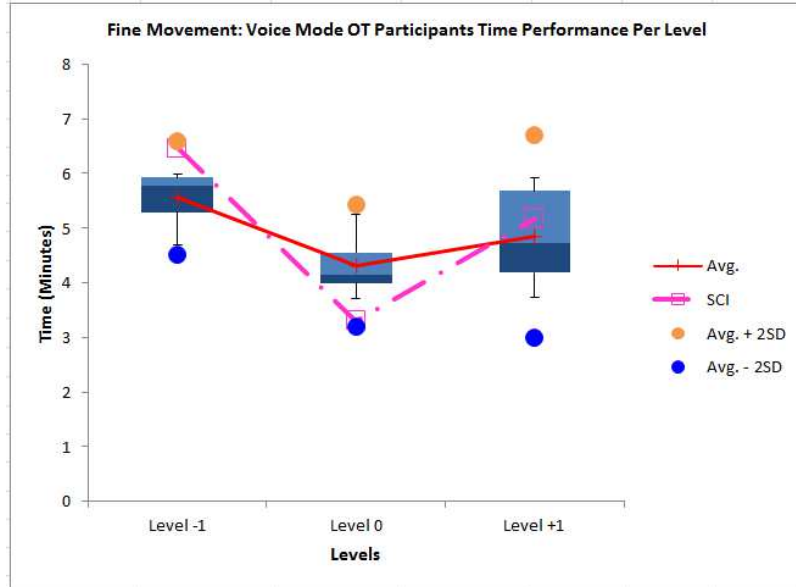


Figure 103: Box and whisker plot of the time performance of occupational therapy participants during the fine movement experiment using the voice modality at all three height levels.

Each occupational therapy participant's completion time and errors per level were recorded for the voice mode for the fine movement experiment.

Levels	Mean	Std. Error	95% Confidence Interval	
			Lower Bound	Upper Bound
-1	5.561	.212	5.016	6.105
0	4.313	.228	3.728	4.898
+1	4.849	.378	3.876	5.822

Table 20: Estimated marginal mean of time (minutes) values and the standard error are reported for the fine movement experiment at each of the three levels using the voice control mode. Values are calculated using data from the occupational therapy participants only.

There was a significant main effect based on height level of the test bench ($F(2, 22) = 12.271, p < 0.001$) for the occupational therapy participants using the voice control mode during the fine movement experiment. The pairwise comparisons for the main effect of level were corrected using Bonferroni adjustments. Table 21 shows that the significant main effect reflects a significant difference between levels -1 and 0 (lower and middle; $p = 0.007$) but there was no

significant difference between levels -1 and 1 (lower and upper; $p = 0.132$) or between levels 1 and 0 (upper and middle; $p = 0.318$).

(I) Levels	(J) Levels	Mean Difference (I-J)	Std. Error	Sig. ^b	95% Confidence Interval for Difference ^b	
					Lower Bound	Upper Bound
-1	0	1.248*	.216	.007	.483	2.013
	+1	.712	.266	.132	-.227	1.650
0	-1	-1.248*	.216	.007	-2.013	-.483
	+1	-.536	.272	.318	-1.499	.427
+1	-1	-.712	.266	.132	-1.650	.227
	0	.536	.272	.318	-.427	1.499

Table 21: ANOVA results for fine movement experiment of occupational therapy participants using the voice mode, based on estimated marginal means. *The mean difference was significant at the 0.05 level. ^b Bonferroni adjustment for multiple comparisons.

4.5.3.2.1 Time Performance of the SCI Participant vs. Occupational Therapy Participants Using One Mode at All Levels

Figure 104 below shows the individual time performance of each occupational therapy participant for the fine movement experiment using the button modality at each of the three height levels.

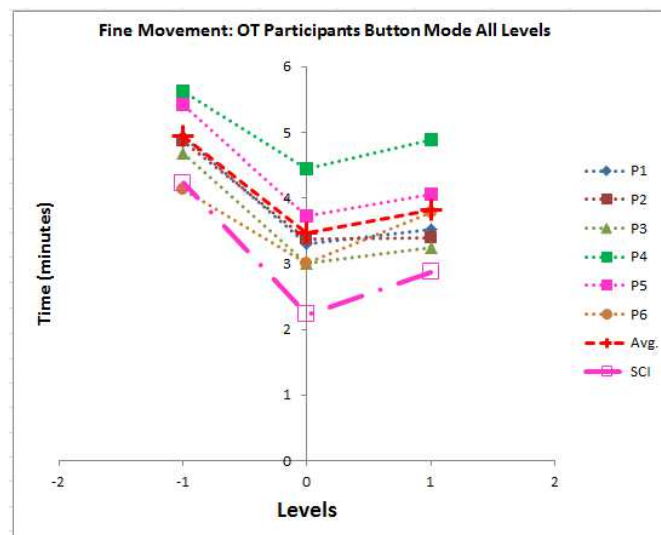


Figure 104: Individual time performances of the occupational therapy participants, their average, and the SCI participant's performance during the fine movement experiment using the button modality at all three height levels.

Figure 105 below shows the individual time performance of each occupational therapy participant for the fine movement experiment using the slider modality at each of the three height levels.

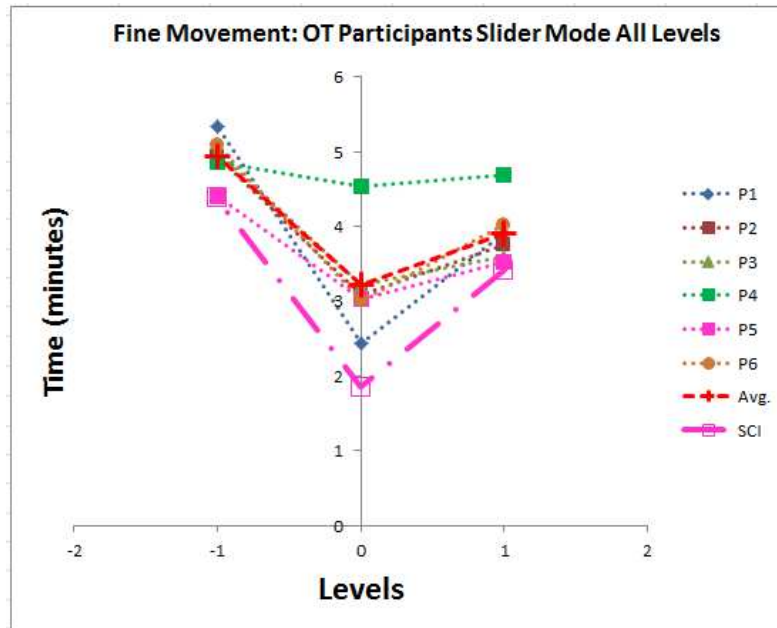


Figure 105: Individual time performances of the occupational therapy participants, their average, and the SCI participant's performance during the fine movement experiment using the slider modality at all three height levels.

Figure 106 below shows the individual time performance of each occupational therapy participant for the fine movement experiment using the voice modality at each of the three height levels.

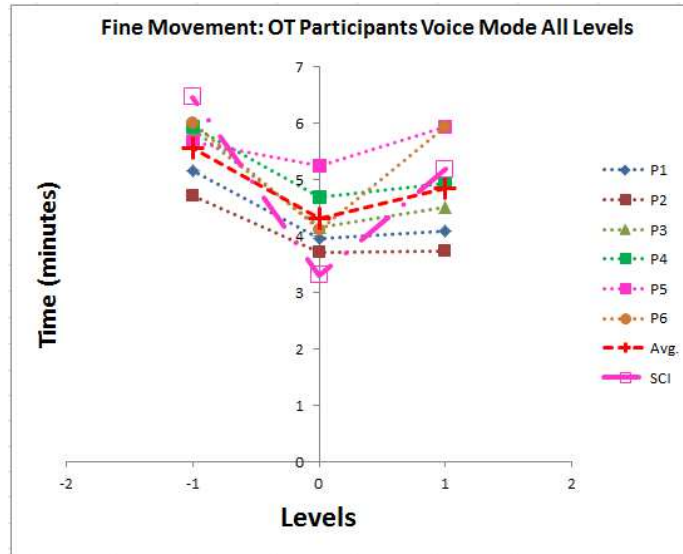


Figure 106: Individual time performances of the occupational therapy participants, their average, and the SCI participant's performance during the fine movement experiment using the voice modality at all three height levels.

4.5.3.2.2 Time Performance of the SCI Participant vs. Occupational Therapy Participants Using All Mode at One Levels

Figure 107 below shows the individual time performance of each occupational therapy participant for the fine movement experiment at level +1 (chest) using all three control modalities.

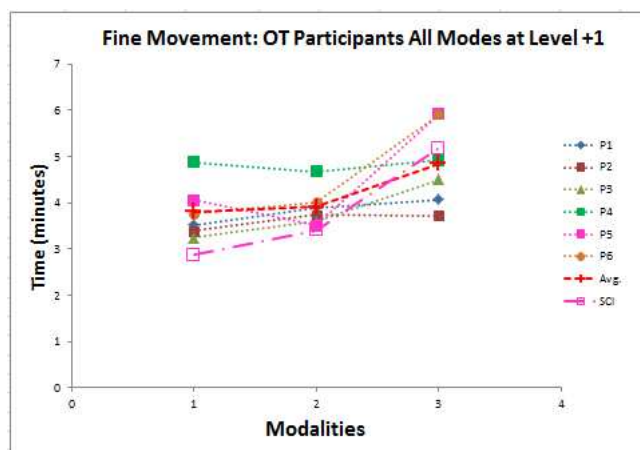


Figure 107: Individual time performance of the occupational therapy participants, their average, and the SCI participant's performance during the fine movement experiment on level +1 using all three control modalities; (1=button, 2=Slider, 3=Voice).

Figure 108 below shows the individual time performance of each occupational therapy participant for the fine movement experiment at level 0 (waist) using all three control modalities.

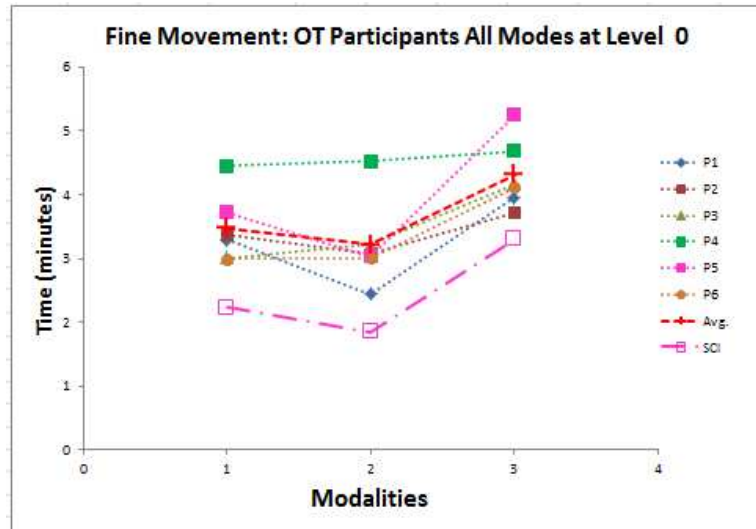


Figure 108: Individual time performance of the occupational therapy participants, their average, and the SCI participant's performance during the fine movement experiment on level 0 using all three control modalities; (1=button, 2=Slider, 3=Voice).

Figure 109 below shows the individual time performance of each occupational therapy participant for the fine movement experiment at level -1 (mid-shin) using all three control modalities.

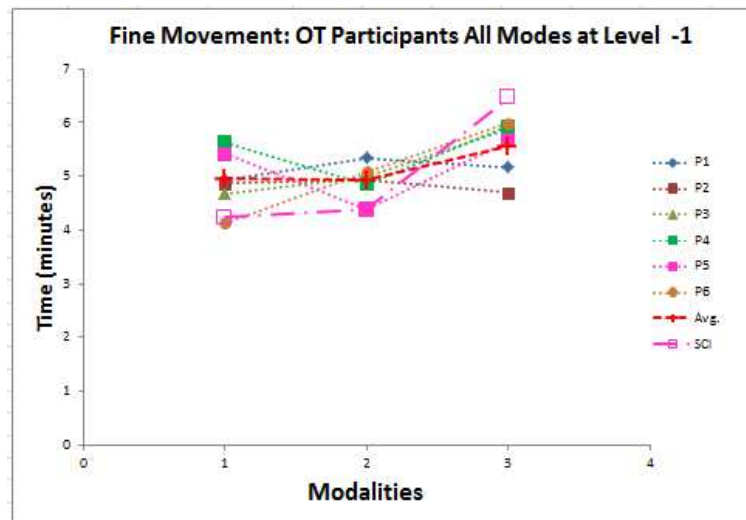


Figure 109: Individual time performance of the occupational therapy participants, their average, and the SCI participant's performance during the fine movement experiment on level -1 using all three control modalities; (1=button, 2=Slider, 3=Voice).

4.5.3.3 All Participants (Healthy and Occupational Therapy Students) in Comparison with the SCI Participant

In this section, time performances of all healthy participants (groups 1 and 2) were combined and compared to that of the SCI participant. Comparisons were made for ‘one mode, all levels’ and ‘all modes, one level’, where mode indicates the three control modalities and level indicates the three height levels of the test bench. In all subsequent plots, blue dotted lines with solid triangles represent the healthy participants (group 1) with their average shown by red solid line with triangles. Green dashed lines with solid circles represent individual occupational therapy participants with their average indicated by an orange solid line with solid circles. The SCI participant’s performance is represented by the magenta dot-dash line with hollow squares.

4.5.3.3.1 Time Performance of the SCI Participant vs. All Participants Using One Mode at All Levels

Figure 110 below shows the time performance of all participants for the fine movement experiment at all three levels using the button modality.

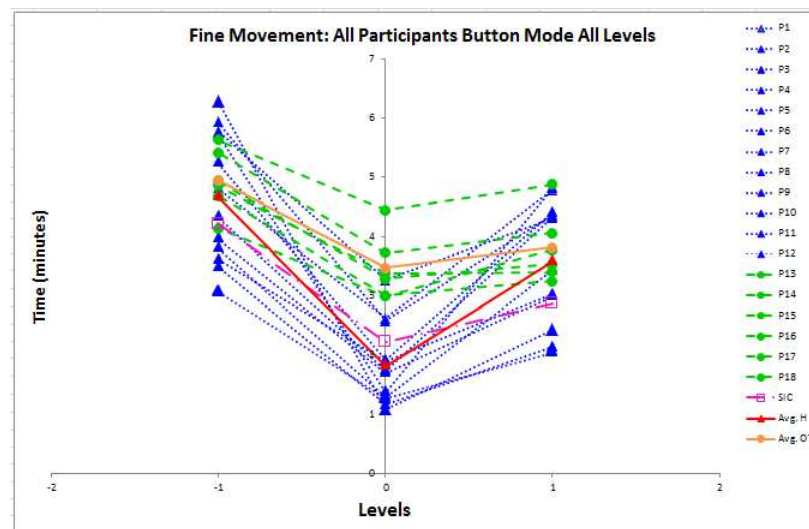


Figure 110: Individual time performances of all participants, and healthy participant averages (groups 1 and 2), during the fine movement experiment using the button modality on all three height levels.

Figure 111 below shows the time performance of all participants for the fine movement experiment at all three levels using the slider modality.

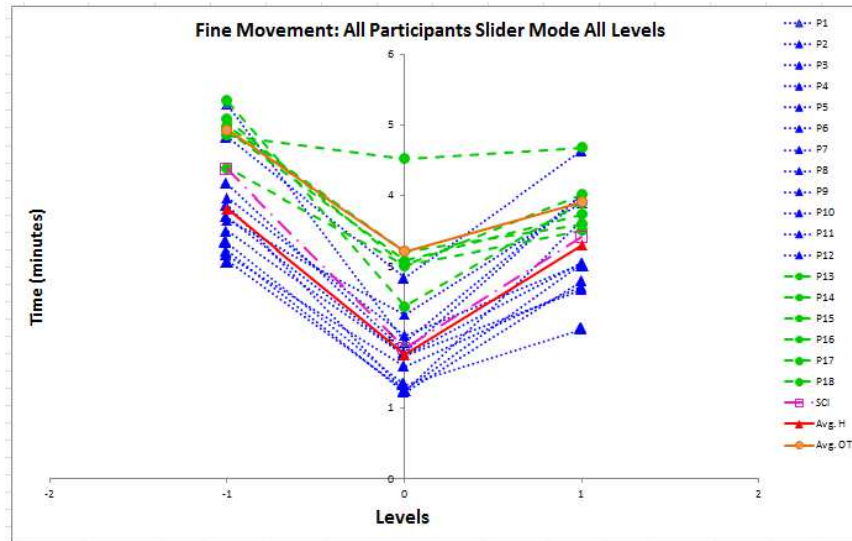


Figure 111: Individual time performances of all participants, and healthy participant averages (groups 1 and 2), during the fine movement experiment using the slider modality on all three height levels.

Figure 112 below shows the time performance of all participants for the fine movement experiment at all three levels using the voice modality.

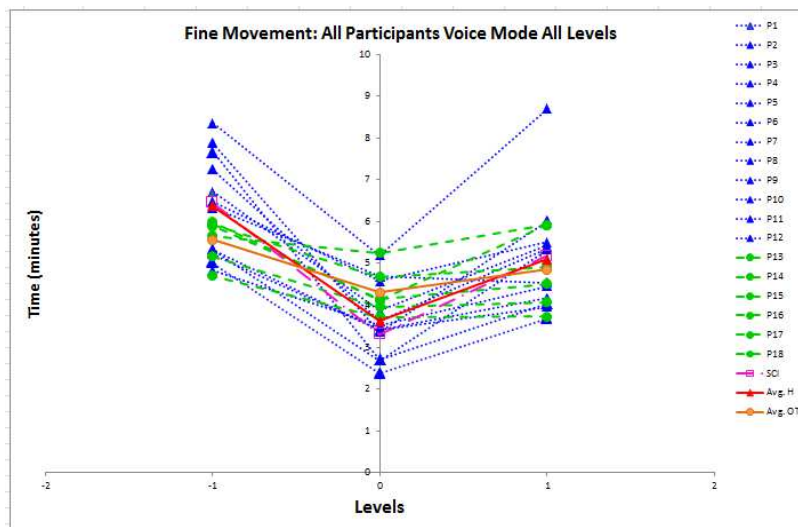


Figure 112: Individual time performances of all participants, and healthy participant averages (groups 1 and 2), during the fine movement experiment using the voice modality on all three height levels.

4.5.3.3.2 Time Performance of the SCI Participant vs. All Participants Using All Modes at One Level

Figure 113 below shows the individual time performances of all participants for the fine movement experiment at level +1 using the all three control modalities.

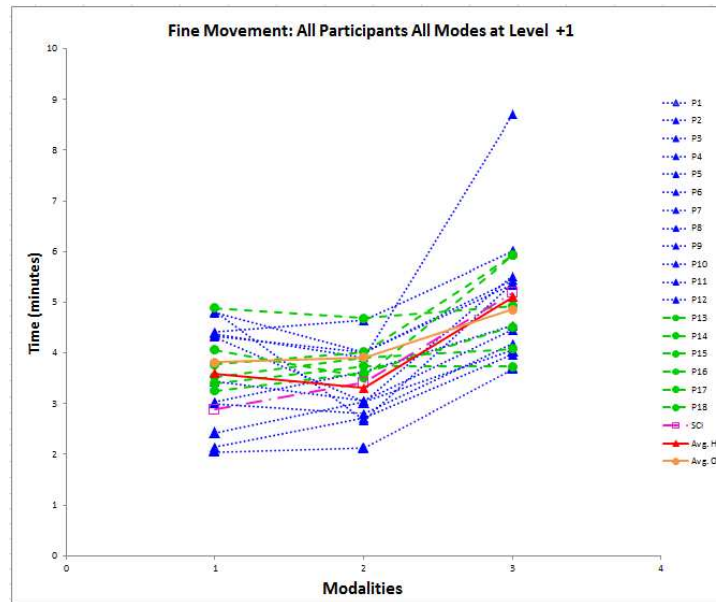


Figure 113: Individual time performances of all participants, and healthy participant averages (groups 1 and 2), during the fine movement experiment at level +1 using all three control modalities; (1=button, 2=Slider, 3=Voice).

Figure 114 below shows the individual time performances of all participants for the fine movement experiment at level 0 using the all three control modalities.

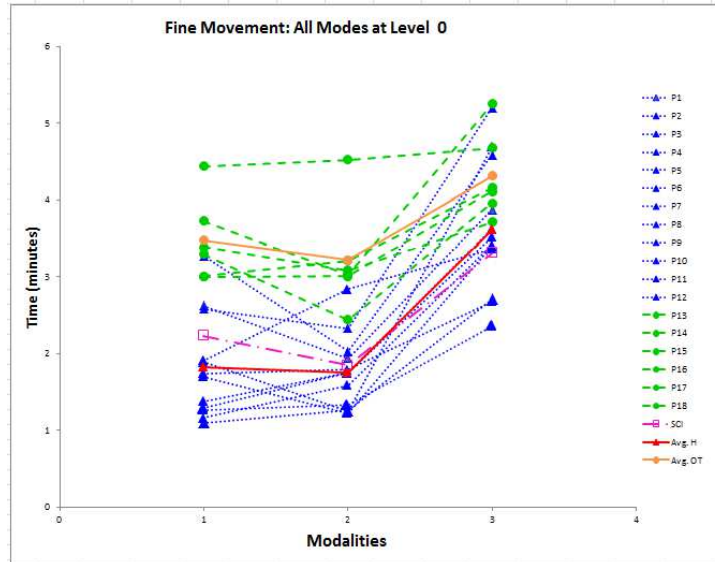


Figure 114: Individual time performances of all participants, and healthy participant averages (groups 1 and 2), during the fine movement experiment at level 0 using all three control modalities; (1=button, 2=Slider, 3=Voice).

Figure 115 below shows the individual time performances of all participants for the fine movement experiment at level -1 using the all three control modalities.

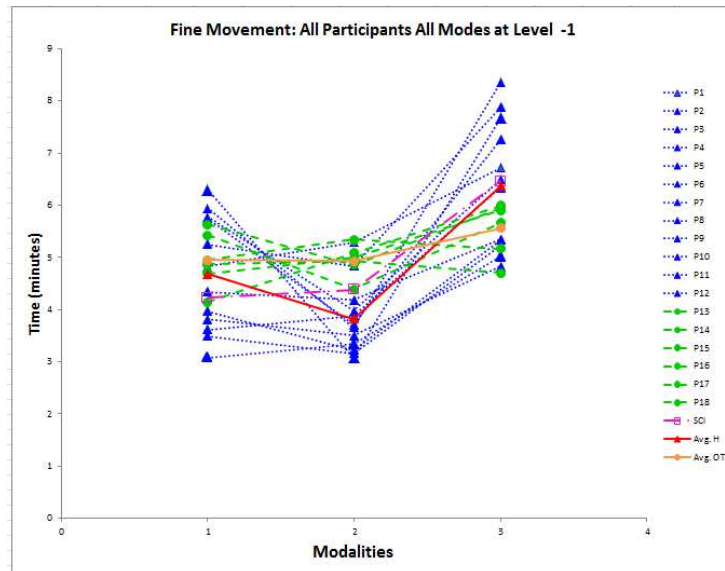


Figure 115: Individual time performances of all participants, and healthy participant averages (groups 1 and 2), during the fine movement experiment at level -1 using all three control modalities; (1=button, 2=Slider, 3=Voice).

4.5.4 Summary

The SCI participant's time performance was within 1 standard deviation of the average of group 1 (healthy participants/general population). The SCI participant's time performance was generally faster than the average time performance of group 2 (Occupational Therapy students). The difference was within 1 or 2 standard deviation. However, when the SCI participant's time performance was assessed against all the participants (group 1 + group 2), the performance difference falls within 1 standard deviation. It was noted that all participants took the longest to complete the lower level (-1 level/ mid-shin level). The fastest level was noted to be the middle level (level 0/ waist level).

4.6 EXPERIMENT 2: Gross Movement Experiment

4.6.1 Methods

4.6.1.1 Materials

A second test was conducted using the eSARA arm and the same groups of participants from experiment 1 in order to test gross movements. For the gross movements test, bottles of various weights were used with the test-bench. The test-bench and these bottles are shown in Figure 116a and 116b, respectively. The bottles weighed 0.5, 1, 1.5, and 2 lbs. Similar to the pegs in the fine movement experiment, the bottles were also color-coded. Participants were tasked with moving the color coded bottles to corresponding color coded positions on the test-bench. Bottles were also marked with their respective weights allowing the participant to know how much weight they were handling.

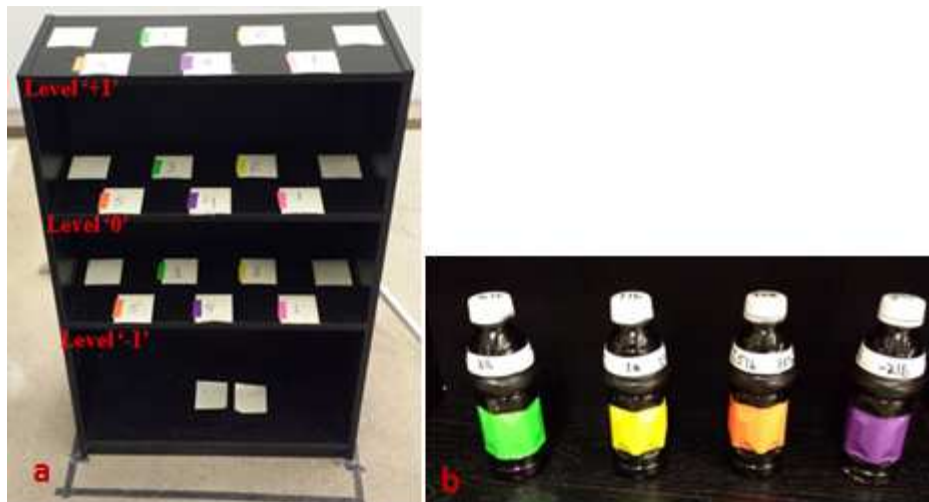


Figure 116: (a) The test-bench (b) Color-coded bottles of various weights.

4.6.1.2 Protocol

To test gross movements with the eSARA platform, the participants were required to perform what was called the Bottle-Weight Transfer Experiment. The lift assist feature of the device was activated during testing at all levels of the experiment. This completed one modality

(e.g. buttons). The same experiment was repeated with the remaining two modalities. All of the bottles were the same size and shape, but each had a different weight. Figure 117 below shows the start point and expected end point of the experiment for the three levels of the test bench.



Figure 117: Start and end points for the gross movement experiment.

To avoid fatigue, participants were allowed to take breaks during testing. Breaks within levels were 3 minutes and breaks between modalities were 5 minutes. The number of breaks

taken was subject to the individual participant's desire. Participants who required even more rest due to excessive fatigue were allowed to rest after completing each level. An option was also given to all the participants to complete the test over the course of one or two days if preferred. The total time to take the test without any breaks was approximately 45 minutes.

4.6.1.3 Error Tracking

Bottle diameters were increased to approximately 2.5 inches (see Figure 118) to improve grasping and prevent slipping of the bottles from the end-effector.

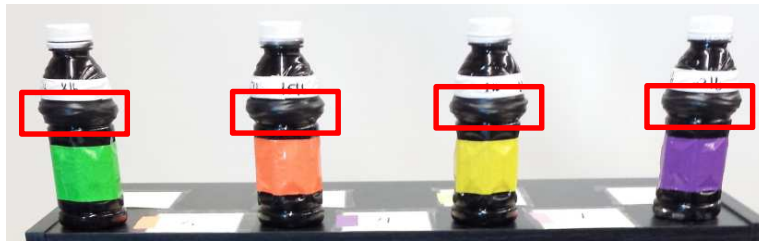


Figure 118: Bottles are marked with a red rectangle to show the additional support during the gross test to have a better grasp on the bottle. The diameter of the rings were noted to be approximately 0.75 inches wide 0.8 inches

Figure 119 shows possible errors committed by the participants during the gross movement tests. An error was recorded if the bottle was knocked down (Figure 119a) but it was determined that participants would not waste additional time and effort to make the bottle stand up. However, if the bottle was placed more than halfway off of its color coded slot (Figure 119b), it was considered an error that must be fixed before moving on. Figure 119c illustrates a failed bottle-weight transfer, which was recorded along with the specific bottle and the respective level.

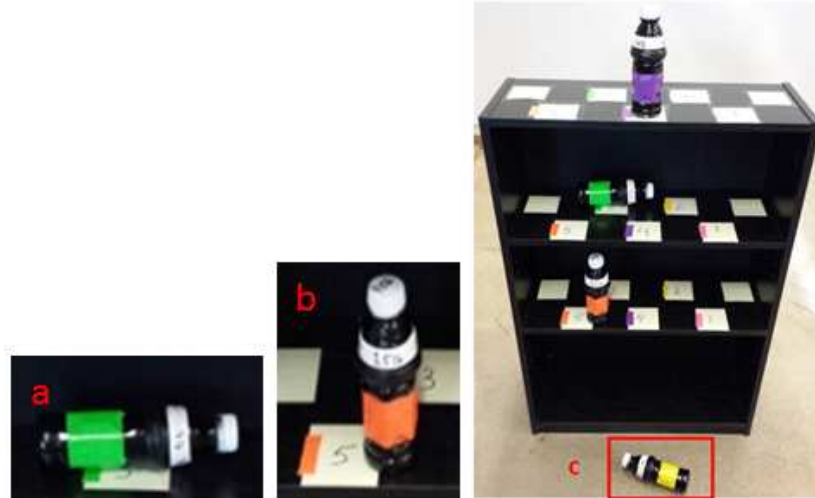


Figure 119: (a) and (b) Examples of errors for the gross movement experiment within the test bench. Only error type (b) required correction before moving on. (c) Errors outside of the test bench are considered a failed bottle transfer for that specific bottle and level.

4.6.2 Data Analysis

For the entire series of experiments the mean estimation and Analysis Of Variance (ANOVA) were calculated for able-bodied participants only. This compiled control data was then compared with the time performance of the SCI participant. Data was analyzed using SPSS (IBM) [97] statistical software. Descriptive data were provided for each participant. Differences in time between levels for all participants were compared using Analysis of Variance (ANOVA) with the Bonferroni correction for multiple comparisons. Significance was established at $p < 0.05$. Overlaying the plots was the average time of the healthy participants took to complete the experiment in each level. This average time of the healthy participants was represented by a thick dashed line, the SCI participant was represented by a thick dot and dash line. The plots also indicate the upper limits (marked with a dot) and lower limits (marked with a dot) for standard deviations. Participants did not report experiencing any discomfort or fatigue, and the principal investigator did not observe any signs of discomfort or fatigue over the course of the experiments.

Figure 120 shows how participants performed tasks for a given mode on all three levels. The time the participant took to complete each level was recorded in order to study the effect of change in height in relation to the modality. Level 0 represented natural working position in contrast to out of reach positions (level +1 and level -1).

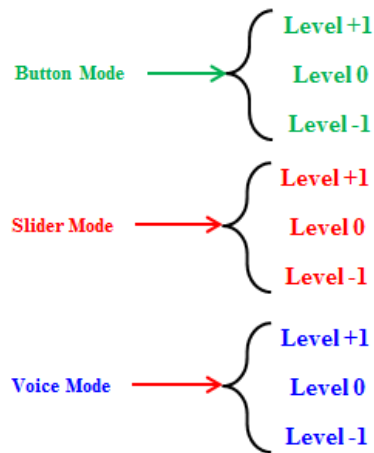


Figure 120: One Mode all level for gross movement

Figure 121 shows how participants were asked to perform tasks using all three control modalities on each of the height levels. For a given level, the participant completed the tasks using all three modalities. The time the participant took to complete each level was recorded in order to study the effect of change in the control mode at a given height (level). Level 0 represented a natural working position in contrast to out of reach positions (level +1 and level -1).

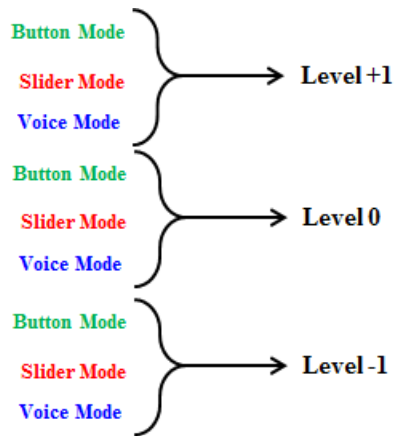


Figure 121: All Modes One level for gross movement

4.6.3 Results

4.6.3.1 Healthy Participants in Comparison with SCI Participant

All summary statistics (e.g. mean estimation and analysis of variance) were conducted on data collected from the healthy participants and occupation therapy participants only. Their combined data was then compared with that of the SCI participant. Figure 122 below shows a box and whisker plot of results from the healthy participants for the gross movement experiment using the button control mode. The SCI participant finished testing at levels +1 (chest) and 0 (waist), faster than the average healthy participants by 21.2% and 29.2%, respectively. At level -1 (mid-shin) the SCI participant was 10.7% slower than the average healthy individual. However, his performance was still within one standard deviation of the average.

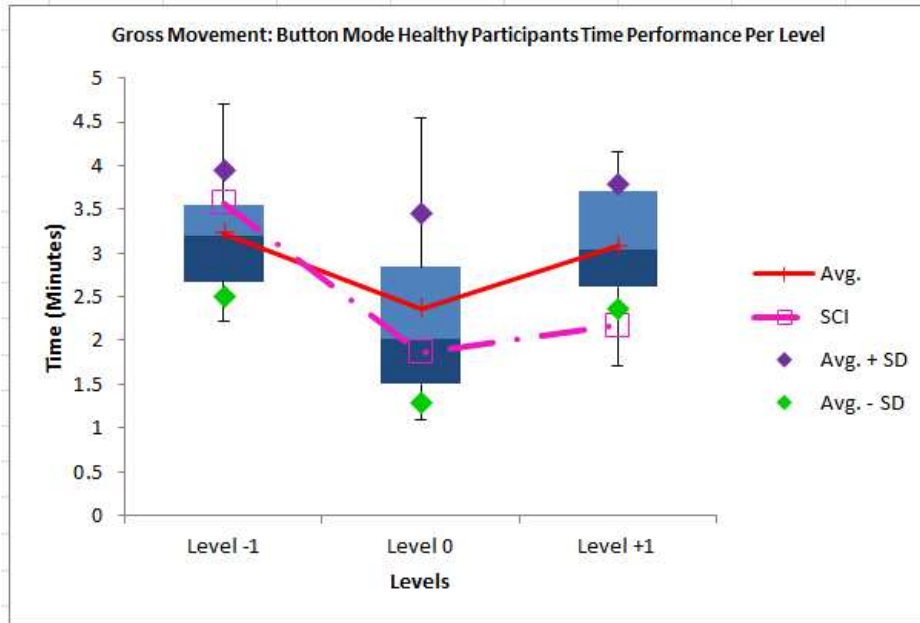


Figure 122: Box and whisker plot of the time performance of healthy participants during the gross movement experiment using the button control modality at each of the three height levels.

Each healthy participant's completion time and errors per level were recorded for the button mode for the gross movement experiment.

Levels	Mean	Std. Error	95% Confidence Interval	
			Lower Bound	Upper Bound
-1	3.228	.210	2.766	3.690
0	2.366	.311	1.680	3.051
+1	3.074	.207	2.618	3.530

Table 22: Estimated marginal mean of time (minutes) values and the standard error are reported for the gross movement experiment at each of the three levels using the button control mode. Values are calculated using data from the occupational therapy participants only.

There was a significant main effect for level height ($F(2, 22) = 6.763, p < 0.001$) in the gross movement experiment for the healthy participants using the button control modality. The pairwise comparisons for the main effect of level were corrected using Bonferroni adjustments and are displayed in the following table. Table 23 reveals a significant difference between levels

-1 and 0 (lower and middle; $p = 0.044$), but no significant differences between levels -1 and 1 (lower and upper; $p = 0.794$) or between levels 1 and 0 (upper and middle; $p = 0.091$).

(I) Levels	(J) Levels	Mean Difference (I-J)	Std. Error	Sig. ^b	95% Confidence Interval for Difference ^a	
					Lower Bound	Upper Bound
-1	0	.862 [*]	.299	.044	.020	1.705
	+1	.154	.131	.794	-.216	.524
0	-1	-.862 [*]	.299	.044	-1.705	-.020
	+1	-.708	.285	.091	-1.512	.095
+1	-1	-.154	.131	.794	-.524	.216
	0	.708	.285	.091	-.095	1.512

Table 23: ANOVA results for the gross movement experiment with healthy participants using the button mode, based on estimated marginal means *The mean difference was significant at the 0.05 level. ^b Bonferroni adjustment for multiple comparisons.

Figure 123 summarizes the results of the gross movement experiment for healthy participants using the slider control modality at each of the three height levels. The SCI participant finished testing at levels +1 (chest) and 0 (waist), faster than the average healthy participants by 14.3% and 18.5%, respectively. At level -1 (mid-shin) the SCI participant was 7.3% slower than the average healthy individual but his performance was still within one standard deviation from the average.

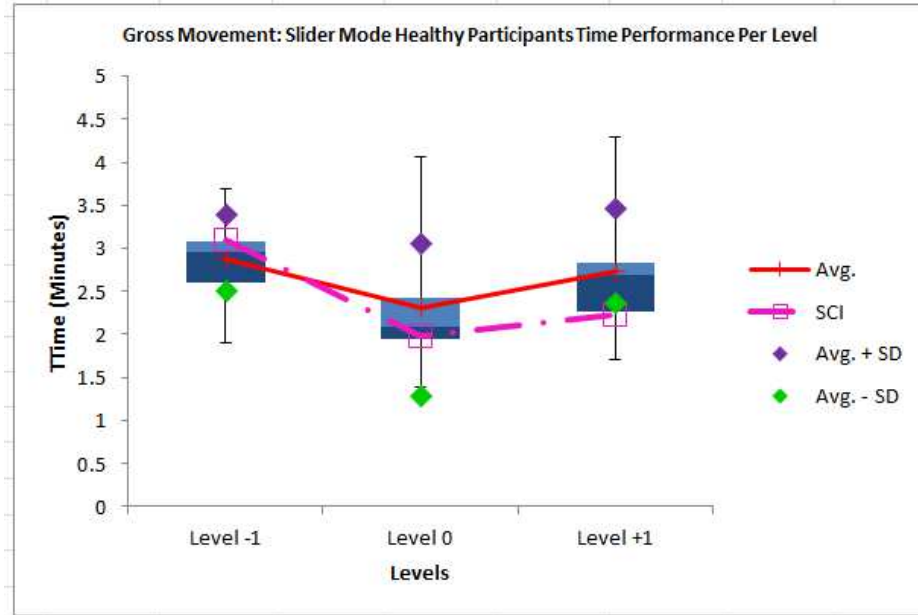


Figure 123: Box and whisker plot of the time performance of healthy participants during the gross movement experiment using the slider control modality at each of the three height levels.

Each healthy participant's completion time and errors per level were recorded for the slider mode for the gross movement experiment.

Levels	Mean	Std. Error	95% Confidence Interval	
			Lower Bound	Upper Bound
-1	2.883	.145	2.563	3.202
0	2.311	.213	1.842	2.781
+1	2.731	.209	2.271	3.192

Table 24: Estimated marginal mean of time (minutes) values and the standard error are reported for the gross movement experiment at each of the three levels using the slider control mode. Values are calculated using data from the occupational therapy participants only.

There was a significant main effect for level height ($F(2, 22) = 4.373, p < 0.001$) in the gross movement experiment for the healthy participants using the slider control mode. The pairwise comparisons for the main effect of level were corrected using Bonferroni adjustments and are displayed in Table 25. Main effect statistical analysis reveals no significant difference ($p = 0.086$)

between any of the pairs of levels. Levels -1 and 0 (lower and middle), between levels -1 and 1 (lower and upper) ($p = 1.000$) and between levels 1 and 0 (upper and middle) ($p = 0.197$).

(I) Levels	(J) Levels	Mean Difference (I-J)	Std. Error	Sig. ^a	95% Confidence Interval for Difference ^a	
					Lower Bound	Upper Bound
-1	0	.571	.227	.086	-.069	1.211
	+1	.151	.163	1.000	-.307	.610
0	-1	-.571	.227	.086	-1.211	.069
	+1	-.420	.205	.197	-.999	.159
+1	-1	-.151	.163	1.000	-.610	.307
	0	.420	.205	.197	-.159	.999

Table 25: ANOVA results for the gross movement experiment with healthy participants using the slider mode, based on estimated marginal means ^aThe mean difference was significant at the 0.05 level. ^b Bonferroni adjustment for multiple comparisons.

Figure 124 below shows a box and whisker plot of only the healthy participants for the gross movement experiment using the voice mode. The SCI participant finished testing at levels +1 (chest) and 0 (waist), faster than the average healthy participants by 2.6% and 0.7%, respectively. At level -1 (mid-shin) the SCI participant was 4.2% slower than the average healthy individual but still within one standard deviation of the average.

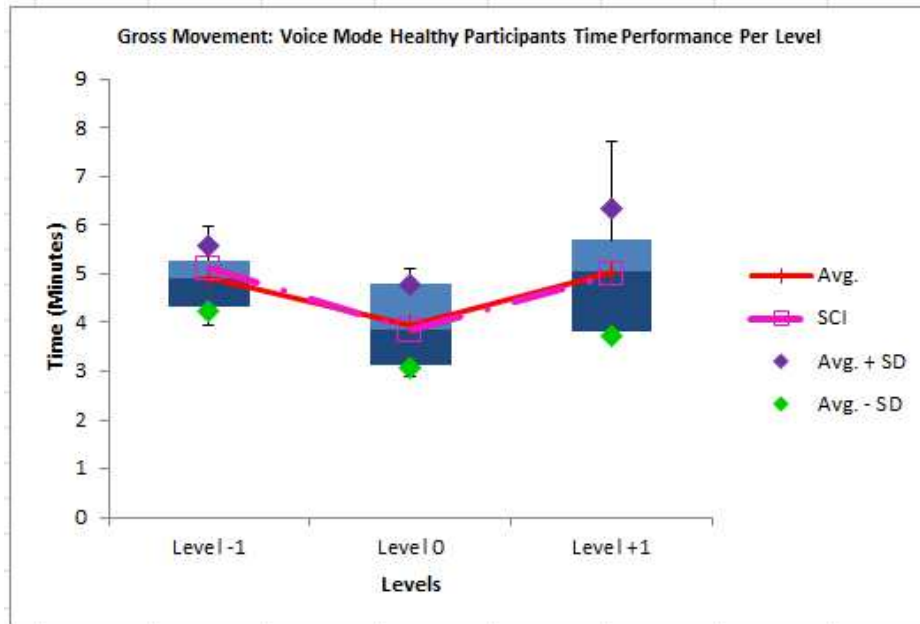


Figure 124: Box and whisker plot of the time performance of healthy participants during the gross movement experiment using the voice modality on all three height levels.

Each healthy participant's completion time and errors per level were recorded for the voice mode for the gross movement experiment.

Levels	Mean	Std. Error	95% Confidence Interval	
			Lower Bound	Upper Bound
-1	4.909	.195	4.481	5.338
0	3.943	.247	3.399	4.487
+1	5.032	.376	4.203	5.860

Table 26: Estimated marginal mean of time (minutes) values and the standard error are reported for the gross movement experiment at each of the three levels using the voice control mode. Values are calculated using data from the occupational therapy participants only.

There was a significant main effect for level height ($F(2, 22) = 12.320, p < 0.001$) in the gross movement experiment for healthy participants using the voice control modality. The pairwise comparisons for the main effect of level were corrected using Bonferroni adjustments. Table 27 shows that the significant main effect reflects a significant difference between levels -1 and 0 (lower and middle; $p = 0.001$) and between levels 1 and 0 (upper and middle; $p = 0.010$). However, there was no significant difference between levels -1 and 1 (lower and upper; $p = 1.000$).

(I) Levels	(J) Levels	Mean Difference (I-J)	Std. Error	Sig. ^b	95% Confidence Interval for Difference ^b	
					Lower Bound	Upper Bound
-1	0	.967*	.197	.001	.410	1.523
	+1	-.122	.220	1.000	-.742	.498
0	-1	-.967*	.197	.001	-1.523	-.410
	+1	-1.089*	.293	.010	-1.916	-.262
+1	-1	.122	.220	1.000	-.498	.742
	0	1.089*	.293	.010	.262	1.916

Table 27: ANOVA results for the gross movement experiment with healthy participants using the voice mode, based on estimated marginal means *The mean difference was significant at the 0.05 level. ^b Bonferroni adjustment for multiple comparisons.

4.6.3.1.1 Time Performance of the SCI Participant vs. Healthy Participants Using One Mode at All Levels

Figure 125 below shows the individual time performance of each healthy participant for the gross movement experiment at all three levels using the button modality.

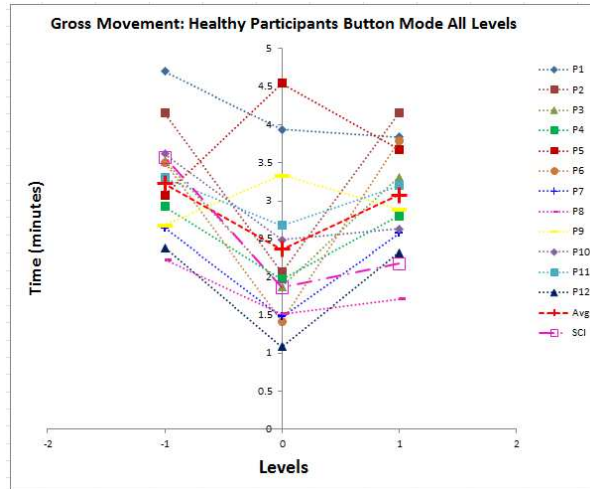


Figure 125: Individual time performance of healthy participants, their average, and the SCI participant's performance are shown for the gross movement experiment conducted at all three height levels using the button modality.

Figure 126 below shows the individual time performance of each healthy participant for the gross movement experiment at all three levels using the slider modality.

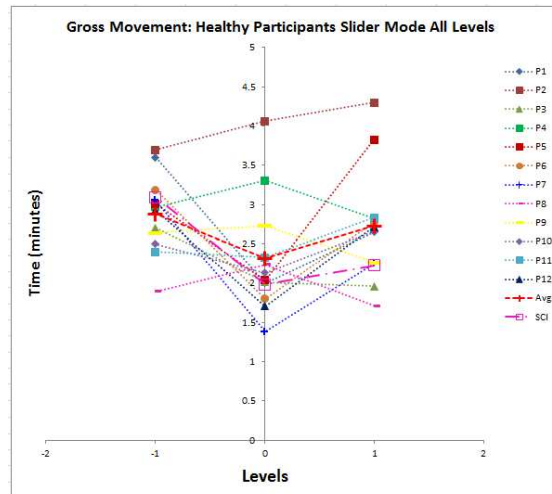


Figure 126: Individual time performance of healthy participants, their average, and the SCI participant's performance are shown for the gross movement experiment conducted at all three height levels using the slider modality.

Figure 127 below shows the time performance of each healthy participant for the gross movement experiment at all three levels using the voice modality.

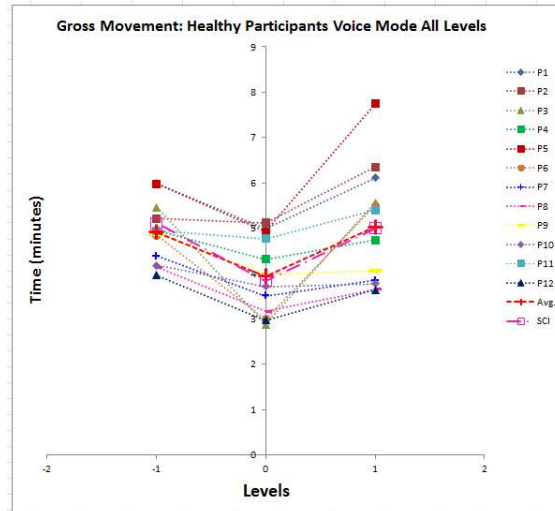


Figure 127: Individual time performance of healthy participants, their average, and the SCI participant's performance are shown for the gross movement experiment conducted at all three height levels using the voice modality.

4.6.3.1.2 Time Performance of the SCI Participant vs. Healthy Participants using All Modes at One Level

Figure 128 below shows the individual time performance of each healthy participant for the gross movement experiment at level +1 (chest) using all three control modalities.

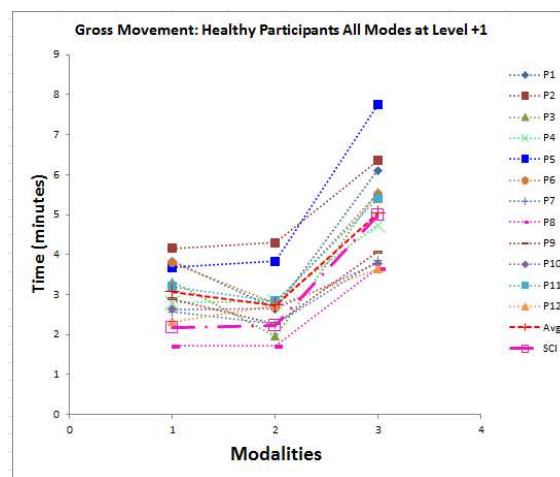


Figure 128: Individual time performance of healthy participants, their average, and the SCI participant's performance during the gross movement experiment on level +1 using all the three modalities; (1=button, 2=Slider, 3=Voice).

Figure 129 below shows the time performance of each healthy participant for the gross movement experiment at level 0 using all three control modalities.

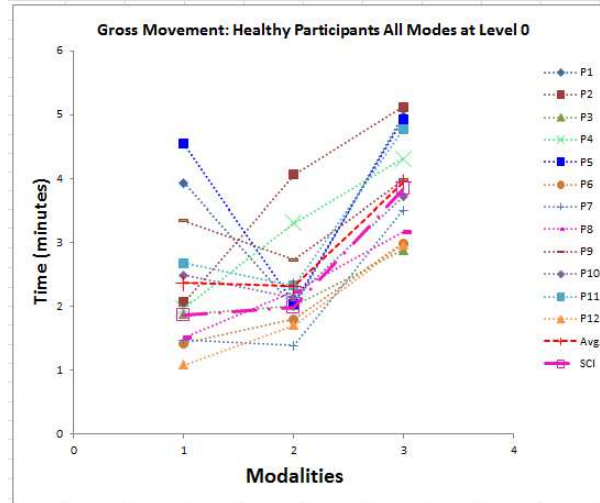


Figure 129: Individual time performance of healthy participants, their average, and the SCI participant's performance during the gross movement experiment on level 0 using all the three modalities; (1=button, 2=Slider, 3=Voice).

Figure 130 below shows the time performance of each healthy participant for the gross movement experiment at level -1 using all three control modalities.

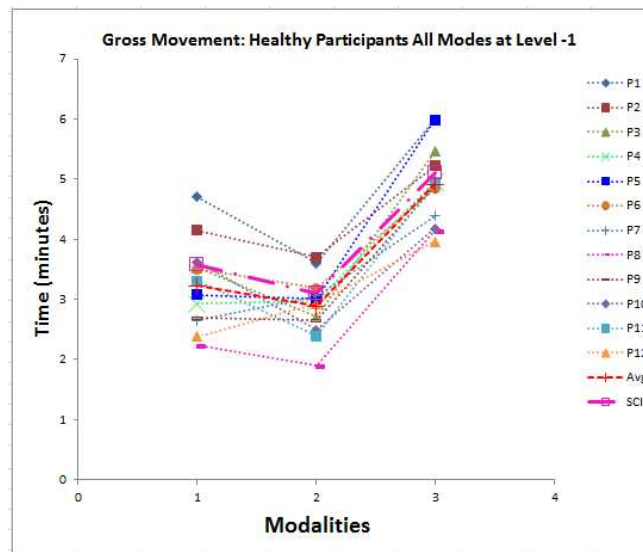


Figure 130: Individual time performance of healthy participants, their average, and the SCI participant's performance during the gross movement experiment on level -1 using all the three modalities; (1=button, 2=Slider, 3=Voice).

4.6.3.2 Healthy Restricted Participants (Occupational Therapy Students) in Comparison with SCI Participant

The above analysis for the healthy participants (group 1) has been repeated for the healthy participants restricting their movements (occupational therapy participants/group 2).

Figure 131 below shows a box and whisker plot of only the occupational therapy participants for the gross movement experiment using the button mode. The SCI participant finished testing at levels -1 (mid-shin), 0 (waist), and +1 (chest), faster than the average of the occupational therapy participants by 20.1%, 35.7%, and 31.1%, respectively. However, his performance was still within two standard deviations of the average.

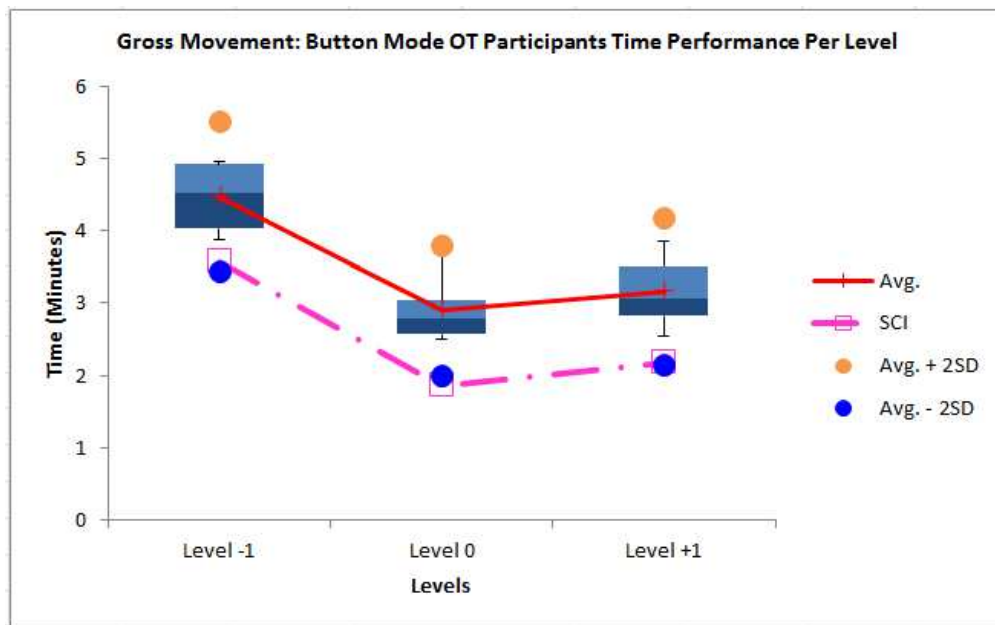


Figure 131: Box and whisker plot of the time performance of occupational therapy participants during the gross movement experiment using the button modality on all three levels.

Each occupational therapy participant's completion time and errors per level were recorded for the button mode for the gross movement experiment.

Levels	Mean	Std. Error	95% Confidence Interval	
			Lower Bound	Upper Bound
1	4.471	.212	3.927	5.016
2	2.898	.184	2.425	3.370
3	3.157	.206	2.628	3.687

Table 28: Estimated marginal mean of time (minutes) values and the standard error are reported for the gross movement experiment at each of the three levels using the button control mode. Values are calculated using data from the occupational therapy participants only.

There was a significant main effect for level height ($F(2, 10) = 50.689, p < 0.001$) in the gross movement experiment occupational therapy participants using button mode. The pairwise comparisons for the main effect of level were corrected using Bonferroni adjustments. Table 29 shows that the significant main effect reflects a significant difference between levels -1 and 0 (lower and middle; $p = 0.002$), between levels -1 and 1 (lower and upper; $p = 0.003$), but was not significant between levels 1 and 0 (upper and middle; $p = 0.094$).

(I) Levels	(J) Levels	Mean Difference (I-J)	Std. Error	Sig. ^b	95% Confidence Interval for Difference ^a	
					Lower Bound	Upper Bound
-1	0	1.573 [*]	.206	.002	.846	2.300
	+1	1.314 [*]	.185	.003	.660	1.968
0	-1	-1.573 [*]	.206	.002	-2.300	-.846
	+1	-.259	.087	.094	-.568	.049
+1	-1	-1.314 [*]	.185	.003	-1.968	-.660
	0	.259	.087	.094	-.049	.568

Table 29: ANOVA results for the gross movement experiment with occupational therapy participants using the button mode, based on estimated marginal means ^aThe mean difference was significant at the 0.05 level. ^b Bonferroni adjustment for multiple comparisons.

Figure 132 below shows a box and whisker plot of the time performances of the occupational therapy participants for the gross movement experiment using the slider mode. The SCI participant finished testing at levels -1 (mid-shin), 0 (waist), and +1 (chest), faster than the average of the occupational therapy participants by 27.1%, 30.0%, and 30.8%, respectively. However, his performance was still within two standard deviations of the average.

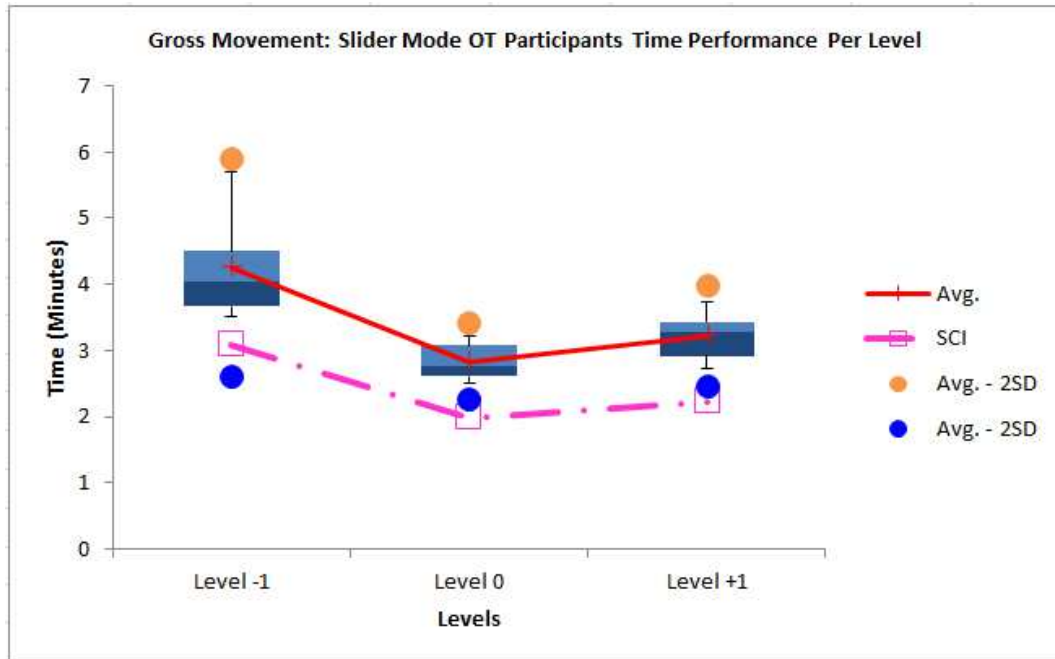


Figure 132: Box and whisker plot of the time performance of the occupational therapy participants during the gross movement experiment using the slider modality on all three height levels.

Each occupational therapy participant's completion time and errors per level were recorded for the slider mode for the gross movement experiment.

Levels	Mean	Std. Error	95% Confidence Interval	
			Lower Bound	Upper Bound
-1	4.245	.335	3.384	5.106
0	2.833	.119	2.527	3.139
+1	3.218	.156	2.816	3.619

Table 30: Estimated marginal mean of time (minutes) values and the standard error are reported for the gross movement experiment at each of the three levels using the slider control mode. Values are calculated using data from the occupational therapy participants only.

There was a significant main effect for level height ($F(2, 10) = 19.379, p < 0.001$) in the gross movement experiment for the occupational therapy participants using slider mode. The pairwise comparisons for the main effect of level were corrected using Bonferroni adjustments.

Table 31 shows that the significant main effect reflects a significant difference between levels -1

and 0 (lower and middle; $p = 0.016$), between levels -1 and 1 (lower and upper; $p = 0.026$), but no significant difference existed between levels 1 and 0 (upper and middle; $p = 0.067$).

(I) Levels	(J) Levels	Mean Difference (I-J)	Std. Error	Sig. ^a	95% Confidence Interval for Difference ^b	
					Lower Bound	Upper Bound
-1	0	1.412*	.301	.016	.347	2.478
	+1	1.028*	.246	.026	.159	1.896
0	-1	-1.412*	.301	.016	-2.478	-.347
	+1	-.385	.118	.067	-.800	.031
+1	-1	-1.028*	.246	.026	-1.896	-.159
	0	.385	.118	.067	-.031	.800

Table 31: ANOVA results for the gross movement experiment with occupational therapy participants using the slider mode, based on estimated marginal means *The mean difference was significant at the 0.05 level. ^b Bonferroni adjustment for multiple comparisons.

Figure 133 below shows a box and whisker plot of the occupational therapy participants' time performance for the gross movement experiment using the voice mode. The SCI participant finished testing at levels -1 (mid-shin), 0 (waist), and +1 (chest), faster than the average of the occupational therapy participants by 7.9%, 13.9%, and 0.4%, respectively. However, his time performance at each of the three height levels were all within 1 standard deviation of the occupational therapy participants' average.

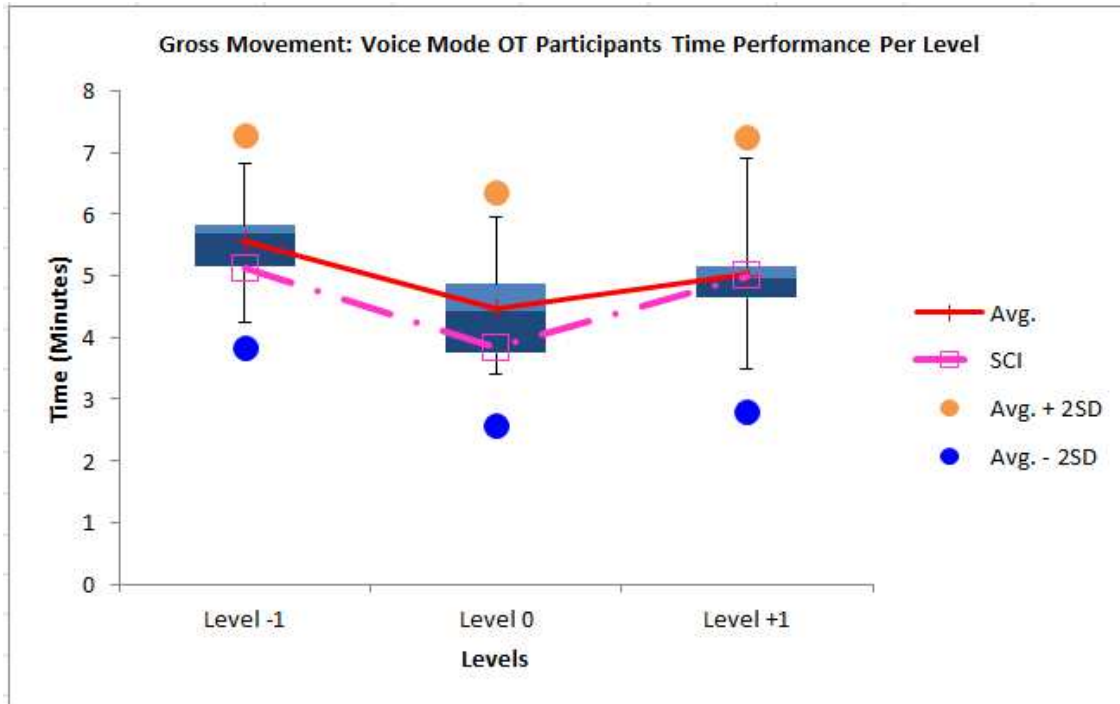


Figure 133: Box and whisker plot of the time performance of occupational therapy participants during the gross movement experiment using the voice modality on all three levels.

Each occupational therapy participant's completion time and errors per level were recorded for the voice mode for the gross movement experiment.

Levels	Mean	Std. Error	95% Confidence Interval	
			Lower Bound	Upper Bound
-1	5.554	.354	4.644	6.463
0	4.459	.386	3.466	5.452
+1	5.017	.454	3.849	6.185

Table 32: Estimated marginal mean of time (minutes) values and the standard error are reported for the gross movement experiment at each of the three levels using the voice control mode. Values are calculated using data from the occupational therapy participants only.

There was a significant main effect for level height ($F(2, 10) = 24.651, p < 0.001$) in the gross movement experiment for the occupational therapy participants using voice mode. The pairwise comparisons for the main effect of level were corrected using Bonferroni adjustments.

Table 33 shows that the significant main effect reflects a significant difference between levels -1

and 0 (lower and middle; $p = 0.003$), between levels -1 and 1 (lower and upper; $p = 0.045$), but not between levels 1 and 0 (upper and middle; $p = 0.053$).

(I) Levels	(J) Levels	Mean Difference (I-J)	Std. Error	Sig. ^b	95% Confidence Interval for Difference ^b	
					Lower Bound	Upper Bound
-1	0	1.094*	.159	.003	.532	1.657
	+1	.536*	.148	.045	.013	1.060
0	-1	-1.094*	.159	.003	-1.657	-.532
	+1	-.558	.160	.053	-1.124	.008
+1	-1	-.536*	.148	.045	-1.060	-.013
	0	.558	.160	.053	-.008	1.124

Table 33: ANOVA results for the gross movement experiment with occupational therapy participants using the voice mode, based on estimated marginal means *The mean difference was significant at the 0.05 level. ^b Bonferroni adjustment for multiple comparisons.

4.6.3.2.1 Time Performance of the SCI Participant vs. Occupational Therapy Participants Using One Mode at All Levels

Figure 134 below shows the individual time performance of each occupational therapy participant for the gross movement experiment at all three levels using the button modality.

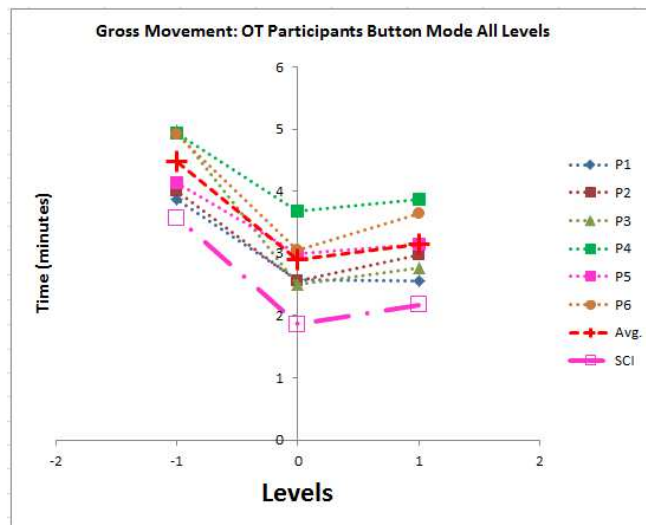


Figure 134: Individual time performance of occupational therapy participants, their average, and the SCI participant’s performance during the gross movement experiment using the button modality on all three height levels.

Figure 135 below shows the time performance of each occupational therapy participant for the gross movement experiment at all three levels using the slider modality.

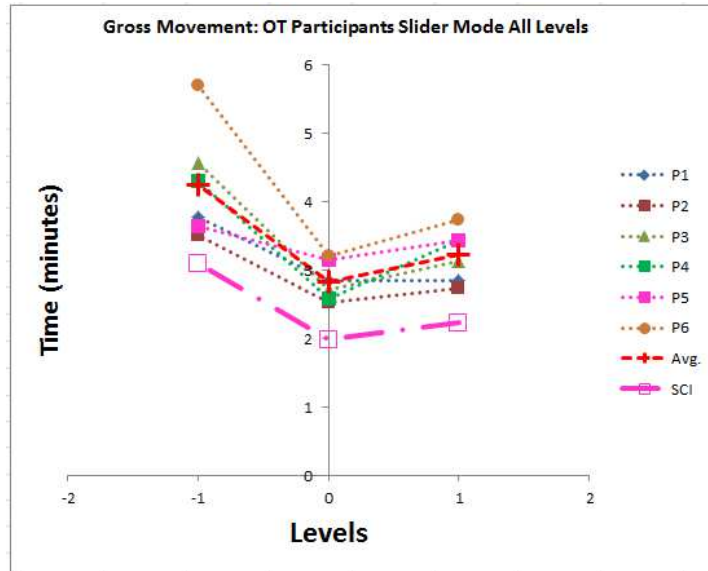


Figure 135: Individual time performance of occupational therapy participants, their average, and the SCI participant’s performance during the gross movement experiment using the slider modality on all three height levels.

Figure 136 below shows the time performance of each occupational therapy participant for the gross movement experiment at all three levels using the voice modality.

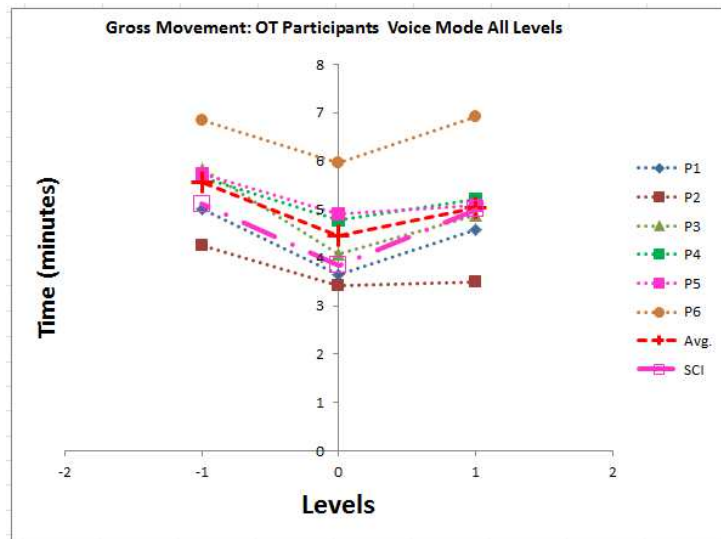


Figure 136: Individual time performance of occupational therapy participants, their average, and the SCI participant’s performance during the gross movement experiment using the voice modality on all three height levels.

4.6.3.2.2 Time Performance of the SCI Participant vs. Occupational Therapy Participants Using All Mode at One Levels

Figure 137 below shows the time performance of each occupational therapy participant for the gross movement experiment at level +1 using all three control modalities.

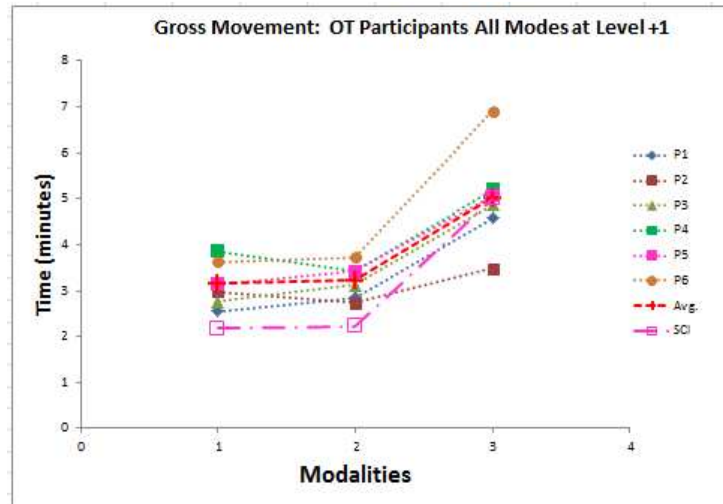


Figure 137: Individual time performance of the occupational therapy participants, their average, and the SCI participant's performance during the gross movement experiment on level +1 using all three modalities; (1=button, 2=Slider, 3=Voice).

Figure 138 below shows the time performance of each occupational therapy participant for the gross movement experiment at level 0 using all three modalities.

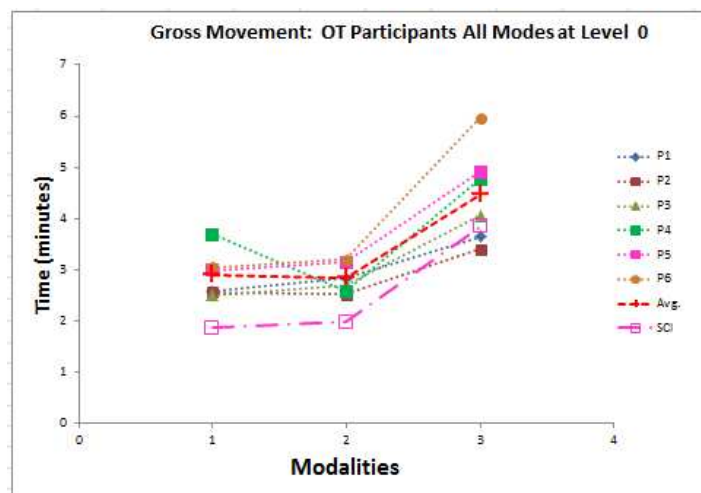


Figure 138: Individual time performance of the occupational therapy participants, their average, and the SCI participant's performance during the gross movement experiment on level 0 using all three modalities; (1=button, 2=Slider, 3=Voice).

Figure 139 below shows the time performance of each occupational therapy participant for the gross movement experiment at level -1 using all three modalities.

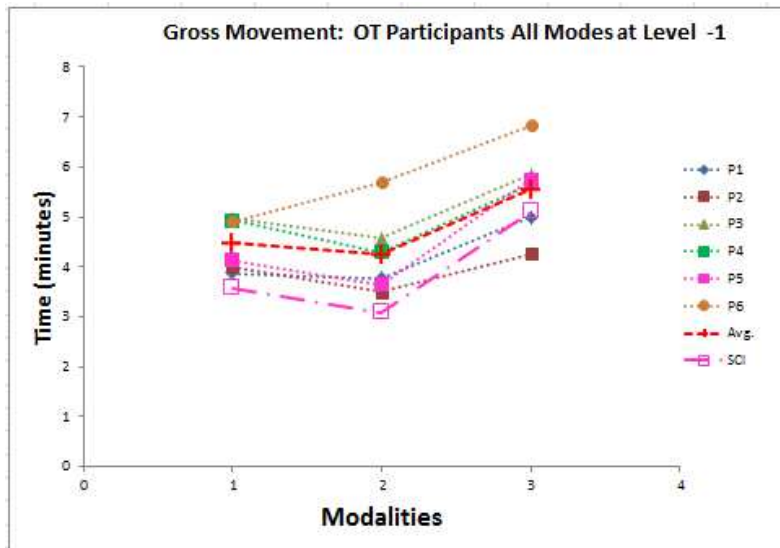


Figure 139: Individual time performance of the occupational therapy participants, their average, and the SCI participant's performance during the gross movement experiment on level -1 using all three modalities; (1=button, 2=Slider, 3=Voice).

4.6.3.3 All Participants (Healthy and Occupational Therapy Students) in Comparison with SCI Participant

In this section, time performances of all healthy participants (groups 1 and 2) were combined and compared to that of the SCI participant. Comparisons were made for 'one mode, all levels' and 'all modes, one level', where mode indicates the three control modalities and level indicates the three height levels of the test bench. In all subsequent plots, blue dotted lines with solid triangles represent the healthy participants (group 1) with their average shown by red solid line with triangles. Green dashed lines with solid circles represent individual occupational therapy participants with their average indicated by an orange solid line with solid circles. The SCI participant's performance is represented by the magenta dot-dash line with hollow squares.

4.6.3.3.1 Time Performance of the SCI Participant vs. All Participants Using One Mode at All Levels

Figure 140 below shows the time performance of all participants for the gross movement experiment at all three levels using the button modality.

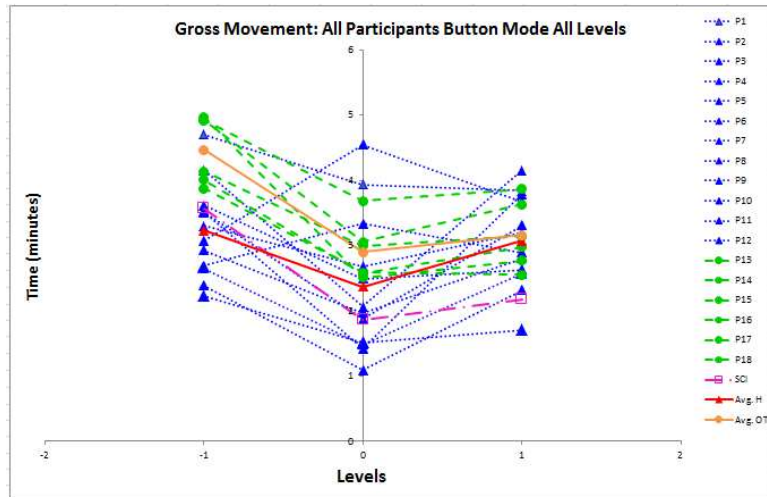


Figure 140: Individual time performance of all participants, and their average along with the SCI participant's performance during the gross movement experiment on all the three levels using the button modality.

Figure 141 below shows the time performance of all participants for the gross movement experiment at all three levels using the slider modality.

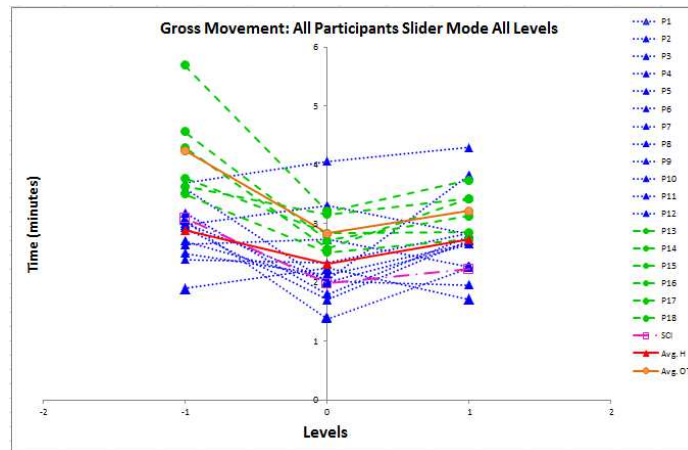


Figure 141: Individual time performance of all participants and their average along with the SCI participant's performance during the gross movement experiment on all the three levels using the slider modality.

Figure 142 below shows the time performance of all participants for the gross movement experiment at all three levels using the voice modality.

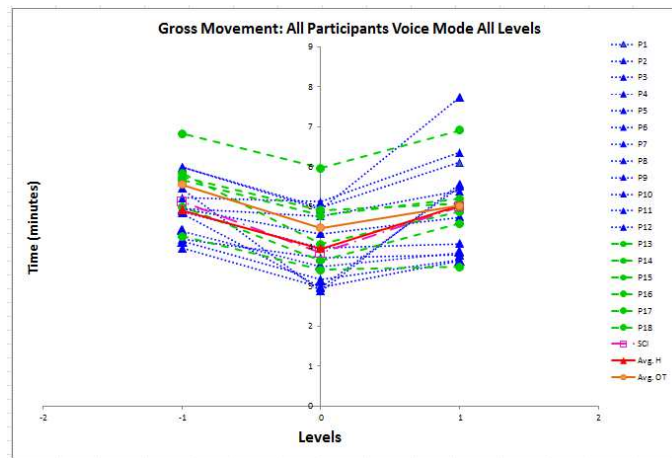


Figure 142: Individual time performance of all participants and their average along with the SCI participant's performance during the gross movement experiment on all the three levels using the voice modality.

4.6.3.3.2 Time Performance of the SCI Participant vs. All Participants Using All Modes at One Level

Figure 143 below shows the time performance of each participant for the gross movement experiment at level +1 using all three modalities.

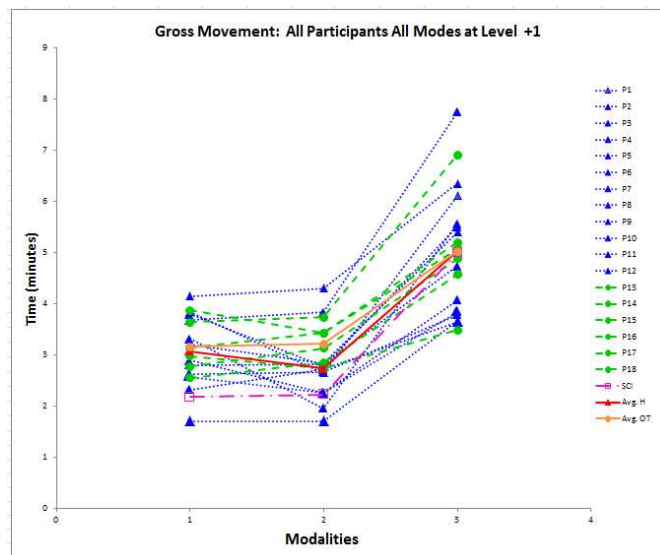


Figure 143: Individual time performance of all participants and their average along with the SCI participant's performance during the gross movement experiment on level +1 using all three modalities; (1=button, 2=Slider, 3=Voice).

Figure 144 below shows the time performance of each participant for the gross movement experiment at level 0 using all three modalities.

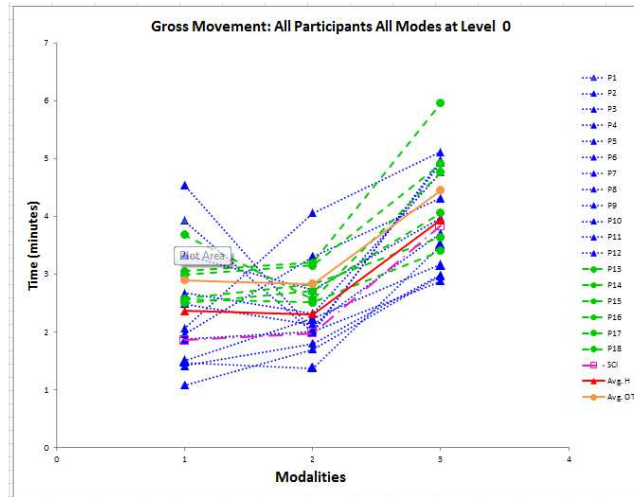


Figure 144: Individual time performance of all participants and their average along with the SCI participant's performance during the gross movement experiment on level 0 using all three modalities; (1=button, 2=Slider, 3=Voice).

Figure 145 below shows the time performance of each participant for the gross movement experiment at level -1 using all three modalities.

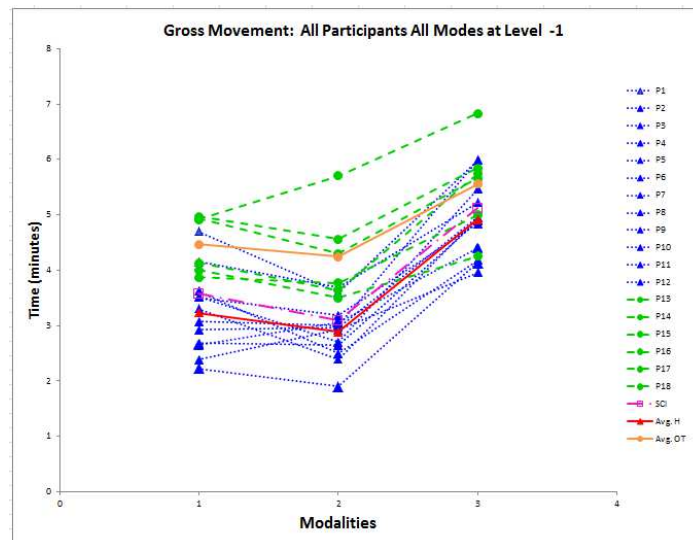


Figure 145: Individual time performance of all participants and their average along with the SCI participant's performance during the gross movement experiment on level -1 using all three modalities; (1=button, 2=Slider, 3=Voice).

4.6.4 Summary

The SCI participant's time performance was within 1 standard deviation of the average of Group 1 (healthy participants (general population)). The SCI participant's time performance was generally faster than the average time performance of group 2 (Occupational Therapy students). The difference was within 1 or 2 standard deviation. However when the SCI participant's time performance was assessed against all the participants (group 1 + group 2), the performance difference falls within 1 standard deviation. It was noted that all participants took the longest to complete the lower level (-1 level/ mid-shin level). The fastest level was noted to be the middle level (level 0/ waist level).

4.7 NASA TLX Results

This section discusses the results of the NASA TLX data collected after the completion of both experiment 1 and experiment 2. The subscales (as described in section 4.4) include Mental Demands (MD), Physical Demands (PD), Temporal Demands (TD), Performance (PF), Effort (EF) and Frustration (FR). The 'Scores' represent the 'Weighted Mean Workload'.

4.7.1 Healthy Participants

Table 34 shows the average of the NASA TLX results of the healthy participants (subscale averages denoted by their acronym + prime, e.g. MD'). These results were compared to that of the SCI participant's with columns immediately to the right of each subscale average (red text).

	Levels	MD'	MD	PD'	PD	TD'	TD	PF'	PF	EF'	EF	FR'	FR	Score'	Score
Fine Movement	1	34.2	35.0	40.0	40.0	36.3	30.0	17.1	15.0	36.3	55.0	32.5	60.0	33.0	40.0
	0	21.7	30.0	24.2	50.0	31.7	30.0	15.4	20.0	20.8	55.0	22.5	75.0	23.0	43.0
	-1	45.4	50.0	53.3	60.0	44.2	60.0	34.6	35.0	49.6	90.0	40.8	75.0	45.1	61.0
Gross Movement	1	46.3	35.0	50.8	65.0	39.2	40.0	36.3	15.0	46.7	65.0	46.3	70.0	47.2	48.0
	0	27.5	30.0	33.8	45.0	33.3	40.0	27.9	25.0	36.3	60.0	31.7	75.0	32.1	45.0
	-1	48.8	60.0	62.9	80.0	49.6	65.0	44.2	30.0	59.6	90.0	43.3	65.0	55.4	65.0

Table 34: Average of the NASA TLX results for the healthy participants compared with that of the SCI participant.

4.7.2 Healthy Restricted (Occupational Therapy Students) Participants

Table 35 shows the average results from the NASA TLX assessment taken by the occupational therapy participants (these averages are shown by each subscale acronym, e.g. MD'). These results were compared to that of the SCI participant's with columns immediately to the right of each subscale average (red text).

	Levels	MD'	MD	PD'	PD	TD'	TD	PF'	PF	EF'	EF	FR'	FR	Score'	Score
Fine Movement	1	27.5	35.0	22.5	40.0	25.0	30.0	15.0	15.0	26.7	55.0	26.7	60.0	25.3	40.0
	0	25.8	30.0	19.2	50.0	32.5	30.0	10.0	20.0	20.8	55.0	21.7	75.0	21.1	43.0
	-1	32.5	50.0	38.3	60.0	30.8	60.0	11.7	35.0	49.2	90.0	31.7	75.0	34.5	61.0
Gross Movement	1	55.8	35.0	50.0	65.0	42.5	40.0	21.7	15.0	56.7	65.0	32.5	70.0	43.7	48.0
	0	26.7	30.0	30.0	45.0	30.8	40.0	8.3	25.0	35.0	60.0	32.5	75.0	30.8	45.0
	-1	60.0	60.0	65.8	80.0	50.8	65.0	34.2	30.0	65.8	90.0	45.8	65.0	52.1	65.0

Table 35: Average of the NASA TLX results for the occupational therapy participants compared with that of the SCI participant.

These two tables reveal that the mid-shin level (-1) required the most effort (EF) and physical demand (PD) for both the fine movement and gross movement experiments.

4.7.3 NASA TLX Result Summary

In table 36 below, each NASA TLX subscale has been marked with a cross (X) to indicate which height level the participants found most challenging. The index marked in red with MD represents the SCI participant whereas the unmarked index MD represents the combined replies

of both the healthy and healthy restricted participants. The table shows that both the SCI and all other participants faced the most challenges at level -1 (mid-shin level).

	Level	MD'	MD	PD'	PD	TD'	TD	PF'	PF	EF'	EF	FR'	FR	Score'	Score
Fine	1														
	0														
	-1	X	X	X	X	X	X	X	X	X	X	X	X	X	X
Gross	1														
	0														
	-1	X	X	X	X	X	X	X	X	X	X	X	X	X	X

Table 36: Most challenging level.

4.8 Modality Rating

After the completion of the two experiments, the participants were asked to rank the modalities based on preference. Table 37 summarizes the results of these modality rankings. 5 of the 12 healthy participants preferred the slider control modality. The next most popular control modality was voice mode, the fewest number of healthy participants liked the button mode. Similarly, 4 of the 6 occupational therapy participants (healthy participants asked to restrict their movements) liked the slider mode the best, followed by the button mode, and voice mode was least preferred. The table also shows the SCI participant's ranking of the modalities. The SCI participant liked the voice mode the best, followed by the slider mode, and liked the button mode least.

Modality Rating			Healthy (12)	PT (6)	SCI (1)
1st choice	2nd choice	3rd choice			
Button	Slider	Voice	1	-	-
Button	Voice	Slider	2	-	-
Slider	Button	Voice	2	4	-
Slider	Voice	Button	5	-	-
Voice	Button	Slider	-	-	-
Voice	Slider	Button	2	2	1

Table 37: Control modalities ranked by the participants.

4.9 Discussion and Conclusion

The results in section 4.8 above revealed that the majority of the healthy participants preferred the continuous mode of control (slider mode) out of the three control modalities. Despite his rankings above, the SCI participant also mentioned liking the slider mode (continuous mode of control) best. However, because the slider modality required the SCI participant to use one arm for balancing and stabilizing his body (related to his level of injury), he ultimately preferred the voice mode.

These extensive experiments demonstrated that the multimodal exo-skeletal reacher arm with lift assist designed here, is useful for assisting an SCI individual in moving objects of different shape, size, and weight in a similar time, and with no more errors, than an average healthy young adult without discomfort or fatigue.

The first experiment was designed to assess the participants' ability to perform a 'fine movement' task by arranging particular pegs into corresponding slots within a confined space. Successful completion of this task by the SCI participant with all the given modes and within a comparable time as the healthy participants clearly demonstrated that the SCI participant was comfortable using the eSARA platform.

The second experiment was designed to assess the participants' ability to perform a 'gross movement' task by moving bottles of different weights within a confined space and in a particular arrangement. Experiment two required a more careful approach and consequently the lift assist function played a vital role here. The extension and lift assist features greatly improved the lifting and placing of heavier objects, especially from the perspective of the SCI participant whose normal lifting capabilities are very limited (<2.5 lbs).

Using the eSARA platform allowed the SCI participant to achieve all of the objectives from the two experiments, which he otherwise was unable to complete. eSARA also allowed the SCI participant to maneuver similar to healthy, young adults using the same device, measured by the time required to complete the experiments. Based on these results, his answers to the NASA TLX assessment, and his ranking of the different modalities, a methodology to fit SCI individuals with the eSARA device was successfully achieved. The results of these experiments also confirmed the second hypothesis of this thesis, which stated that a methodology to evaluate the multiple control modes of the eSARA could be created.

Ultimately, this multimodal, exo-skeletal robotic arm resolved previously unmet needs for an individual with severe spinal cord injury. The eSARA device was particularly useful for giving this individual independence, especially for reaching and grasping otherwise out-of-reach (located at various height levels) objects. Furthermore, the lift assist feature enabled the SCI individual to manageably lift and retract objects that would otherwise weigh too much. Movement between mid-shin and mid-chest levels of these objects not only became feasible, but was completed with comparable movement times and number of errors as a control group of healthy young adults. Finally, the SCI individual was able to accomplish all of this without distress or fatigue (either reported by the participant or observed by the investigator). Based on these findings, the researcher, with additional technical improvement, may provide significant and meaningful assistance to people with high level SCI.

This research provided strong proof of concept that, using the eSARA platform, a methodology can be developed to match a specific mode of device control to the functionality of an SCI individual, based on his or her level of injury. Technical improvements for the next generation of the researcher have been identified and are discussed in the next chapter. The next

chapter discusses the future work proposed for the eSARA platform based on feedback from the majority of the participants.

Chapter 5: Discussion, Conclusion, and Future Work

Summary: One of the fundamental problems with designing a user interface for assistive devices is addressing functional deficits in the matching of user capability with device control modalities. Solving this problem was the primary goal of this thesis—that is, how to create a methodology that allows for technology customization, bringing individuals from the target population (high level spinal cord injury) towards greater self-sufficiency. The thesis was framed around the main hypotheses that:

- (1) Reach and grasp tasks with platforms designed with multiple modes of control and other useful features would be feasible and usable by an SCI participant and
- (2) A methodology to evaluate multiple modes of operating such a device can also be created.

The first prototype device, and its associated experiments, addressed hypothesis 1 and were described in chapter 2. User testing confirmed the device's utility as a low cost, light weight, voice-activated reaching and grasping device for people with reach limitation. Furthermore, the device allowed a SCI participant to perform at the same level as a healthy individual using the same device. The reach limitations were tested in a specially designed test environment simulating real life scenarios. The experiments were expanded with a control group of healthy participants. The SCI participant repeated the experiment with results similar to those of the average of the healthy participants using the same device. These results showed promising usability, but the device was restricted in its capabilities and modes of operations.

In chapter 3 the research was taken further with the design of a new wearable robotic device with multi-modal controls. Greater functionality (lift assist and extendibility) was also

added to the device to better assist individuals with severe SCI and upper extremity limitations in their daily lives. Two different tests were designed to target various aspects of functionality and movability of the Human Machine Interface (HMI). All participants were to complete both experiments with the three given modalities of control. Healthy participants were divided into two groups. Group 1 participants were allowed to make any movements while group 2 was asked to restrict themselves to imitate movements that would be made by an individual with severe SCI. At the end of the two experiments with all the modalities, participants took a task load index test to determine the most challenging aspect of the experiments.

Finally, the SCI participant completed the two experiments with all three available modalities. The results of the experiments confirmed that the SCI participant was able to perform equal to the average healthy participant (using the same device) while achieving all the tasks accurately. No visual signs of fatigue were observed and all participants confirmed not feeling fatigue when asked.

5.1 Discussion and Conclusion

This research validates the methodology of matching the ability of the SCI individual with the mode of control using the eSARA platform. The eSARA platform enabled individuals with high level of SCI or upper extremity limitations to move objects within a 1D planar level and across three levels in 3D. The SCI participant was able to use all the available modes of control, but due to limitations from his SCI, he selected the ballistic mode of control with minimal/no limb movement. Without the methodology developed using eSARA, the SCI participant was unable to perform any of the functional tasks. With the use of the reacher it was validated that the SCI participant was able to perform all of the assigned tasks and was able to lift substantial weight (beyond his normal limit) with the help of the lift assist feature. His time performance

was comparable to both control groups. This result was the key to the methodology because it demonstrates that a successful level of control was achieved by the SCI individual.

The methodology devised in this research has proven on positive impact, and great potential to improve, the life of SCI participants by matching their deficits with appropriate control modalities. One drawback of this research was that there were not enough SCI participants (due to a lack of availability) to fully test the methodology. In addition, the device was a prototype that still needs usability improvements. Thus, future work is based on these main factors:

1. Participant Study: A larger group of individuals with SCI needs to be evaluated on the test platform developed in chapters 2 and 3.
2. Device update: The device will be updated to increase its usability with a number of improvements suggested below.
3. Enhanced Human Machine Interface (HMI): The future HMI should be tested with SCI participants with various levels of injury. These participants will then take part in experiments similar to the ones in chapter 2 and chapter 3. Control modes will be categorized as described previously:
 1. Ballistic modality with no extremity movement required (e.g. voice activated)
 2. Ballistic control mode (e.g. pushing buttons) that requires minimal movement of the extremities
 3. Continuous control mode (e.g. joystick) that may require major (continuous) movement of the extremities

Other modalities could be added depending on the range of disabilities. For instance, if speech was an issue, neck or eye movements could be used to control the device.

The methodology will include having the participant use a given control mode and assessing the results of the experiment to see if the participant's data corresponds to that of a healthy participant. If a SCI participant's performance falls outside two standard deviations of the mean performance of healthy participants, the SCI participant will be asked to select a different (less movement requiring) modality and repeat the experiment. A simple test of evaluation could be created to determine the capabilities of any given participant. For instance, a simple computer game could help determine the ease of use of a given modality. A joystick or differently sized buttons could all be used to complete the gaming tasks. The information collected from the gaming tasks would be utilized to design a modality study for the SCI participants.

5.1.1 Modality Selection for the SCI Injury Level

The participant will be required to perform a simple experiment that will determine which of the three modes is best suited for that participant (like those in chapter 2). The participant will then engage in a more intensive experiment (like those in chapter 3) multiple times. A number of participants, with various levels of SCI, will be compared to the following control groups similarly to the controls used in chapters 2 and 3:

1. Healthy participants with no restrictions
2. Healthy participants with temporary physical constraints
3. SCI participants with various levels of injury
4. Participants with arthritis
5. Participants with temporary upper extremity limitations

The methodology for modality selection will be similar for all of these participants in order to create a user interface that matches the capability of the participant with his or her respective upper extremity limitations.

5.1.2 Modality Match Methodology

Once the participant is matched to a given modality, that mode will be available in various ergonomic and user friendly options. If the participant was matched with the ballistic modality with no extremity movement, there will be various microphones available for enhanced voice communication. If the participant was matched with ballistic control mode with minor extremity movement, there will be buttons with various sizes and touch sensitivities available. If the participant was matched with continuous control mode, there will be a variety of options for the participant to select from including a rotary dial, a slider, or a joystick. To further customize the matched modality, the participants will be required to repeat a series of experiments with their modality's different options. The following figure helps explain this ideology for the future work.

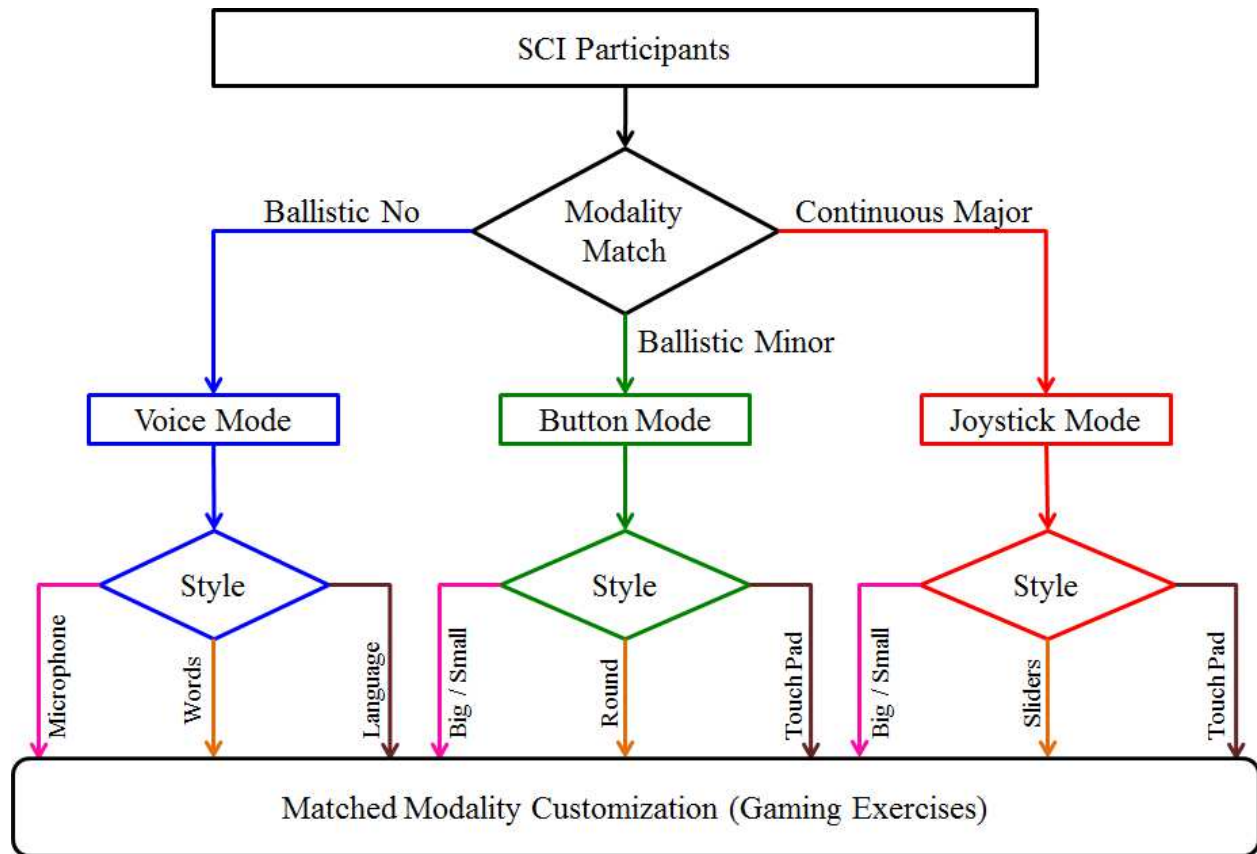


Figure 146: Methodology for modality selection for SCI participants.

Stating from various participants the modality match experiments will determine what mode the participant can use given their physical restrictions. Once the modality is matched, ballistic no extremity movement, ballistic minor extremity movement or continuous with major extremity movement, the participants will be provided with options available for the matched modality. To determine the best fit specifications of the matched modality the participants will be asked to perform a simple test of evaluation. For instance the gaming exercises from section 5.2. This will help the participant to choose to customize the matched modality.

5.2 Future Work

5.2.1 Device Upgrades

The current generation of the assistive arm is a fully operational device that meets all desired expectations and functional requirements. However, the current Exo-Skeletal Assistive Robotic Arm (eSARA) could be modified to a lighter and easier to customize device. Now that the platform is functional, and shown to be useful for developing a strategy for SCI participants, only a few adjustments are needed to enhance future generations of the assistive arm. The following are a few suggestions and ideas for the next generation of eSARA.

5.2.1.1 Weight Reduction

The current assistive device weighs 7.42 lbs. with the majority of this weight coming from the steel components (forearm plate, bottom arm plate, biceps bracket, triceps bracket, etc.) of eSARA. In the future design these parts could be replaced by aluminum, high density polymer, or carbon-fiber, all of which would significantly reduce the weight of the arm. Another weight contributing factor is the handle. Although the current handle is made of aluminum, it contains many components. The central cylinder holding the top and bottom plate of the handle

is a solid aluminum piece. That solid aluminum cylinder is housed within a hollow aluminum cylinder to have a floating mechanism for the handle. In the future these pieces could be replaced by a simpler piece of high density polymer or plastic. These parts could also be 3D printed in low-cost, high strength plastics. 3D printing would also allow the parts to be made modular such that if something breaks, a replacement part could be printed. Finally, the electronics could be housed within the arm's length, avoiding weight generated by the individual housing units for lift assist and modality selection.

5.2.1.2 New Structural Design

The current generation of eSARA inherited its structure from the air-brace system with slight modifications to accommodate the needs of the user. Now that different functionalities of eSARA have been well-defined with the current platform, a fresh design could not only improve the look and weight of the device, but could also accommodate channels for the electrical features. This design feature would help to integrate and conceal the electrical wires, connections, and battery within the structure.

The current generation of eSARA consists of a cushion and four Velcro straps to fasten the device to the user. These Velcro straps are located at the wrist, forearm, bottom of the bicep, and top of the bicep. The cushion and Velcro combination makes the current generation look bulky and maladroit. This system can also be very cumbersome while putting on or taking off the arm. Better ways of securing the user's arm to the device are being considered. For example, a one buckle system could provide a quick and secure release for the arm.

5.2.1.3 End-Effector Enhancement

The end-effector used for the current generation was a servo based grasping claw. The claw assembly worked sufficiently well but the end-effector could be greatly enhanced for future device generations using some of the following ideas.

5.2.1.4 Camera Based Adaptive End-Effector Orientation

If a micro camera with the capability of object recognition is added at the end effector, it could greatly improve the ease of grasping an object. Once the camera recognizes the object, the end-effector would rotate and adjust its orientation based on the object's position. This recognition would allow the users to perform the grasping task faster and more efficiently. However, a training period would be required for the users to get acclimated with the new device.

5.2.1.5 Better Gripper

The current gripper works excellently but further improvements in the quality and grasping ability could be very useful. A gripper with integrated sensors for slip detection, force feedback, and dexterity would allow the users to be more informed about the grasp on the object.

5.2.1.6 Feedback Mechanism

The future generation of this robotic device should provide more information to the user based on suggestions from the current participants. Feedback from the various functionalities of the current assistive arm would help the user to be more confident in moving various objects. Feedback requirements, and how they would enhance the current device, follow.

5.2.1.6.1 Lift Assist Feedback

The current generation of eSARA lacked feedback from the pressure sensors. A multicolor Light Emitting Diode (LED) could be added to the pressure sensors. The LED would

stay 'on' while the arm is in motion, with a simple change in color when the maximum or minimum angle between the forearm and biceps is reached. This color coded LED will make the user aware of the maximum and minimum limits of the arm's rotation.

5.2.1.6.2 Extension Feedback

The current generation of eSARA also lacks extension feedback. This feedback could also be in the form of an LED. This LED can stay luminous while the extension is taking place and changes to a different color if the maximum extension is reached. The same can be true when the arm collapses and the minimum extension is reached.

5.2.1.6.3 Gripper Feedback

Feedback from the gripper would also improve the current generation of eSARA by providing feedback regarding the grip strength. A tactor (small vibrating motor) [93] would be very helpful for the user. The tactor's intensity can be linked to pressure sensor in the gripper end of the device. The pressure sensor can be directly proportional to the tactor's vibration. The strongest grasp by the end-effector will make the tactor vibrate intensely. The intensity of vibrations will reduce as the grip is reduced. This feedback could also be achieved using an LED instead of a tactor. When the luminosity of the LED is the brightest, that would suggest the tightest grip by the end-effector.

5.2.1.6.4 Modality Feedback

The current generation eSARA had only one modality control switch that indicated the mode in use, but a feedback mechanism could be incorporated that allows users to know what mode the platform is in without checking the switch. This feature could be done by connecting an LED or a speaker using the inputs from the modality control switch. Based on the switch position, when the device is turned on, the modality feedback will say which modality is

currently being used (in case of the speaker feedback). In case of the LED feedback, once the device is turned ‘on’ the feedback for various modalities can be color coded. For example, if the button modality was selected the LED will blink red for a few seconds and turn off. Once the modality is switched (slider modality) the led will blink yellow a few times and turn off. Again if the modality is switched to voice the led will blink blue for a few second and turn off.

5.2.1.6.5 Power Feedback (Low Battery Feedback)

The power feedback feature will allow the user to know if the battery needs to be recharged. This can be achieved by using a low energy LED. Once the power reaches a certain value the power feedback LED turns on. This will be a clear visual indication to recharge the battery. Current generation of eSARA does not have an indicator that allows the users to know if the battery needs to be recharged.

5.2.1.7 Modality Selection and Exchange

In the current platform, the modality selection switch was concealed to limit access. In the future generation it would be made visible making it easier for users to utilize the multi-modal feature. The packaging of the modality and connection wires also needs to be improved for durability.

5.2.1.8 Placement of the Pressure Sensors for Lift Assist

The participant study revealed that placement of the pressure sensors needed to be improved. Currently, the pressure sensor are placed just above the handle. In the next generation of the device, a pressure sensor with a larger contact area will be used. This will improve the contact of the sensor with the user resulting in a better pressure assessment. The threshold adjustment switch was concealed in the current version to see how well the participants adapt with a constant pressure threshold. However, some of the participants showed interest in

changing the pressure threshold making it more (or less) sensitive. Therefore, in the next generation the pressure threshold will be visible and adjustable to suit the participants' desires.

5.2.1.9 Dynamic Lift Assist

The lift assist feature of this device was based on one threshold. Once the threshold was adjusted, the PID controller was set up to maintain a constant speed. A future improvement will be to allow for user adjustment of this threshold. Another improvement will be a dynamic assistive method. In this method, if the pressure sensor is pressed beyond the threshold pressure, the speed of the arm will increase. These adjustments will allow a user to fully adjust the pressure applied at the pressure sensor and also controlling the speed of the rotation of the arm.

5.2.1.10 Ergonomics and Participants

Ergonomics play an important part in designing a commercial device. The current generation served as a platform for concept verification/visualization. Consideration of ergonomics was rather low for the current iteration of the device. However, now that the device has been demonstrated to be useful for the target population, an improved Human Machine Interface can be styled to allow for a larger user base for the device. In addition to ergonomics, future participant testing should also include individuals with other conditions that result in greatly decreased arm and hand function, such as people with multiple sclerosis, stroke, or arthritis.

This research developed a methodology to select a specific control mode for an assistive device based on the level of injury of a SCI individual. Using this method, individuals can select their preferred modality, while still having the other modes available for use. The platform's evolution is especially beneficial for SCI participants but this same methodology can be applied

to many different individuals with any type of temporary or permanent upper extremity disability.

REFERENCES

1. Connolly, C., *Prosthetic hands from touch bionics*. Industrial Robot: An International Journal, 2008. **35**(4): p. 290-293.
2. Wrathall, J.R., Y.D. Teng, and D. Choiniere, *Amelioration of functional deficits from spinal cord trauma with systemically administered NBQX, an antagonist of non-N-methyl-D-aspartate receptors*. Experimental Neurology, 1996. **137**(1): p. 119-126.
3. Schaefer, P., *Applications of DWI in clinical neurology*. Journal of the neurological sciences, 2001. **186**: p. S25-S35.
4. Sullivan, M. and W. Gullick, *Three-in-one health care system*. 2007, Google Patents.
5. Nguyen, H., et al. *A clickable world: Behavior selection through pointing and context for mobile manipulation*. 2008.
6. Choi, Y., et al. *Laser pointers and a touch screen: intuitive interfaces for autonomous mobile manipulation for the motor impaired*. 2008. ACM.
7. Cyberdyne, *Robot Suit Hybrid Assistive Limb*.

8. Kawamoto, H. and Y. Sankai. *Comfortable power assist control method for walking aid by HAL-3*. 2002. Ieee.
9. Lee, S. and Y. Sankai. *Power assist control for walking aid with HAL-3 based on EMG and impedance adjustment around knee joint*. 2002. Ieee.
10. Sankai, Y. *Leading edge of cybernics: robot suit HAL*. 2006. IEEE.
11. Marchal-Crespo, L. and D.J. Reinkensmeyer, *Review of control strategies for robotic movement training after neurologic injury*. Journal of Neuroengineering and Rehabilitation, 2009. **6**(1): p. 20.
12. Bradberry, T., R. Gentili, and J. Contreras-Vidal, *Reconstructing Three-Dimensional Hand Movements from Noninvasive Electroencephalographic Signals*. Journal of Neuroscience, 2010. **30**(9): p. 3432.
13. Chappell, P.H., et al., *Sensory motor systems of artificial and natural hands*. International Journal of Surgery, 2007. **5**(6): p. 436-440.
14. Engeberg, E.D. and S.G. Meek, *Backstepping and sliding mode control hybridized for a prosthetic hand*. Neural Systems and

- Rehabilitation Engineering, IEEE Transactions on, 2009. **17**(1): p. 70-79.
15. Brown, A.S., *Why hands matter?* Mechanical Engineering, 2008. **130**(7): p. p24-29.
 16. Dalley, S.A., et al., *Design of a multifunctional anthropomorphic prosthetic hand with extrinsic actuation*. Mechatronics, IEEE/ASME Transactions on, 2009. **14**(6): p. 699-706.
 17. Cipriani, C., M. Controzzi, and M.C. Carrozza, *Objectives, criteria and methods for the design of the SmartHand transradial prosthesis*. Robotica, 2010. **28**(06): p. 919-927.
 18. Castellini, C. and P. van der Smagt, *Surface EMG in advanced hand prosthetics*. Biological cybernetics, 2009. **100**(1): p. 35-47.
 19. Castellini, C., et al., *Fine detection of grasp force and posture by amputees via surface electromyography*. Journal of Physiology-Paris, 2009. **103**(3-5): p. 255-262.
 20. Bogue, R., *Exoskeletons and robotic prosthetics: a review of recent developments*. Industrial Robot: An International Journal, 2009. **36**(5): p. 421-427.

21. *Anatomy of the Spinal Cord*. Available from: <http://www.sci-recovery.org/sci.htm>.
22. *Spinal Cord Injury*. Available from: http://www.spinalinjury.net/html/_spinal_cord_101.html.
23. Curt, A. and V. Dietz, *Ambulatory capacity in spinal cord injury: significance of somatosensory evoked potentials and ASIA protocol in predicting outcome*. Archives of physical medicine and rehabilitation, 1997. **78**(1): p. 39.
24. McDonald, J. and C. Sadowsky, *Spinal-cord injury*. The Lancet, 2002. **359**(9304): p. 417-425.
25. Waters, R., et al., *Injury pattern effect on motor recovery after traumatic spinal cord injury*. Archives of physical medicine and rehabilitation, 1995. **76**(5): p. 440-443.
26. Keith, M., et al., *Tendon transfers and functional electrical stimulation for restoration of hand function in spinal cord injury*^{o+}. The Journal of hand surgery, 1996. **21**(1): p. 89-99.

27. Qian, T., D. Campagnolo, and S. Kirshblum, *High-dose methylprednisolone may do more harm for spinal cord injury*. Medical hypotheses, 2000. **55**(5): p. 452-453.
28. Creasey, G., J. Grill, and M. Korsten, *An implantable neuroprosthesis for restoring bladder and bowel control to patients with spinal cord injuries: A multicenter trial* 1*. Archives of physical medicine and rehabilitation, 2001. **82**(11): p. 1512-1519.
29. Marino, R., et al., *Neurologic recovery after traumatic spinal cord injury: data from the Model Spinal Cord Injury Systems*. Archives of physical medicine and rehabilitation, 1999. **80**: p. 1391-1396.
30. Barker, G., *Diffusion-weighted imaging of the spinal cord and optic nerve*. Journal of the neurological sciences, 2001. **186**: p. S45-S49.
31. *SCI-Info*. Available from: <http://www.sci-info-pages.com/>.
32. *Spinal cord injury facts*. Available from: <http://www.fscip.org/facts.htm>.

33. Melton, L., *Neural transplantation: new cells for old brains*. The Lancet, 2000. **355**(9221): p. 2142.
34. Nash, M., B. Montalvo, and B. Applegate, *Lower extremity blood flow and responses to occlusion ischemia differ in exercise-trained and sedentary tetraplegic persons*. Archives of physical medicine and rehabilitation, 1996. **77**(12): p. 1260-1265.
35. *International Classification of Functioning, Disability and Health ICF*. World Health Organization, 2001. **NLM classification W: 15**(ISBN 92 4 154542 9).
36. Schneidert, M., et al., *The role of environment in the International Classification of Functioning, Disability and Health (ICF)*. Disability & Rehabilitation, 2003. **25**(11): p. 588-595.
37. Steiner, W., et al., *Use of the ICF model as a clinical problem-solving tool in physical therapy and rehabilitation medicine*. Physical Therapy, 2002. **82**(11): p. 1098.
38. Stucki, G., *International Classification of Functioning, Disability, and Health (ICF): a promising framework and classification for*

- rehabilitation medicine*. American Journal of Physical Medicine & Rehabilitation, 2005. **84**(10): p. 733.
39. Stucki, G., et al., *Application of the International Classification of Functioning, Disability and Health (ICF) in clinical practice*. Disability & Rehabilitation, 2002. **24**(5): p. 281-282.
40. Bolton, B., J. Bellini, and J. Brookings, *Predicting client employment outcomes from personal history, functional limitations, and rehabilitation services*. Rehabilitation Counseling Bulletin, 2000. **44**(1): p. 10.
41. Dahl, T., *International classification of functioning, disability and health: An introduction and discussion of its potential impact on rehabilitation services and research*. Journal of Rehabilitation Medicine, 2002. **34**(5): p. 201-204.
42. Tetrault, E.O., *PACKAGE-REACHER*. 1912, Google Patents.
43. Tichacek, J., *PACKAGE-REACHER*. 1918, Google Patents.
44. Pedersen, J., *Shelf-reacher*. 1920, Google Patents.
45. Del Johnson, R., *Extendable, non-rotating reacher*. 2002, Google Patents.

46. Liden, D., *Multi-purpose reacher and dressing aid*. 1997, Google Patents.
47. Osborn, G., *Combination cane and reaching apparatus*. 1993, Google Patents.
48. Shimasaki, K., *Self-gripping reacher*. 1988, Google Patents.
49. Van Zelm, W., *Hand-held gripping device with improved support for handicapped persons having limited finger function or wrist strength*. 1986, Google Patents.
50. Keith, G. and P. Rappl, *Pickup tool with variable position limiting and variable axis of operation*. 2003, Google Patents.
51. Al Ferguson, W., *Pick-up tool*. 2005, Google Patents.
52. Traber, A. and R. Traber, *Single-hand actuated pick-up tool*. 1996, Google Patents.
53. Chen, L.-K.P., et al., *An evaluation of reachers for use by older persons with disabilities*. *Assistive Technology*, 1998. **10**(2): p. 113-125.
54. Mokhtari, M., et al., *Toward a human-friendly user interface to control an assistive robot in the context of smart homes*, in

- Advances in Rehabilitation Robotics - Human-Friendly Technologies on Movement Assistance and Restoration for People with Disabilities*, Z.Z. Bien and D. Stefanov, Editors. 2004, Springer-Verlag Berlin: Berlin. p. 47-56.
55. Abdulrazak, B., M. Mokhtari, and B. Grandjean, *Usability of an assistive robot manipulator: Toward a quantitative user evaluation*, in *Advances in Rehabilitation Robotics - Human-Friendly Technologies on Movement Assistance and Restoration for People with Disabilities*, Z.Z. Bien and D. Stefanov, Editors. 2004, Springer-Verlag Berlin: Berlin. p. 211-220.
56. Hillman, M., et al., *Weston wheelchair mounted assistive robot - the design story*. *Robotica*, 2002. **20**: p. 125-132.
57. Asma S. Ali, M.G.M., Danielle C. McGeary, William R. Pruehsner, John D. Enderle, Ph.D., *The Assistive Robotic Arm*. IEEE, 2010.
58. Katsura, S. and K. Ohnishi, *Human cooperative wheelchair for haptic interaction based on dual compliance control*. *Industrial Electronics, IEEE Transactions on*, 2004. **51**(1): p. 221-228.

59. Oh, S., N. Hata, and Y. Hori, *Integrated motion control of a wheelchair in the longitudinal, lateral, and pitch directions*. Industrial Electronics, IEEE Transactions on, 2008. **55**(4): p. 1855-1862.
60. Oonishi, Y., S. Oh, and Y. Hon. *New control method for power-assisted wheelchair based on upper extremity movement using surface myoelectric signal*. 2008. IEEE.
61. Oonishi, Y., S. Oh, and Y. Hori, *A new control method for power-assisted wheelchair based on the surface myoelectric signal*. Industrial Electronics, IEEE Transactions on, 2010. **57**(9): p. 3191-3196.
62. Abellanas, A., et al., *Estimation of gait parameters by measuring upper limb-walker interaction forces*. Sensors and Actuators A: Physical, 2010. **162**(2): p. 276-283.
63. Rapacki, E., C. Niezrecki, and H. Yanco, *An Underactuated Gripper to Unlatch Door Knobs and Handles*.
64. Tsui, K. and H. Yanco. *Simplifying wheelchair mounted robotic arm control with a visual interface*. 2007.

65. Agree, E.M. and V.A. Freedman, *A comparison of assistive technology and personal care in alleviating disability and unmet need*. The Gerontologist, 2003. **43**(3): p. 335-344.
66. Jain, A. and C.C. Kemp, *EL-E: an assistive mobile manipulator that autonomously fetches objects from flat surfaces*. Autonomous Robots, 2010. **28**(1): p. 45-64.
67. Deyle, T., et al., *RFID-Guided Robots for Pervasive Automation*. IEEE Pervasive Computing, 2010.
68. Jain, A. and C. Kemp. *Behaviors for robust door opening and doorway traversal with a force-sensing mobile manipulator*. 2008.
69. Nguyen, H. and C. Kemp. *Bio-inspired assistive robotics: Service dogs as a model for human-robot interaction and mobile manipulation*. 2008.
70. King, C.-H., et al., *Dusty: an assistive mobile manipulator that retrieves dropped objects for people with motor impairments*. Disability and Rehabilitation: Assistive Technology, 2012. **7**(2): p. 168-179.

71. Erico Guizzo, H.G., *The Rise of the Body Bots*. IEEE spectrum, 2005.
72. Ferris, D., G. Sawicki, and A. Domingo, *Powered lower limb orthoses for gait rehabilitation*. Topics in spinal cord injury rehabilitation, 2005. **11**(2): p. 34-49.
73. Zoss, A., H. Kazerooni, and A. Chu, *Biomechanical design of the Berkeley lower extremity exoskeleton (BLEEX)*. IEEE/ASME Transactions On Mechatronics, 2006. **11**(2): p. 128-138.
74. Kazerooni, H., R. Steger, and L. Huang, *Hybrid control of the berkeley lower extremity exoskeleton (bleex)*. The International Journal of Robotics Research, 2006. **25**(5-6): p. 561.
75. Pons, J.L., *Rehabilitation Exoskeletal Robotics*. IEEE, 2010.
76. Kong, K., et al., *Control of an Exoskeleton for Realization of Aquatic Therapy Effects*. Ieee-Asme Transactions on Mechatronics, 2010. **15**(2): p. 191-200.
77. Zelinsky, A., *Robot suit hybrid assistive limb [Industrial Activities]*. Robotics & Automation Magazine, IEEE, 2009. **16**(4): p. 98-98, 102.

78. Kong, K., et al. *Robotic rehabilitation treatments: realization of aquatic therapy effects in exoskeleton systems*. 2009. IEEE Press.
79. Popovic, D., R. Tomovic, and L. Schwirtlich, *Hybrid assistive system-the motor neuroprosthesis*. IEEE Transactions on Biomedical Engineering, 1989. **36**(7): p. 729-737.
80. Ishii, M., K. Yamamoto, and K. Hyodo, *Stand-alone wearable power assist suit-Development and availability*. Journal of robotics and mechatronics, 2005. **17**(5): p. 575.
81. Naruse, K., S. Kawai, and T. Kukichi. *Three-dimensional lifting-up motion analysis for wearable power assist device of lower back support*. 2005. IEEE.
82. Sankai, Y., *HAL: Hybrid Assistive Limb Based on Cybernetics*. Robotics Research, 2011: p. 25-34.
83. Schiele, A. and G. Visentin. *The esa human arm exoskeleton for space robotics telepresence*. 2003.
84. Cavallaro, E., et al., *Hill-Based Model as a Myoprocessor for a Neural Controlled Powered Exoskeleton Arm-Parameters Optimization*.

85. Staubli, P., et al., *Effects of intensive arm training with the rehabilitation robot ARMin II in chronic stroke patients: four single-cases*. Journal of Neuroengineering and Rehabilitation, 2009. **6**.
86. Yagi, E., D. Harada, and M. Kobayashi, *Upper-limb power-assist control for agriculture load lifting*. International Journal of Automation Technology, 2009. **3(6)**: p. 716-722.
87. Perry, J.C., J. Rosen, and S. Burns, *Upper-limb powered exoskeleton design*. Mechatronics, IEEE/ASME Transactions on, 2007. **12(4)**: p. 408-417.
88. Colizzi, L., A. Lidonnici, and L. Pignolo, *The ARMIS project a concept robot and technical design*. Journal of Rehabilitation Medicine, 2009. **41(12)**: p. 1011-1015.
89. du Sart Tilman, P. and R. des Chasseurs Ardennais, *EXOSTATION: 7-DOF HAPTIC EXOSKELETON AND VIRTUAL SLAVE ROBOT SIMULATOR*.
90. Letier, P., et al., *SAM: A 7-DOF Portable Arm Exoskeleton with Local Joint Control*.

91. Bekey, G. and R. Tomovic. *Robot control by reflex actions*. 1986. IEEE.
92. Neri, T. and J. Cregg, *New Prosthetic arms provide greater quality of life for amputees*.
93. Bloomfield, A. and N. Badler, *A low cost tactor suit for vibrotactile feedback*. Technical Reports (CIS), 2003: p. 66.
94. Khalid, U., et al., *DEVELOPMENT AND HUMAN PERFORMANCE EVALUATION OF CONTROL MODES OF A LIGHTWEIGHT SMART-ASSISTIVE ROBOTIC ARM (SARA)*.
95. *Sensory* Available from: <http://www.sensoryinc.com/>.
96. *Firgelli*. Available from: <http://www.firgelli.com/>.
97. Corp., I., *IBM SPSS Statistics for Windows*. 2013 (Version 22).
98. *Zeiss*. Available from: <http://www.zeiss.com/>.
99. *Össur*. Available from: <http://www.ossur.com>.
100. *VEXRobotics*. Available from: <http://www.vexrobotics.com>.
101. *Arduino*. Available from: <http://arduino.cc/>.
102. *Atmel*. Available from: <http://www.atmel.com>.
103. *Veear*. Available from: <http://www.veear.eu>.

104. *Interlink Electronics*. Available from:

<http://www.interlinkelectronics.com/>.

105. Hart, S.G. and L.E. Staveland, *Development of NASA-TLX (Task Load Index): Results of empirical and theoretical research*. Human mental workload, 1988. 1(3): p. 139-183.

ABSTRACT

DEVELOPMENT AND HUMAN PERFORMANCE EVALUATION OF CONTROL MODES OF AN EXO-SKELETAL ASSISTIVE ROBOTIC ARM (eSARA)

by

UMER KHALID

May 2015

Advisor: Dr. Abhilash Pandya

Major: Electrical and Computer Engineering

Degree: Doctor of Philosophy

This research was conducted to assist with functional tasks for a targeted group of individuals with spinal cord injury (SCI); with C5 to C7 level of injury relating to upper extremity movement. The specific population was selected as the existing technology was either too expensive, too bulky or was unable to address their needs in regards to upper extremity mobility. In addition, no platforms allowed multimodal control options for customization or provided a methodology for this crucial evaluation. The motivation of this research was to provide a methodology for selecting the appropriate control of an assistive device based on the range of basic human movements that were possible by the population under consideration (button pushing, lever sliding, and speech). The main idea was to create an evaluation methodology based on a user platform with multiple modes of control. The controls were developed such that they would allow operation of the device with respect to the capabilities of SCI participants.

Engineering advancements have taken assistive robotics to new dimensions. Technologies such as wheelchair robotics and myo-electronically controlled systems have opened up a wide range of new applications to assist people with physical disabilities. Similarly exo-skeletal limbs

and body suits have provided new foundations from which technologies can aid function. Unfortunately, these devices have issues of usability, weight, and discomfort with donning. The Smart Assistive Reacher Arm (SARA) system, developed in this research, is a voice-activated, lightweight, mobile device that can be used when needed. SARA was built to help overcome daily reach challenges faced by individuals with limited arm and hand movement capability, such as people with cervical level 5-6 (C5-6) SCI. The functional reacher arm with voice control can be beneficial for this population. Comparison study with healthy participants and an SCI participant shows that, when using SARA, a person with SCI can perform simple reach and grasp tasks independently, without someone else's help. This suggests that the interface is intuitive and can be easily used to a high-level of proficiency by a SCI individual.

Using SARA, an Exo-Skeletal Assistive Robotic Arm (eSARA) was designed and built. eSARA platform had multiple modes of control namely, voice (ballistic mode with no extremity movement), button (ballistic mode with minor extremity movement) and slider (continuous mode with major extremity movement). eSARA was able to extend a total of 7 inches from its original position. The platform also provided lift assist for users that can potentially enable them to lift up to 20lbs. The purpose of eSARA was to build a platform that could help design a methodology to select the modality for a specific level of SCI injury or capability.

The eSARA platform's Human Machine Interface (HMI) was based on two experiments 'Fine movement experiment' and 'Gross movement experiment'. These experiments tested the reaching, grasping and lifting ability of the platform. Two groups of healthy young adults were selected to perform the experiment. The first group, 12 healthy participants, had no movement restrictions. The second group, 6 Occupational Therapy students, that could mimic restrictions similar to those of a level 5-6 SCI individual. The experiment was also conducted by an SCI

individual. The results of the 2 groups from both the experiments were compared with the results of the SCI participant. It was found that the SCI participant's time performance to finish the tasks was comparable to the average of the healthy participants.

It was concluded that the developed methodology and platforms could be used to evaluate the control modes needed in order to customize the system to the capabilities of SCI individual. . These platforms can be tested for a broader range of participants including participants with arthritis, recovering from paralysis and seniors with movement issues.

AUTOBIOGRAPHICAL STATEMENT

Umer Khalid is an Electrical Engineer at Ford Motor Company and an Adjunct faculty at Wayne State University. He holds a B.S. and M.S. in Electrical and Computer Engineering, and from Wayne State University. His research interests include assistive robotics, prosthetics, medical robotics and surgical robotics.